UNIVERSITÄTSKLINIKUM HAMBURG-EPPENDORF

Institut für Experimentelle Pharmakologie und Toxikologie

Prof. Dr. med. Thomas Eschenhagen

Repolarisation of human induced pluripotent stem cell cardiomyocytes in engineered heart tissue

A systematic comparison to human adult cardiac tissue

Dissertation

zur Erlangung des Grades eines Doktors der Medizin /Zahnmedizin

an der Medizinischen Fakultät der Universität Hamburg.

vorgelegt von:

Tobias Krause

aus Bremen

Hamburg 2021

(wird von der Medizinischen Fakultät ausgefüllt)

Angenommen von der

Medizinischen Fakultät der Universität Hamburg am: 13.09.2021

Veröffentlicht mit Genehmigung der

Medizinischen Fakultät der Universität Hamburg.

Prüfungsausschuss, der/die Vorsitzende: Prof. Dr. Alexander Schwoerer

Prüfungsausschuss, zweite/r Gutachter/in: PD Dr. Torsten Christ

Abstract of the dissertation

Cardiac ventricular tachyarrhythmias are possibly lethal occurrences in patients when they cause too fast myocardial excitation and contraction of the ventricular muscle. A prolongation of action potential (AP) duration and QT interval leads to a substantial risk for Torsade-de-Pointes tachycardias (long QT syndrome, LQTS). Causes for AP prolongation can be ion channel mutations or drug induced channel dysfunction. In safety pharmacology, substances are screened for potential proarrhythmic blocking effect of repolarising potassium channels. The effect on a single ion channel can be monitored in expression systems, but AP measurements are necessary to estimate the net effect of drugs on repolarisation. Since human cardiac tissue is only available to a limited extent, measurements are performed in animal models with notable interspecies differences in AP regulation by different potassium channels. Are human induced pluripotent stem cell cardiomyocytes (hiPSC-CM) able to close the gap to animal models? Thus far, the exact contribution of individual potassium channels to repolarisation of mature hiPSC-CM in engineered heart tissue (EHT) is not fully characterised yet. This work will investigate how closely EHT resembles human ventricular tissue with respect to repolarisation. The final goal is to investigate whether EHT may lead to a superior test system compared to established animal tissue models.

Methods: Engineered heart tissue (EHT) was created from hiPSC-CM. Human left ventricular (LV) tissue was collected from patients undergoing heart surgery. For action potential measurements, the sharp microelectrode technique was used. Action potentials could be measured and remained stable over hours, allowing application of stimulation protocols as well as pharmacologic interventions with ion channel altering drugs.

Results: In contrast to LV, EHT showed spontaneous diastolic depolarisation, excitation and contraction, which could be mostly abolished by ivabradine-induced block of the *funny current* I_f. AP shape in EHT resembled that in human left ventricle, but AP duration in EHT was shorter. I_{Kr} block by E-4031 induced a larger AP prolongation and showed a stronger reverse use dependency than LV. A possible cause for this may be the higher channel density and gene expression of *hERG*-channels. I_{Ks} block prolonged APD only when beta adrenoceptors were stimulated; the increase in APD was much smaller than with I_{Kr} block. Upon I_{Kr} block half of the EHTs developed early afterdepolarisations (EAD), associated with arrhythmia. In contrast, several proarrhythmic factors were necessary to evoke EADs in LV.

Conclusion: Overall, LV and EHT share common features in repolarisation, but repolarisation reserve is much smaller in EHT, in which I_{Kr} dominates repolarisation. Contribution of I_{Ks} is rather small in both preparations and depends on beta adrenoceptor stimulation. The data suggest that EHT is a promising model in safety pharmacology as it provides a complete model of human electrophysiology compared to animal models.

I Table of content

II List of figures

III List of tables

IV List of abbreviations

AP:	action potential
APD_{90}:	action potential duration (at 90% repolarisation)
AVN:	atrioventricular node
β_N-AR:	beta-N adrenergic receptors
CL:	cycle length
DD:	diastolic depolarisation
EAD:	early afterdepolarisation
ECG:	electrocardiogram
EHT:	Engineered heart tissue
ERP:	effective refractory period
DAD:	delayed afterdepolarisation
DD:	diastolic depolarisation
hERG:	human *Ether-à-go-go*-Related Gene
hiPSC-CM:	human induced pluripotent stem cell cardiomyocytes
I_{Kr}:	cardiac rapid activating delayed rectifier potassium current
I_{Ks}:	cardiac slow activating delayed rectifier potassium current
I_{K1}:	inward rectifier potassium current
LQTS:	long QT syndrome
LV:	left ventricle
LVAD:	left ventricular-assist-device
RMP:	resting membrane potential
SN:	sinus node
TdP:	Torsade-de-Pointe
VF:	ventricular fibrillation
VT:	ventricular tachycardia

1 Introduction

Cardiac arrhythmias can trigger sudden cardiac death (SCD) and are therefore one of the most dangerous cardiac events in human medicine. Especially ventricular tachycardia (VT) can cause a lack of synchronised myocardial excitation of the ventricular muscle, hence an asynchronous contraction, reduced ejection and subsequently insufficient blood flow to the brain.

One of these life-threatening cardiac arrhythmias is Torsade-de-Pointes tachycardia (TdP), a polymorphic irregular ventricular tachycardia that occurs, when an excitation wave reaches cells during the vulnerable phase of repolarisation and leads to a circulating macro-reentry of excitation. Factors that increase the likelihood of this event include early and delayed afterdepolarisations (EAD/DAD) of the cardiac action potential (AP). An increase of cardiac action potential duration (APD), and thereby QT-interval in the ECG, prolongs the vulnerable phase of the myocardium during the cardiac cycle and increases the probability of EADs and other proarrhythmic triggers to cause such a severe tachyarrhythmia. This can occur either in genetic diseases like long QT syndrome (LQTS) in which repolarisation is impaired by malfunctioning cation channels or by other conditions affecting repolarising ion channels like certain substances, metabolic conditions and toxic or structural damage.

TdP has the potential to terminate spontaneously, however in certain situations an episode of this tachyarrhythmia can degenerate into ventricular fibrillation during which practically no cardiac output of blood to the brain and organs occurs, leading to SCD if not terminated.

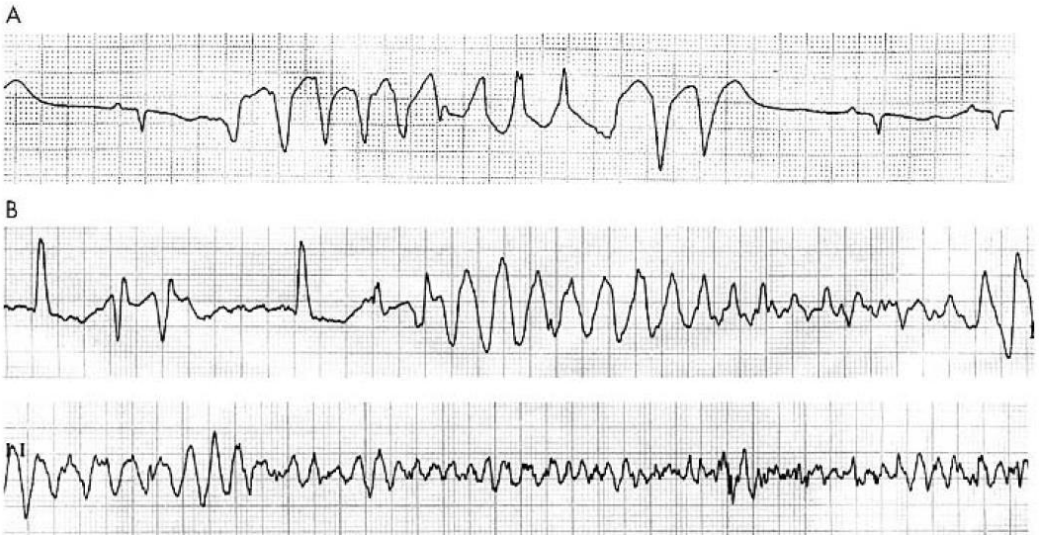

Figure 1. ECG recording of Torsade-de-Pointe tachycardia.

A. Self-limiting Torsade-de-Pointe tachyarrhythmia episode. B. Torsade-de-Pointe degenerating to ventricular fibrillation (Yap and Camm 2003).

In the context of safety pharmacology, reagents are therefore evaluated for their potential to interfere with repolarising ion currents and prolong action potentials. Especially the human ether-a-go-go related gene (*hERG*) channel conducting the rapid delayed inward rectifier potassium current (I_{Kr}) is a critical factor as it dominates repolarisation. Any impairment of repolarising ion currents during the AP can lead to AP prolongation, which favours arrhythmogenesis (Thomas et al. 2004).

Nowadays the effect of a drug on a single ion channel can be monitored very effectively in expression systems. However, for identification of the net effect of a drug on tissue repolarisation, action potential measurements are necessary. Most of these studies are still performed in intact tissue because of the stability of AP parameters compared to work in single cells. Since human cardiac tissue is only available to a limited extent, these measurements are almost exclusively done in animal models. But so far there is no animal model that depicts human cardiac cellular electrophysiology without substantial deviations. Even in the different animal models, there are interspecies differences present, which make comparison quite difficult because contribution of each individual ion current to repolarisation has different significance (Liu and Antzelevitch 1995; Lu et al. 2001; Jost et al. 2013).

A new possibility to test a drug's effect on tissue with regards to arrhythmogenicity and potential to close the gap between animal model and human tissue is brought forth by engineered heart tissue (EHT) generated from human induced pluripotent stem cell cardiomyocytes (hiPSC-CM). Pluripotent stem cells are differentiated into cardiac cells using a previously described protocol and result in cardiac tissue of high similarity to native human heart tissue (Breckwoldt et al. 2017). The EHT format as a three-dimensional tissue shape as opposed to a monolayer of cells or isolated single cells is chosen to reproduce human myocardial conditions as closely as possible regarding tissue structure, culturing and growing conditions such as mechanical strain and nutrient perfusion.

This dissertation specifically investigates the electrophysiological characteristics of hiPSC-CM EHT's cellular repolarisation and repolarisation reserve, which thus far has not been characterised yet. The major goal of it is to investigate the effects of different proarrhythmic influences on arrhythmogenicity in comparison to human left ventricular tissue and to give an answer as to how well this test system can be used in drug testing as an alternative method to animal models and other pre-existing assays.

1.1 Cardiac electrophysiology & arrhythmia

The discipline of cardiac electrophysiology is focused on the electrical activities of the heart on the cellular level, excitation and conduction of electric stimuli as well as on the results on the beating of the heart. Cardiac arrhythmias can occur in a multitude of ways due to many different causes and may certainly present themselves nonuniformly.

In disorders involving cardiac arrhythmia, generally speaking the more threatening manifestations are ventricular tachyarrhythmias as opposed to supraventricular arrhythmias originating from the atria or specific conduction system. One important reason for this is that the atrio-ventricular node's function protects the ventricle from uncontrolled fast excitations and thereby ensures a sufficient time period for repolarisation, relaxation and refilling with blood during the diastole. VTs in their regular, as well as irregular form can lead to a high beating rate and excitation frequency during which the diastole shortens and the refill phase of the cardiac cycle is insufficient, subsequently lowering ejection fraction of the heart and total cardiac output. When VT degenerates into ventricular fibrillation (VF), excitation and contraction work completely asynchronous and irregular, resulting in practically no pump function and cardiac output stops.

In TdP tachyarrhythmia the heart's electrical stimulation is conducted in an undirected way, proceeding in permanently changing reentry circles. Predisposition for development of this kind of rhythm is a prolonged AP and QT duration resulting from repolarisation dysregulations on a cellular level. This LQTS based on disruption of myocardial ion channel functions can either be acquired by iatrogenic influence of certain drugs on ion currents and cell membrane imbalance of electrolytes like potassium, sodium and calcium or results from mutations of genes coding for ion channels in the cell membrane.

The aim of this dissertation is to compare relative contribution of the main repolarising potassium currents to repolarisation and electrical stability in human ventricle and EHT. The basis for the main topic of this work is happening on the tissue level of electrophysiology influenced by cellular mechanisms during repolarisation. The following chapters will therefore start introducing the general electrophysiological functions and mechanisms of the myocardium with a focus on the repolarisation phase of the AP. But the electrical conduction and detailed background of LQTS play a role as well.

1.1.1 The cardiac action potential

The cardiac action potential is the fundamental function of the myocardium to uphold the electromechanical coupling responsible for the pumping function of the cardiac cycle. It is created by membrane currents of ions between the extra- and intracellular compartment and

can be divided into different phases. During phase 0 the initial depolarising upstroke of the membrane potential from a base resting membrane potential (RMP) of around -80 mV up to a voltage of 30 mV is driven by a fast and short influx of Na^+ via SCN5A ion channels. Immediately after this AP peak, repolarisation begins in phase 1 with an outflow of K^+ i.e. via transient outward currents like I_{to}. Afterwards phase 2 (plateau phase) begins and voltage-activated Ca^{2+} currents of the L-type calcium channel allow an inward current from extracellular into the cell. This activates the calcium-triggered Ca^{2+} release from the sarcoplasmic reticulum. The long-lasting influx of positive charges keeps the plateau phase relatively stable until the net transmembrane current leans towards repolarising the membrane potential. Phase 3 (repolarisation phase) in human myocardium which is dominated by potassium outward currents and will be further discussed in the next subchapter. When the membrane potential reaches its initial RMP, the *inward rectifying current* (I_{K1}) stabilises the potential until an excitation stimulus or the *hyperpolarisation-activated cyclic nucleotide–gated* channel's (HCN, funny channel, I_f) currents raise the potential up to the threshold of the next upstroke (Jost et al 2015).

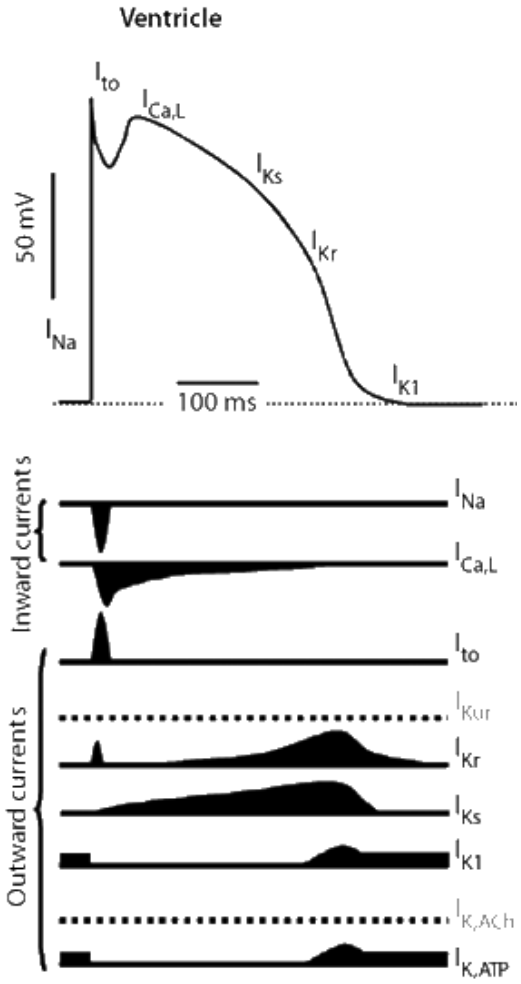

Figure 2. Major ion channel currents in human ventricular myocardium.

A typical human myocardial ventricular action potential is depicted, labelled with the corresponding time-dependent current fluxes shown below separated in inward and outward currents. (adapted from Ravens and Christ 2010, related depictions in Camm et al. 1991).

1.1.2 Repolarisation

The repolarisation phase of the cardiac AP is predominantly carried by potassium outward currents through different ion channels with different characteristics and functions. Most of these channels expressed in the human heart can be found in other animals as well, hence animal models have been studied in electrophysiology for many years. However, the exact contribution of repolarising currents to repolarisation varies between species and produces specific repolarisation patterns. In humans the most significant repolarising K^+ currents are the slowly

(I_{Ks}) and rapidly (I_{Kr}) activating delayed rectifier potassium currents. Additionally, there is the I_{K1} current; another rectifying K^+ current that is responsible for the RMP.

I_{Ks} is activated slowly during the plateau phase and steadily increases over the duration of the AP. Towards the beginning of phase 3 it decreases again and comes to a halt upon reaching the RMP again. The I_{Ks} current is conducted by the Kv7.1 channel which is composed of the KvLQT1 (genetically coded by KCNQ1) and the MinK (genetically coded by KCNE1) subunits (Sanguinetti et al. 1996). I_{Ks} is present in humans and several other animal models, however it is not a major contributor to repolarisation. This changes when there is β-adrenergic stimulation which increases the total I_{Ks} contribution or during simultaneous block of other outward currents, when the relative contribution of I_{Ks} compared to other currents is much higher (Jost et al. 2005).

The I_{Kr} current begins rapidly during AP phase 0 and decreases again just as suddenly. In phase 1 and 2 there is very low activity and the current increases slowly until around 0 mV, when the plateau phase is over. At this point the current increases and carries the fast repolarisation slope of phase 3, after which I_{Kr} deactivates quickly. The channel conducting I_{Kr} is the Kv11.1, which is coded by the KCNH2 gene. I_{Kr} has a significantly higher impact on net repolarisation than other currents and at the same time is often impaired by iatrogenic causes such as medication from many different substance groups.

I_{K1} while inactive during phase 0-2, increases towards the end of Phase 3 and reaches its peak activity close to RMP. Afterwards it decreases again and runs at a steady level to fix the RMP until the next AP upstroke phase 0 and stabilises the potential. For the next AP to trigger a certain amount of current is then required to reach the level of re-excitation (Jost, Muntean, and Christ, 2015).

Other factors to affect repolarisation time include an increased influx of positive charges via gain-of-function mutations of, e.g. sodium or calcium channels. In LQT3 an increased SCN5A coded Na^+ inwards current leads to a prolonged APD as more Na^+ ions have to be transported out in order to reach the RMP level again.

The prolongation of the APD causes an increase in refractory period during which the voltage-activated Na^+ channels remain in an inactivated state and new excitations cannot trigger the next upstroke. Prolongation of APD often leads to an increased dispersion of repolarisation in the tissue, and differences in refractoriness within individual cells can cause micro-reentry on tissue level (Gintant and Valentin 2015).

When the prolongation of the AP during the plateau phase is long enough reactivation of inward currents can happen. This leads to a new influx of cations during the AP which may result either in early or delayed afterdepolarisations (EAD/DAD) or in “triggered activity” (TA). In TA

another quick depolarisation caused by Na^+ produces a fast upstroke in phase 2. EAD/DAD are more likely caused by Ca^{2+} reactivation which causes smaller depolarisations, though both can lead to a significant APD prolongation. Ion channel reactivation and prolongation of

repolarisation (and therefore QT-prolongation) are arrhythmogenic factors that may lead to development of ventricular tachyarrhythmiassuch as TdP (Schleifer and Srivathsan 2015).

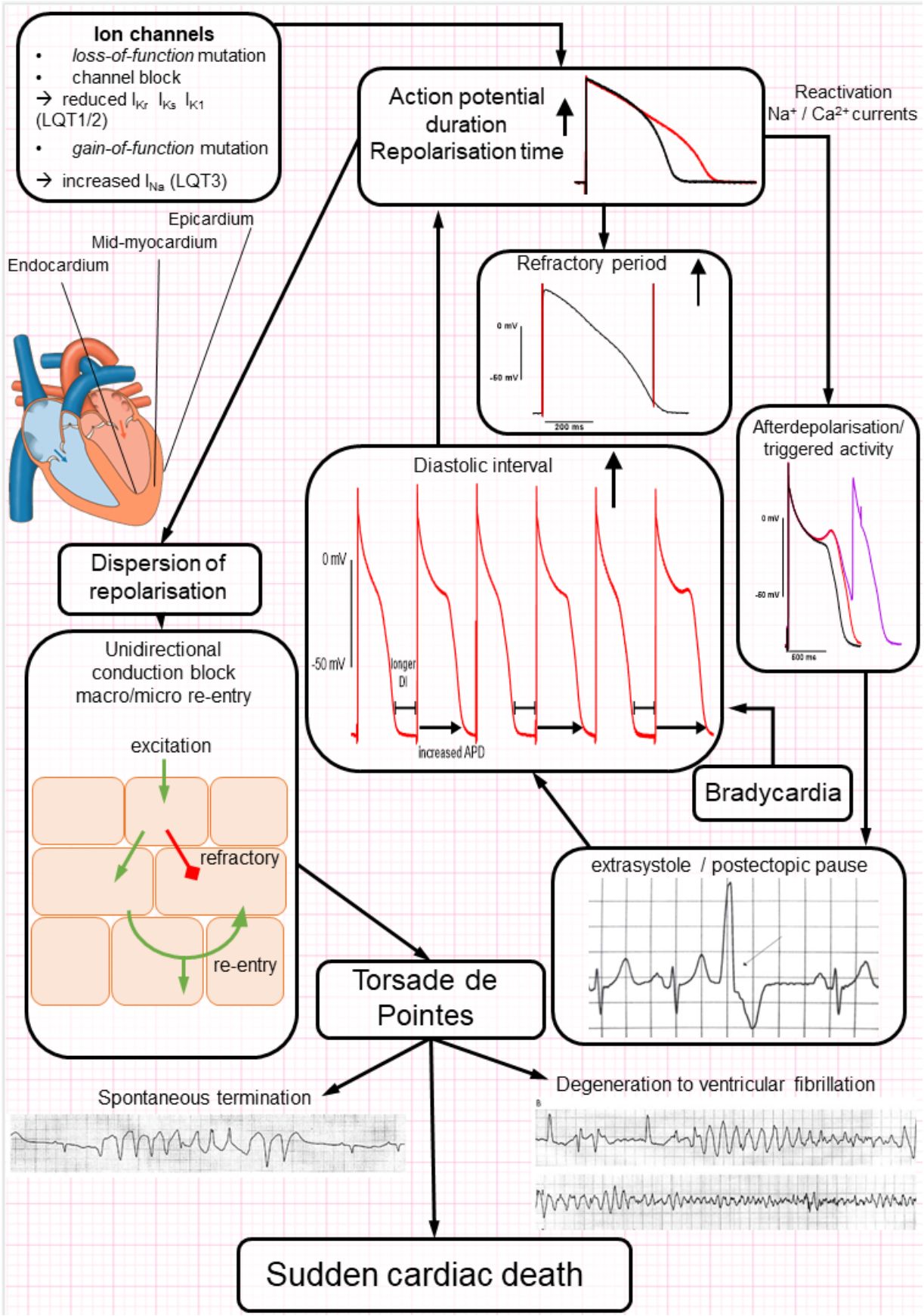

Figure 3. Schematic of mechanisms in arrhythmogenesis.

Interaction of factors that play into arrhythmogenesis escpecially in Long QT syndrome and Torsade-de-Pointe. (ECG elements modified from Yap and Camm 2003).

1.1.3 Specific electrical conduction system of the heart

In the human heart ejection of blood is synchronised by the simultaneous mechanical contraction of the myocardium in both ventricles. Origin of the electrical stimulus in the heart is the sinoatrial node in the high right atrium. These cells produce an automated activity and cyclical depolarisation of the membrane potential to start the conduction of APs throughout the atria. Since the myocardium works as a functional syncytium via the intercalated discs and gap junctions the electrical impulse spreads over the atrial muscle cells (as well as the internodal pathways) and causes their contraction. Atria and ventricles are electrically isolated from each other by the valvular apparatus and its fibrous non-conducting structures. Via the atrioventricular node near the coronary sinus the conduction is delayed and directed through the bundle of His towards the specific cardiac conduction system of the ventricles. These bundle branches propagate a much faster conduction and lead to a nearly simultaneous excitation of the myocardial ventricles via specialised cells called Purkinje fibres. The different cardiac cell's ion channel compositions and AP characteristics facilitate the proper function of the cardiac electro-mechanical-coupling.

A coordinated electrical excitation of the muscle is required in order not to develop suboptimal pumping function and ultimately heart failure. Coordination of excitation can be disrupted either by structural damage such as bundle branch blocks or by a cellular change of membrane currents leading to increased dispersion of repolarisation and excitation. AP prolongations because of ion channel blocks are the prime example of this, ischemia or inflammation may be other causes of cardiac electrophysiological malfunctions. Damage to different cardiac structures can cause a number of rhythm disturbances, including AVN blocks, bundle branch blocks, ventricular extrasystoles and ventricular tachycardia of multiple manifestations such as monomorphic VT or potentially lethal TdP and VF.

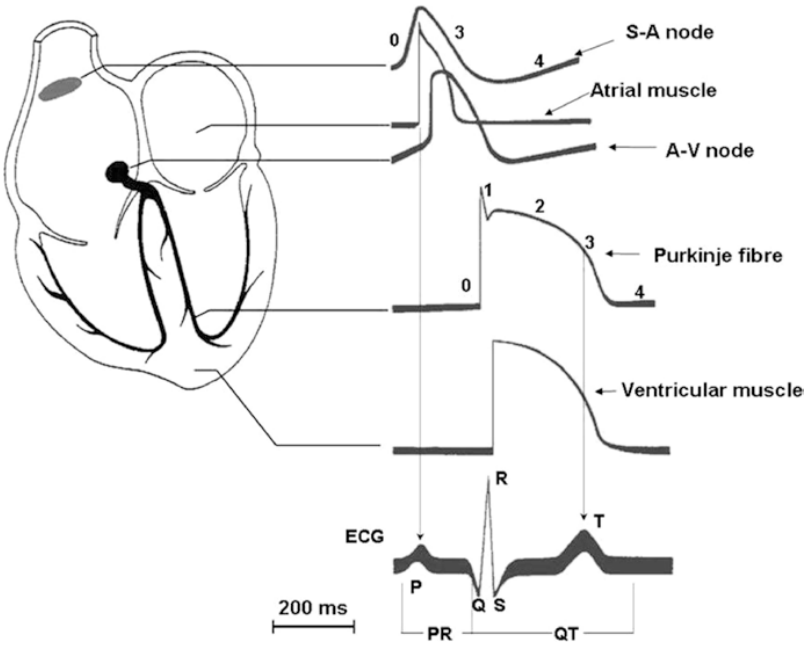

Figure 4. Specific cardiac conduction system.

Corresponding typical action potential waveforms with numbered action potential phases of different cell types and locations are represented in relation to the surface ECG (Jost et al 2015).

1.1.4 Long QT syndrome

Congenital LQTS is classified in different subsyndromes depending on the gene and ion channel affected. They overall share the prolongation of the cardiac AP and QT interval. The most common congenital LQTS forms (major forms) are LQT1 (40-55%), LQT2 (30-45%) and the less common LQT3 (5-10%). The other less common minor forms of the disease are rare with occurrence rates of <1% (Wallace et al. 2019).

In LQT1, a mutation of the gene KCNQ1 leads to a loss of function of the Kv7.1 protein, resulting in a reduced I_{Ks} potassium ion current conducted by the corresponding channel. During beta-adrenergic stimulation this current plays a bigger role for repolarisation in total. This becomes clinically important, since episodes of tachycardia and TdP tachyarrhythmia occur more often during physically or emotionally stressful situations (Goldenberg et al. 2012).

LQT2 presents with a mutation in the KCNH2 gene producing a smaller I_{Kr} K^+ outward current. I_{Kr} is also affected in most acquired forms of LQTS when it is caused by drugs interacting with the human ether-a-go-go related gene (*hERG*) channel. In this work the focus of most aspects is on the level of ion currents in the cell membrane, therefore discussion will mostly evolve around the term I_{Kr} (current). Other terms such as *hERG*-channel, LQT2, KCNH2 or K^+ might be used synonymously in certain situations. LQT2 patients have cardiac events predominantly in resting situations, e.g. during sleep, bradycardia or caused by sudden triggers such as

startling or emotional distress. This suggests a connection to arrhythmogenesis involved mechanisms connected with a long diastolic interval or postextrasystolic pauses. Arrhythmias during physical exercise are very rare in LQT2 (Tester and Ackerman 2011). Different than in LQT1 and 2, in LQT3 syndrome there is no mutation in a potassium channel gene, but in the SCN5A gene coding for the sodium ion channel. Also, it is not a loss- but a gain-of-function mutation leading to an increased Na^+ inward current during the initial phase 0 of the AP. This causes a higher influx of positive charged ions into the cell which leads to an increased repolarisation time as more cations have to be transported out to reach a repolarised membrane state again (Lemoine et al. 2011). Arrhythmic events are common during sleep, rarely also caused by stress or other triggers (Tester and Ackerman 2011).

More rare minor forms of LQTS mostly show reduced I_{Kr} or I_{Ks} as well and are often inherited in an autosomal dominant manner. But there are other factors leading to long AP in minor LQTS, e.g. caused by impaired I_{K1} (KCNJ2 mutation) or I_{KACh} current (KCNJ5), dysfunctional transport proteins (Ankyrin B) or calcium handling dysregulation (Calmodulin 1/2 or CACNA1C mutations) (Schwartz et al. 2013).

1.1.5 Drug-induced LQTS and safety pharmacology

In acquired LQTS APD prolongation is usually caused by the interaction of certain compounds with ion channels, mostly I_{Kr} which has the highest impact on repolarisation. When outwards K^+ channels are impaired the time for repolarising the membrane potential increases and the time window of the refractory period as well as reactivation window of depolarising channels gets wider. This APD and QT prolonging effect is seen in many different substance classes such as neuroleptics, antidepressants, antibiotics, antihistaminic drugs but also in antiarrhythmic substances with potential to block I_{Kr}, like sotalol or chinidine. A detailed list of substances can be found at https://www.crediblemeds.org/. Another important factor for interference with membrane currents is electrolyte balance. Especially low levels of potassium, magnesium and calcium increase arrhythmogenicity. Furthermore structural cardiac damage, intoxication and inflammation can lead to a more vulnerable tissue (Khan 2002).

Research of substances which are prone to cause a *hERG*-block or other interactions with ion channels is a central point in safety pharmacology. Different testing systems have been developed and used over the years in order to find proarrhythmic factors of substances and to use as a screening method before further clinical use of the drug is proposed. These include the use of rabbit and canine Purkinje fibres (Nattel and Quantz 1988; Lu et al. 2005; Jonsson et al. 2010), slices of myocardial tissue (Bussek et al. 2009), dissociated canine and human papillary muscle cells (Koncz et al. 2011), guinea pig single myocytes (Altomare et al. 2015), as well as human ventricular-like embryonic stem cell-derived cardiomyocytes (hESC-CMs)

(Jonsson et al. 2010). Other currents have been studied as well, such as I_{K1} and I_{Ks} in dog, rabbit and guinea pig cardiomyocytes, reporting much lower I_{Ks} and I_{K1} current densities in human compared to dogs (Jost et al. 2013). I_{Ks} current investigations find dog and rabbit ventricular tissue to be closer to human physiology than guinea pig but still incongruent (Heath and Terrar 1996; Salata et al. 1996).

All these models have the problem in common that they do not accurately represent the electrophysiological properties of the human heart. Only certain aspects such as channel function, single cell behaviour or tissue physiology can be compared with human *in vivo* data. Additionally, interspecies differences represent data in sometimes contradictory or unclear fashion which makes accurate predictions about human *in vivo* physiology even harder. The translation of animal models to human myocardium is often insufficient and lacks precision to come to a perfect conclusion. Stem cell derived cardiomyocytes have shown a higher sensitivity towards arrhythmogenicity than animal tissue assays from canine and rabbit Purkinje fibres (Peng et al. 2010).

In order to eliminate the error of the interspecies differences of the testing system a new method to produce human ventricular myocardial cells is introduced by hiPSC. This project is designed to find out if EHT from hiPSC-CM is superior to animal models and how it can be used to accurately compare to real human tissue. Another focus is to see if EHTs are an appropriate method to detect proarrhythmic potential of substances.

1.2 Human induced pluripotent stem cell derived cardiomyocytes and engineered heart tissue

In order to close the gap between common animal models for cell physiological research and real human tissue with the most accurate representation of *in vivo* systems we need flexible cell systems with a human genome. This eliminates at least most of the confounding factors that come up due to genetic ambivalence. In the best-case scenario it can reproduce an accurate human tissue similar in behaviour to actual samples from patients. Additionally, genetic disease modelling for diseases like channelopathies (LQTS, Brugada syndrome, short QT syndrome, catecholaminergic polymorphic ventricular tachycardia) and other genetic mutations in the heart can be achieved via this approach.

One viable method to reach this goal is the use of hiPSC, which can be developed into cardiomyocytes. In either commercially available cells or reprogrammed cells from a donor skin biopsy, a new genetic template can be induced for the cell to develop into. This creates genetically identical tissues to a defined organ system and can still be manipulated via methods like CRISPR-Cas9 DNA manipulation to suit individual needs of activated genes and can be

used for detailed biochemical and electrophysiological studies (Prondzynski et al. 2019). From these reprogrammed cells whole tissues of different organs can be formed with the right culture methods. In this project hiPSC-CM were used to produce engineered heart tissue, consisting of 70-97% troponin T positive ventricular cardiomyocytes and fibroblasts or stromal cells for connective tissue structure and form (Breckwoldt et al. 2017).

The goal of this dissertation is to do electrophysiological experiments and measurements on these EHTs to figure out how exactly they compare to human myocardial tissue under equal baseline conditions with regard to cellular electrophysiology and arrhythmia. Furthermore, their use for research in safety pharmacology is examined to find out how well hiPSC-CM EHTs can be used to study proarrhythmic substances and conditions, especially concerning repolarisation impairment and APD prolongation. For this purpose, human LV myocardium tissue samples are compared to *in vitro* generated EHT from hiPSC-CM to examine their specific physiological properties.

1.3 Presentation of the problem and hypothesis

In the context of safety pharmacology, all compounds are tested for potential ion channel blocking effects. Repolarising potassium channels of the cardiac AP (I_{Kr}, I_{Ks}, I_{K1}) are of interest in this regard, since AP prolongation is associated with life threatening arrhythmias.

Nowadays the effect on a single ion channel can be monitored very effectively in expression systems. To identify the total effect of a blocked channel on repolarisation, action potential measurements are necessary though. Since human cardiac tissue is only available to a rather limited extent these measurements are usually done in animal models. There are substantial interspecies differences in individual contribution of each ion current to total repolarisation (repolarisation reserve). It is expected that human induced pluripotent stem cell cardiomyocytes (hiPSC-CM) are able to close this gap, but thus far the repolarisation reserve of hiPSC-CM is not characterised yet.

In this project, the repolarisation reserve of hiPSC-CM will be compared to that of human ventricular tissue to answer some questions: Are hiPSC-CM suitable to represent the repolarisation reserve of human ventricle better than animal tissue? Is hiPSC-CM engineered heart tissue an appropriate system to model arrhythmia relevant ion channel assays? What predictions and prognosis can be made using EHT? Where lie the biggest advantages and most concerning disadvantages of the model?

2 Materials and methods

This chapter will describe the materials and methods that were used in this project. First the utilised materials are listed and described, then the execution of the measurements will be explained.

2.1 Materials

2.1.1 Tissue samples

2.1.1.1 Human left ventricular tissue

The human myocardial ventricular tissue samples were provided by the University Heart Centre's department of cardiovascular surgery. The study followed the declaration of Helsinki and all patients gave written informed consent. Local ethics committee approved the study protocol (permit number PV3759). Samples from patients with terminal heart failure, as well as samples from patients with valvular heart disease and hypertrophic cardiomyopathy were used. The heart failure group was composed of patients who underwent heart transplantation (HTX) or left ventricular assist device (LVAD) implantation. The former group's samples were obtained from the ventricular trabeculae, the latter one's was from the implantation site of the device in the left ventricular apex.

The other patient's samples were parts of the interventricular septum, which were excised during myectomy of hypertrophic cardiomyopathy (HCM) or valve reconstruction due to valvular aortic stenosis (AS) or aortic insufficiency (AI). The excisional tissue was then stored in cardioplegic transport solution (see table 2) and transported to the laboratory.

Macroscopic preparation of up to 0.5 cm long trabeculae was performed in a petri dish (Nunclon Delta). The samples were then placed in the silicone recording chamber and perfused with Tyrode's solution for at least 30 minutes to wash out the transport solution.

2.1.1.2 Engineered heart tissue

Engineered heart tissues (EHT) were produced and provided by Ingra Mannhardt, Maksymilian Prondzynski, Marta Lemme, Umber Saleem, Bärbel Ulmer and Mirja Schulze (all IEPT, UKE). The human induced pluripotent stem cell cardiomyocytes (hiPSC-CM) in this project were developed from three different cell lines: two house internal cell lines ERC018 (differentiated from a healthy subject's skin fibroblasts using the CytoTune™-iPS Sendai Reprogramming Kit, Thermo Fisher Scientific) and C25 (undifferentiated hiPSC gifted by Alessandra Moretti,

Munich Germany) as well as one commercially available one by Cellular Dynamics International (iCell² cell line).

Cell culture, mesoderm induction, cardiac differentiation and EHT generation, development and cultivation were performed as previously described by a group from the institute of experimental pharmacology and toxicology (Breckwoldt et al. 2017).

Briefly summarised, the hiPSC cell lines were differentiated to cardiomyocytes using specific growth factors and from these hiPSC-cardiomyocytes (hiPSC-CM) engineered heart tissue samples were produced. In agarose casting moulds EHTs with 10^6 hiPSC-CM each, formed around silicone/PDMS posts in a fibrin matrix. In culture conditions of 37°C, 7% CO_2, 40% O_2 and 90% humidity EHTs were incubated in a culture medium of Dulbecco's Modified Eagle Medium (DMEM, Gibco), 10% heat-inactivated horse serum (Thermo Fisher scientific, Gibco 26050), 1% penicillin/streptomycin (Thermo Fisher scientific, Gibco), insulin (Sigma-Aldrich) and aprotinin (Sigma-Aldrich) which was changed three times per week. Around two weeks after moulding EHTs started auxotonic contraction on the flexible silicone racks and were used for electrophysiological measurements from day 25 to 100. A more detailed description and operating instruction can be found in the publication by Breckwoldt et al. (2017).

2.1.2 Solutions

2.1.2.1 Tyrode's solution

For perfusion during the experiment and washout of transport medium, Tyrode's solution composed of ion concentrations in table 1 was used. In addition to the standard solution a modified Tyrode's solution with a lower potassium ion concentration of 2.7 mmol/L and 133.3 mmol/L Cl^- was used in order to generate a more arrhythmogenic ion homeostasis and provoke early afterdepolarisations in human left ventricular tissue (Zaza 2009).

Table 1. Tyrode's solution composition. Ion concentrations of different Tyrode's solutions and stock solutions used for preparing.

Compound	Manufacturer	Standard Tyrode's Concentration (mmol/L)	Modified Tyrode's Concentration (mmol/L)	Tyrode's solution Stock A (g/2L H_2O)	Tyrode's solution Stock B (g/2L H_2O)
NaCl	Roth	136.0	133.3	296.17	
KCl	Sigma	5.40	2.70	16.10	
MgCl H_2O	Merck	1.00	1.00	8.54	
NaH_2PO_4	Merck	0.42	0.42		2.32
$NaHCO_3$	Merck	22.0	22.0		73.93
$CaCl_2$	Roth	1.80	1.80	10.59	
pH	Adjusted with Mettler Toledo pH meter	7.40	7.40		

A fresh solution was prepared from two Tyrode's Stock solutions (A & B) every week. 100 ml of each stock solution were diluted up with distilled water to a total volume of 2 litres and 2 g glucose were added. Addition of stock solutions and glucose was done under constant centrifugal mixing via a magnetic stirrer.

2.1.2.2 Glass pipette electrode solution

The KCl solution inside of the glass electrode used for the sharp microelectrode method had a concentration of 3 mol/L. It was filled up using a standard intravenous cannula or thin filament cannula on a 2 mL syringe. The glass electrode was then de-aired of bubbles in the tip by slightly tapping it from the side without damaging the sharp intracellular edge. This allowed proper conduction of electric current from the measuring end to the wire electrode inside the glass pipette.

2.1.2.3 Transport solution

Human myocardial tissue samples were transported from the operating theatre to the laboratory in a special cardioplegic Ca^{2+}-free transport solution at 20–25 °C. The substance composition is noted in table 2. Before the start of an experiment tissue samples were superfused with Tyrodes's solution at 36.5±0.5 °C for at least 30 minutes to wash out the high potassium cardioplegic transport solution. The cardioplegic state of the system allows for a maximised survival time of tissue in the low oxygen supply liquid solution, by stopping the energy consuming aerobic processes of the tissue.

Table 2. Transport solution composition.

Compound	Manufacturer	Ca^{2+}-free transport solution (mmol/L)
NaCl	Roth	100.0
KCl	Sigma	10.0
KH_2PO_4	Merck	1.20
$MgSO_4$	Merck	5.0
Taurin	Merck	50.0
MOPS	Sigma	5.0
Butanedionemonoxime (BDM)	Sigma	30.0
pH		7.0
Temperature		20-25°C

2.1.2.4 Nutrient medium for engineered heart tissue

The nutrient medium used during conservation and culture of EHTs consisted of DMEM, 1% penicillin/streptomycin, 10% horse serum, 10 mg/ml insulin, and 33 mg/ml aprotinin. Culture medium was changed on Mondays, Wednesdays, and Fridays by filling fresh solution in wells next to the EHT containing wells and switching the racks over with minimal time outside of the medium.

2.1.3 Drugs and substances

2.1.3.1 E-4031

E-4031 is a specific blocker of the *hERG*-type potassium channel Kv11.1 which conducts the rapidly activating delayed rectifier potassium (K^+) current (I_{Kr}) (Sanguinetti 1992; Nerbonne and Kass 2005). It is a synthesised methanesulfonalidine that binds to a target structure in the open *hERG*-Channel with an IC_{50} of 10 nmol/L (Spector et al. 1996; Weinsberg et al. 1997). The hydrophobic aromatic groups of many *hERG*-blockers such as E-4031, amiodarone, terfenadine, or propafenone are known to bind to the aromatic residues of the S6 helix in the inner cavity of the channel once it has opened (Vandenberg et al. 2012). The blocked channel will then be unable to allow potassium ions to pass through the membrane to contribute to the rectifying current. Since I_{Kr} is the biggest contributor to outward potassium currents in the late phase of the human ventricular cardiac AP, its inhibition delays repolarisation tremendously. AP prolongation may lead to early afterdepolarisations, heterogeneity of repolarisation and subsequently to LQTS (Roden and Viswanathan 2005). For the following experiments E-4031 by manufacturer Tocris (1808, 1 mmol/L in distilled water) was used.

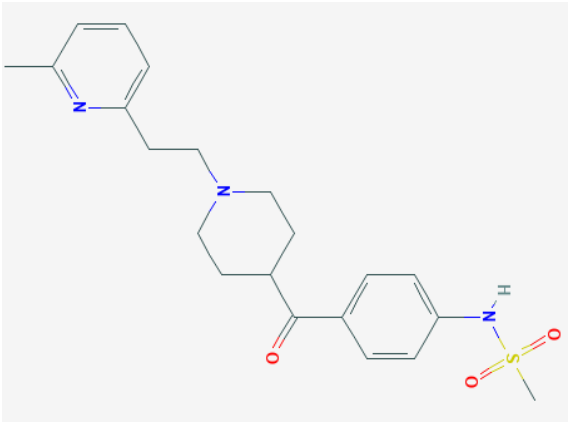

Figure 5. Structural formula of E-4031.

(PubChem CID: 3087190, 2D-structure) E-4031 is a class III antiarrhythmic drug exclusively used for research as it counterintuitively also produces proarrhythmic effects like QTc prolongation (Okada et al. 1996).

2.1.3.2 HMR-1556

Just as E-4031 is a specific blocker for the rapid delayed rectifier current, HMR-1556 acts as a specific blocker of the slowly activating delayed rectifier potassium current (I_{Ks}), which contributes to the repolarisation of the cardiac AP as well (Thomas et al. 2003). Therefore, the mechanism of arrhythmogenicity is explained the same way Long QT Syndrome 1 and 5 are, which is via AP prolongation and the risk of TdP tachyarrhythmia (Sanguinetti et al. 1996). HMR-1556 is a chromanol derivate with a higher potency and specifity for I_{Ks} inhibition than its predecessors presenting with an IC_{50} of 10.5 nmol/L in canine ventricle (Thomas et al. 2003). Higher concentrations in the 10-30 micromolar range showed to have an inhibitory effect on I_{Kr}, the transient outward current (I_{to}), and L-type calcium channels (I_{CaL}) although not on the inward rectifier current (I_{K1}) (Thomas et al. 2003). The substance used in this project is HMR-1556 by manufacturer: Tocris, 5011, 10 mmol/L in 100% DMSO.

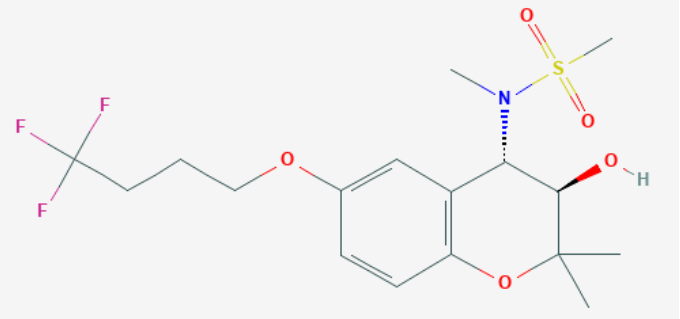

Figure 6. Structural formula of HMR-1556.

(PubChem CID: 9887834, 2D-structure) The I_{Ks} blocking drug HMR-1556 has been used in many electrophysiological studies. Especially its role in LQTS and β-AR modified activity are of interest.

2.1.3.3 Barium chloride

In this project $BaCl_2$ was used to block channels of the $K_{ir}2.x$ family (genetically coded by *KCNJX*) responsible for the repolarising inward rectifier potassium current (I_{K1}). The I_{K1} current primarily stabilises the resting membrane potential but also contributes to the final repolarisation of the cardiac AP (Dhamoon and Jalife 2005). When Ba^{2+} enters the channel it strongly binds to the potassium selectivity filter, causing a blockade of the current. The IC_{50} barium to block the different $K_{ir}2.x$ subfamily members varies between 0.15 – 30 µmol/L ($K_{ir}2.1$), 6-40 µmol/L ($K_{ir}2.2$), 13 µmol/L ($K_{ir}2.3$) and 755 - 792 µmol/L ($K_{ir}2.4$) (Bhoelan et al. 2014; Horváth et al. 2018).

Dysfunction of the $K_{ir}2.1$ caused by channelopathy due to mutations of the KCNJ genes are linked to Andersen's syndrome (LQT7) which involves arrhythmias and the proarrhythmic Short QT Syndrome (Tristani-Firouzi and Tawil).

2.1.3.4 Ivabradine

Ivabradine is a specific inhibitor of the hyperpolarisation-activated cyclic nucleotide–gated channels (HCN) conducting the *funny current* (I_f) which is also described as the pacemaker current and is considered to be the characterising current of spontaneously active cardiac cells such as the sinoatrial node (SAN), atrioventricular node (AVN) and Purkinje fibres. Its specific property presents as an inward current of cations activated by hyperpolarisation in a voltage range of -70 to -40 mV. This contributes to a cyclic activation following the repolarisation of the AP and initiating the upstroke of the voltage gated sodium channels (DiFrancesco and Ojeda 1980; DiFrancesco 1993). Another trait of the *funny current* is that it is activated by cyclic nucleotides such as cyclic adenosine monophosphate (cAMP) that bind directly to the channel and shift the activation curve to less negative voltage. Sympathetic stimulation raises cAMP levels, thereby generating current even at not so negative voltages, increases steepness of diastolic depolarisation and consequently heart rate (DiFrancesco and Tortora 1991).

HCN channels have four isotypes and belong to the family of voltage-dependent K+ (Kv) channels and cyclic nucleotide gated (CGN) channels. Ivabradine's binding-unbinding reactions are restricted to the open state of the channel and the molecule blocks it more efficiently from the intracellular side due to its positively charged quaternary ammonium ion and current-dependency (Baruscotti et al. 2005).

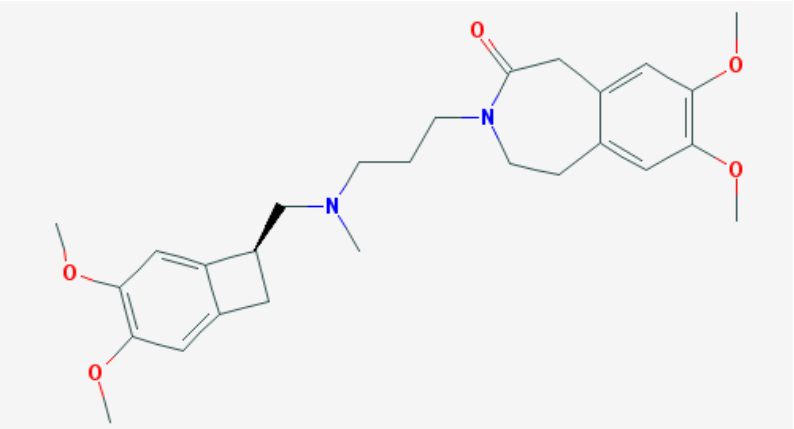

Figure 7. Structural formula of ivabradine.

(PubChem CID: 132999, 2D-structure) The compound ivabradine is a substance used to treat patients with stable chronic heart failure and reduced ejection fraction (HFrEF) not sufficiently treated with beta blockers and a higher than 70 bpm heart rate. The benefit lies in reducing hospitalisation rate, as it slows down the heart rate (Shen et al. 2017).

2.1.3.5 Isoprenaline

Isoprenaline is a selective β-adrenergic receptor (β-AR) agonist. Chemically it is closely related to adrenaline, as it is a synthetic isopropyl analogue. However, it does not activate α-

adrenergic receptors. Following activating of β-AR the intracellular adenylyl cyclase converts adenosine triphosphate to cyclic adenosine monophosphate. In activating β_2 adrenoceptors it causes vascular and bronchiolar smooth muscle cell relaxation. In the human heart both β_1 and β_2 -AR mediate positive chronotrope and inotrope effects of catecholamines and thereby increase cardiac output.

The drug is therefore used in patients for treatment of bradycardia, atrioventricular heart block and in emergency situations before pacemaker therapy can initiated. In addition, isoprenaline was used as a relief of obstructive bronchospasms in asthma or chronic bronchitis. Another use is in cardiac shock situations because of low cardiac output, like in acute congestive heart failure.

In this project isoprenaline by supplier Sigma Aldrich was used for activation of an adrenergic stimulus in a concentration of 100 nmol/L to specifically target myocardial β-receptors. The following cAMP increase and activation of protein kinase A phosphorylation of *KCNQ1*

subunit of the I_{Ks} channel protein cause an increase in I_{Ks} current. This is important since slow delayed rectifier potassium current in humans and several animal models, is not a major contributor to repolarisation, unless there is β-adrenergic stimulation or simultaneous block of other outward currents like I_{Kr} present (Stengl et al. 2003). Isoprenaline was used to increase the effect of I_{Ks} and thereby to provoke arrhythmogenesis in LV tissue in an attempt to unmask the contribution of I_{Ks} to human repolarisation reserve (Jost et al. 2005; Li et al. 2019).

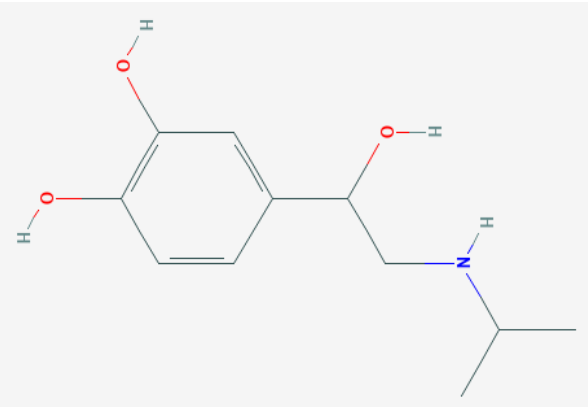

Figure 8. Structural formula of isoprenaline.

(PubChem CID: 3779, 2D-structure) The β-adrenoceptor agonist isoprenaline is used to stimulate tissues and cells via the signalling pathway activated in sympathetic activation by catecholamines like adrenaline.

2.1.3.6 Moxifloxacin

Moxifloxacin is an antibiotic drug from the group of fluoroquinolones, commonly used in treatment of bacterial infections of the gram-positive and anaerobic spectrum. Typical applications are acute exacerbation of chronic bronchitis or chronic obstructive pulmonary disease, sinusitis, pneumonia, skin infections, diabetic foot syndrome as well as infections with germs like legionella or mycoplasma. The mechanism of action is a bactericidal inhibition of gyrase enzymes, which are responsible for untwisting bacterial DNA for replication. Drug interactions can occur when combined with NSAID, causing tendon damage or in use with vitamin-K antagonists, causing INR variations of the coagulation system. A rare, but serious side effect can be severe liver injury. Notable is the tendency to prolong QT interval in patients treated with moxifloxacin. However, although an inhibition of *hERG*-channels has been shown, the compound rarely did lead to development of TdP *in vivo*. Therefore, the agent is frequently used in preclinical research to test for false positive results. Still, the combination with other QT-prolonging factors or drugs should be avoided (National Center for Biotechnology Information 2020, Pubchem CID:152946).

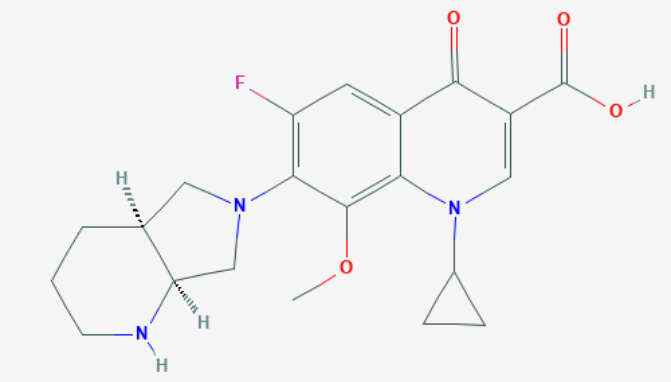

Figure 9. Structural formula of moxifloxacin.

(PubChem CID:152946, 2D-structure) Moxifloxacin is a fluoroquinolone antibiotic used in a broad spectrum of bacterial infections, but it may also cause QT prolongation.

2.1.3.7 Verapamil

Verapamil is an agent with calcium channel blocking properties, used to inhibit the influx of Ca^{2+} in myocardial and vascular smooth muscle cells. This leads to vasodilatation, slowed sinus node rate, and AV conduction but also weakens myocardial contractility. It is therefore predominantly used in treatment of hypertension and angina pectoris in coronary artery disease and hypertrophic obstructive cardiomyopathy. Verapamil is also effective in supraventricular tachycardia due to its negative dromotropic effect on excitation conduction on the AV node. As a non-dihydropyridine it is eponymous for the group of verapamil-type calcium channel blockers. Typical adverse effects occur especially in combination with other

cardiodepressive drugs such as betablockers and include bradycardia, AVN-blockade, hypotension, and low cardiac output. Other side effects are cephalgia or vertigo. An inhibition of CYP3A4 enzymes can cause further potential drug interactions. The compound also blocks I_{Kr}, however, there is no dangerous increase in APD or QT interval leading to potential arrhythmias (National Center for Biotechnology Information 2020, Pubchem CID: 2520).

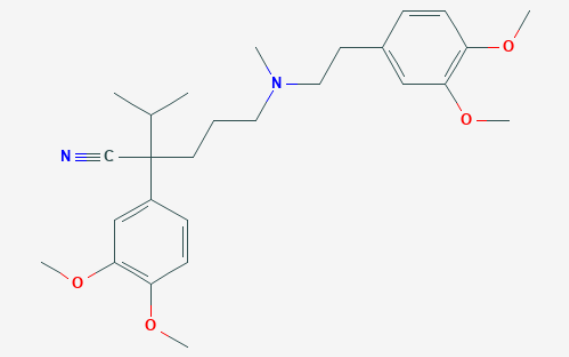

Figure 10. Structural formula of verapamil.

(PubChem CID: 2520, 2D-structure) The calcium channel blocker verapamil is usually used in treatment of hypertension and angina pectoris due to its blood vessel dilating effects or in supraventricular tachycardia because of its negative chronotropic and dromotropic effect.

2.1.3.8 SEA0400

The sodium-calcium exchanger (NCX) is a membrane protein that functions as an electrogenic antiporter of Na^+ and Ca^{2+} ions, transporting one calcium ion in exchange for three sodium ions. It plays a major role in cardiac Ca^{2+} balance and regulation of membrane voltage. The aniline derivate SEA0400 selectively blocks the NCX with a high potency in human atrial CM (-log EC_{50} 6.77 mol/L Christ et al. 2016). At higher concentrations (3 µmol/L) block of other channels such as the L-type Ca^{2+} channel was reported (Tanaka et al. 2002; Birinyi et al. 2005). In human atrial cardiomyocytes even 10 µmol/L SEA0400 did not block L-type Ca^{2+} channels (unpublished observation Christ).

At voltages close to the resting membrane potential NCX allows extracellular Na^+ to enter the cell and Ca^{2+} is transported out (“forward mode”). This contributes to the reduction of intracellular Ca^{2+} alongside with the reuptake of Ca^{2+} into the sarcoplasmic reticulum (SR) via the SR-Ca2+-ATPase (SERCA). Other mechanisms that bring Ca^{2+} back to low levels are the uptake into mitochondrial calcium storage and the extrusion via plasma membrane Ca^{2+} ATPase. After the initial AP upstroke when Na^+ has entered the cell, the NCX works in the opposite direction and transports Na^+ out of the cell while taking up Ca^{2+} back into the cell. This switch from “forward” into “reverse mode” only lasts a short time though, before calcium

triggered calcium release from the SR increases intracellular Ca^{2+} again, turning the NCX back into depolarising “forward mode” (Bers 2002; Santulli et al. 2015).

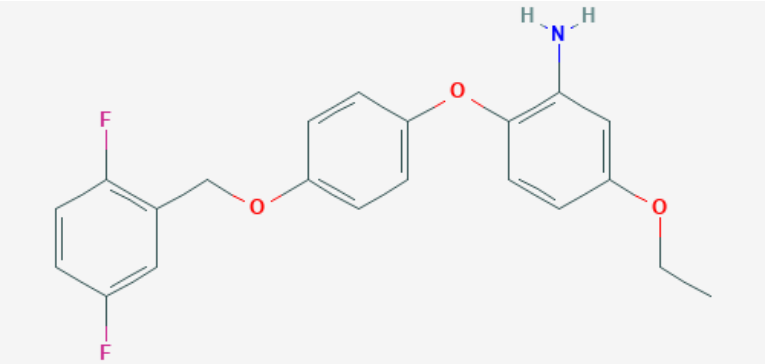

Figure 11. Structural formula of SEA0400.

(PubChem CID: 644100, 2D-structure) The selective NCX blocking aniline derivate SEA0400.

2.1.4 Equipment and tools

Table 3. Devices used in the experimental setup. Manufacturer of the device and brief description of its use and function are listed.

Device	Product name/ manufacturer	Description
Stimulator	UHS20 Biotronik, Berlin Germany	Adjustment of frequency and stimulation protocols in electrophysiology
Pre-amp headstage	npi electronic, Tamm, Germany	Connection from glass electrode holder to electrode amplifier, connection to grounding electrode
Amplifier	BA 1S/BA-01X, npi electronic, Tamm, Germany	Electrode amplifier for increasing measured signal leading into analogue-digital converter
Stimulator	SD9 Stimulator Grass Product Group, West Warwick, USA	Device sending out stimulation signal to stimulation electrode in recording chamber
A-D converter	ADInstruments Model ML 826 Powerlab 2/26, Dunedin, New Zealand	Conversion of analogue electric signal into digital output for computation in measuring software
Position Micromanipulator	MM-3, Narishige group, Tokyo, Japan	Three axis cogwheel-micromanipulator for general placement of measuring electrode
Impalement Micromanipulator	MMO-203, Narishige group, Tokyo, Japan	Hydraulic micromanipulator for gentle impalement of the tissue
Heating system	Lohmann Research Equipment LTR-2 P.I.D. Temperature Controller, Dortmund, Germany	Passage heating system of thin tubing in water bath with high surface area
Rolling pump	Ismatec Rolling Pump, Wertheim, Germany	Standard rolling pump system creating forward and/or backwards flow in tubes
Silicone bath	Lohmann Research, Dortmund, Germany	Soft silicone chamber for fixating tissues with needles
Glass electrodes	HILG1103227; Hilgenberg, Malsfeld, Germany	Borosilicate glass pipettes (external diameter 1.5 mm, internal diameter 0.87 mm)
Electrode puller	Zeitz DMZ-Universal Puller, Munich, Germany	Mechanical heating and pulling device creating fine glass electrode tips
Faraday cage	custom build	Aluminium cage surrounding the whole setup to isolate electromagnetically
Microscope	Olympus SZ61 SZ-STB1 zoom stereo microscope, Tokyo, Japan	Optical microscope for easier placement of the tissue and electrodes

2.2 Methods

2.2.1 Sharp microelectrode technique

2.2.1.1 General concept of the method

The first intracellular action potential in animal tissue was measured in a giant squid axon in 1939 by Hodgkin and Huxley. A sharp hollow glass pipette filled with sea water (electrically connected via a silver wire) was inserted in the tissue and a second reference electrode was placed outside the axon (Hodgkin and Huxley 1939). For their discoveries concerning the ionic mechanisms involved in excitation and inhibition in nerve cells Hodgkin, Eccles and Huxley were awarded with the Nobel Prize in Physiology or Medicine in 1963. In 1949 Ling and Gerard expanded on previous intracellular recordings by developing pulled glass microelectrodes with a sharp tip that could penetrate the cell with little damage (Brette and Destexhe 2012). Breakthroughs in cardiac cellular electrophysiology were particularly achieved by Weidmann in the 1950's and 60's. He first described many of the crucial underlying cardiac action potential characteristics relevant to this day, such as the initial fast sodium upstroke, resting membrane potentials, voltage clamp methods and gap junctions in Purkinje fibres even before modern utility like structural analysis was available (Niggli et al. 2006).

This sharp electrode technique is the method of choice in this project as it is a viable way of recording many sequential action potentials in live contracting tissue at stable conditions over several hours. At the same time, it is possible to stimulate the tissue electrically to provoke contractions and thereby control the beating frequency of the system. At the same time, it is possible to apply pharmacological compounds and to wash them out again. Another advantage is that intracellular homeostasis is untouched and ion channels are not affected by enzymatic dissociation. Generally, the technique is quite simple yet elegant and easy to learn. Since the tip is very thin there is no dialysis of the cell and the electric resistance is very high (25 – 125 MΩ). Though, a disadvantage of the method is that the seal between the tip and the cell is not as tight as it is when using other methods such as patch clamp. This can lead to high noise in the signal and possibly have effects on linearity and predictability of the experiment. Overall the experimental setup is similar to previously described methods and setups used in electrophysiological research (Wettwer et al. 2004).

2.2.1.2 Setup

The measuring setup, along with a schematic depiction of intracellular impalement is shown in the figure below. It shows a general depiction of the chamber and the containing instruments as well as zoomed in sections of the cell impalement and the stimulation electrodes and a side view cross section of the recording chamber itself. Different key parts of the setup will be explained in further detail below.

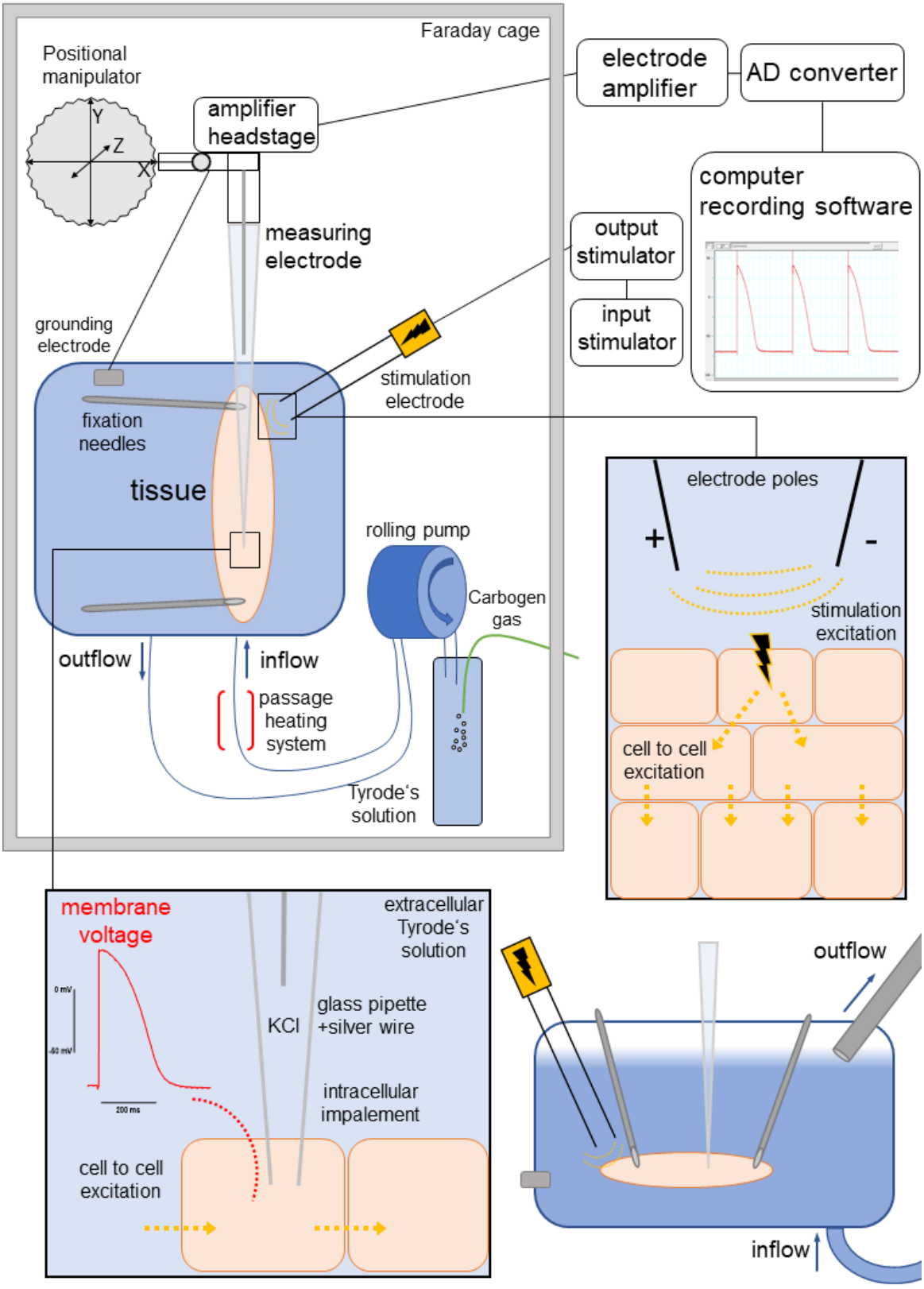

Figure 12. Schematic representation of the measuring setup.

Shown is the recording chamber inside the Faraday cage with the fixated tissue being impaled by the measuring electrode and stimulated by the stimulation electrode. Outside the cage the different electric devices for acquiring the data are pictured. The inset zoom-ins show the excitation process during stimulation (right) and the impalement of the glass pipette (bottom).

2.1.2.3 Electrodes

The sharp microelectrodes used to measure action potentials were manufactured from 1.5 mm diameter hollow borosilicate glass tube pipettes (Hilgenberg), which were inserted in the microelectrode puller (DMZ-Universal Puller Zeitz), heated to 285° C in the centre and pulled apart. During this process, the middle part thins, stretches and ultimately breaks apart, resulting in two sharp electrodes with a tip diameter down to 0.2 µm which results in an electric resistance up to 100 MΩ.

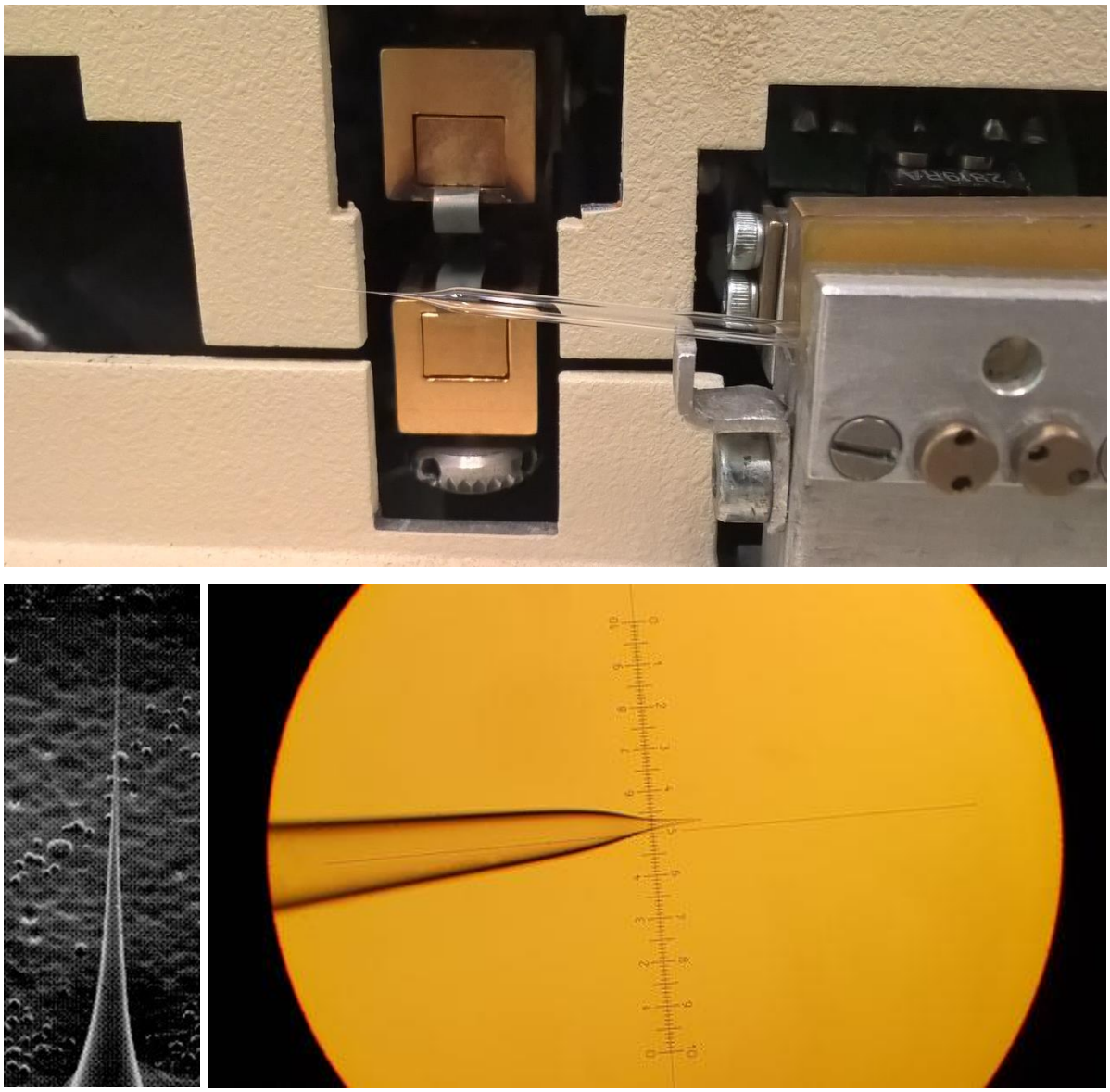

Figure 13. Sharp microelectrode glass pipettes.

Sharp microelectrodes produced using DMZ-Universal Puller Zeitz (top, original photograph), taken with scanning electron microscope (bottom left) and through light microscope in 100 times magnification (bottom right, bottom images provided by electrode puller manufacturer Zeitz).

The glass pipettes were then filled with a 3 mol/L KCl solution, which in combination with the chlorinated silver wire acts as the electrode. Electron exchange conducts in the following reaction: $Cl^- + Ag \leftrightarrow AgCl + e^-$

2.1.2.4 Amplifier and AD converter

The measuring electrode (mounted on the micromanipulator used for movement in three axis directions) was connected to a pre-amplifier, which then connected to the amplifier. This headstage was used for several things. Signals were so small that they need to be amplified before they were sent to the amplifier. The amplifier could also be used to apply an additional electric “buzz” stimulus with a set duration for readjusting or capturing a good signal in the tissue. In many instances this stimulus could get rid of slight deterioration of the signal or movement artefacts in the signal.

The A-D converter (Powerlab 2/26 AD Instruments) was connected to the amplifier to translate the analogue signal into a digital one to be processed by the computer software Lab-Chart (ADInstruments, Spechbach, Germany).

Figure 14. Amplifier for signal increase of voltage.

Amplification settings for the measured voltage, ZIP stimulus duration, capacity compensation, offset adjustment and the display indicating electrode resistance.

2.1.2.5 Table and cage

The whole setup was placed in a faraday cage made of aluminium to provide isolation of external electromagnetic disturbances. The operational devices were resting on a gas cushion buffered table (Science Products, Hofheim, Germany) that minimised mechanical movement interference from the outside.

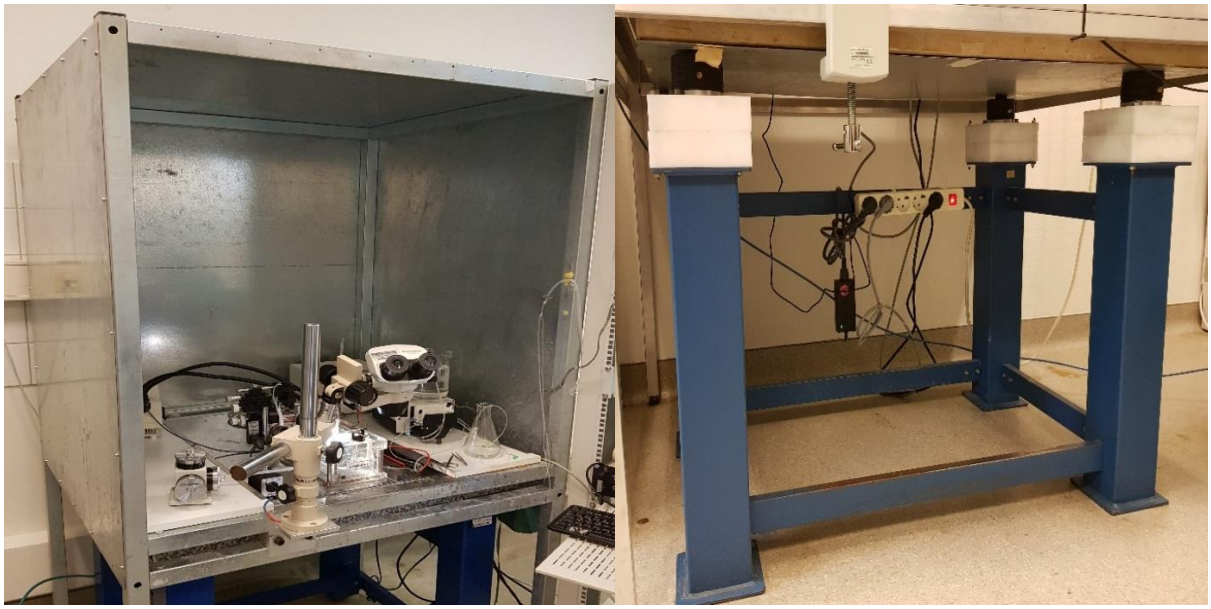

Figure 15. Table and Faraday cage setup.

Aluminium cage for electric isolation from outside interference (left) and air cushion-buffered table for prevention of mechanical tremors affecting the measurement (right).

2.1.2.6 Positional manipulators

Movement of the measuring electrode was performed with a mechanical gear wheel micromanipulator bringing the microelectrode into general position. The fine adjustment and impalement of the tissue was done with the hydraulic micromanipulator (Narishige MO-203).

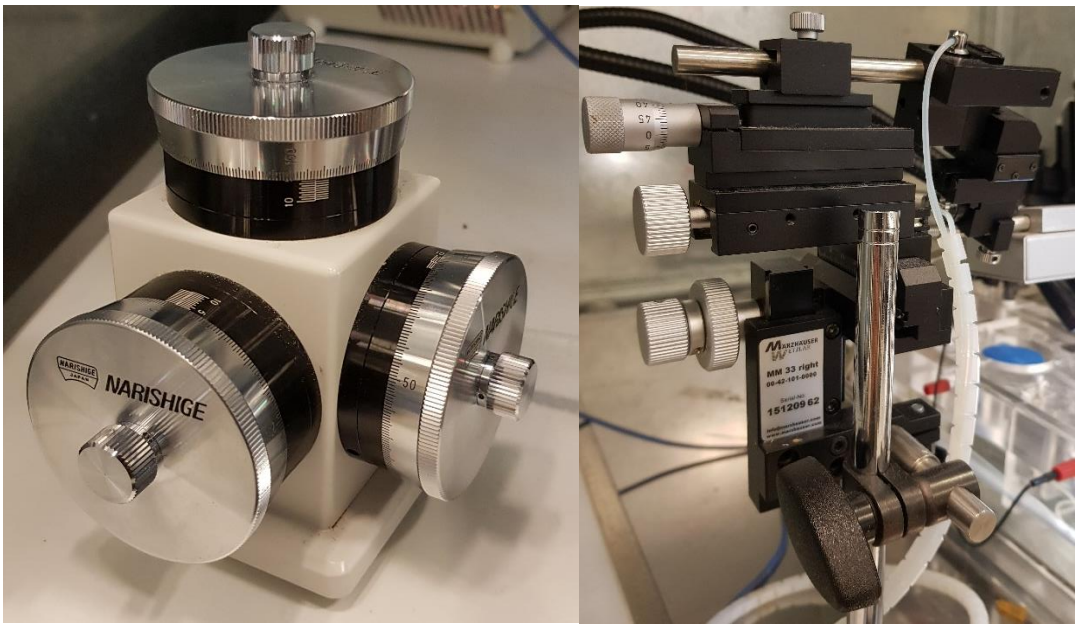

Figure 16. Positional manipulators for the measuring electrode.

Micromanipulators used for fine movement of the glass pipette microelectrode consisting of hydraulic three axis wheel manipulator (left) and stand mounted cogwheel manipulator for general positioning in the setup (right).

2.1.2.7 Chamber and pump system

The 2 cm diameter silicon bath chamber in which the tissue samples were placed, was connected via rubber tubes leading through the heating system (Lohmann Research Equipment LTR-2 P.I.D.) to bring the perfused solutions to a physiological temperature of 36.5°C. The tubing system consisted of a suction for the source of the solution, leading though a roller pump (Ismatec) into the heating water bath and into the tissue chamber. From there a suction is manually placed at the upper rim of the chamber pumping the solution into a waste repository. In order to recycle the solution, for example to maintain the same volume in the system to administer drugs, the waste tube was placed inside the source solution vessel. For source and waste vessels standard Erlenmeyer flasks or measuring cylinders were used. Gas tubes providing carbogen gas were placed inside the source vessel as well to provide oxygenation and pH adjustment.

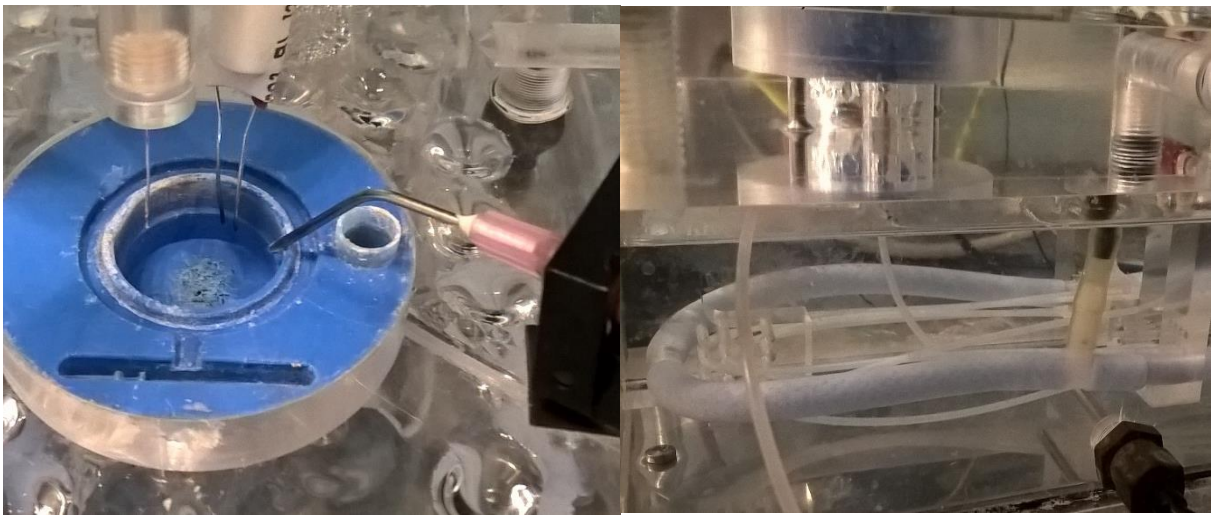

Figure 17. Chamber setup and heating water bath system.

The left picture shows the empty silicone chamber with suction cannula on the right rim, stimulation electrode fork and measuring electrode. In the right picture the chamber is visible from the side above the water bath heating system through which the tubing system leads to the chamber from below.

2.1.2.8 Stimulator

Tissue stimulation was controlled via two different stimulators which were serially connected to a platinum wire stimulation fork in the recording chamber. The first UHS20 Biotronik stimulator (originally a stimulator from a clinical electrophysiological laboratory setting) was used to adjust frequency and to allow complex stimulation protocols. The output signal was used to trigger a second stimulator (SD9 Stimulator Grass Product Group). Stimulation voltage was always set 50% over stimulation threshold at an impulse duration of 0.5 ms (unipolar field-stimulation). From the second device a connection led to the stimulation fork placed in proximity to the tissue in a way that the electrical field between both electrode poles was able to excite the electrically coupled cardiomyocytes. This stimulation fork was also position adjustable via a three-dimensional cogwheel micromanipulator.

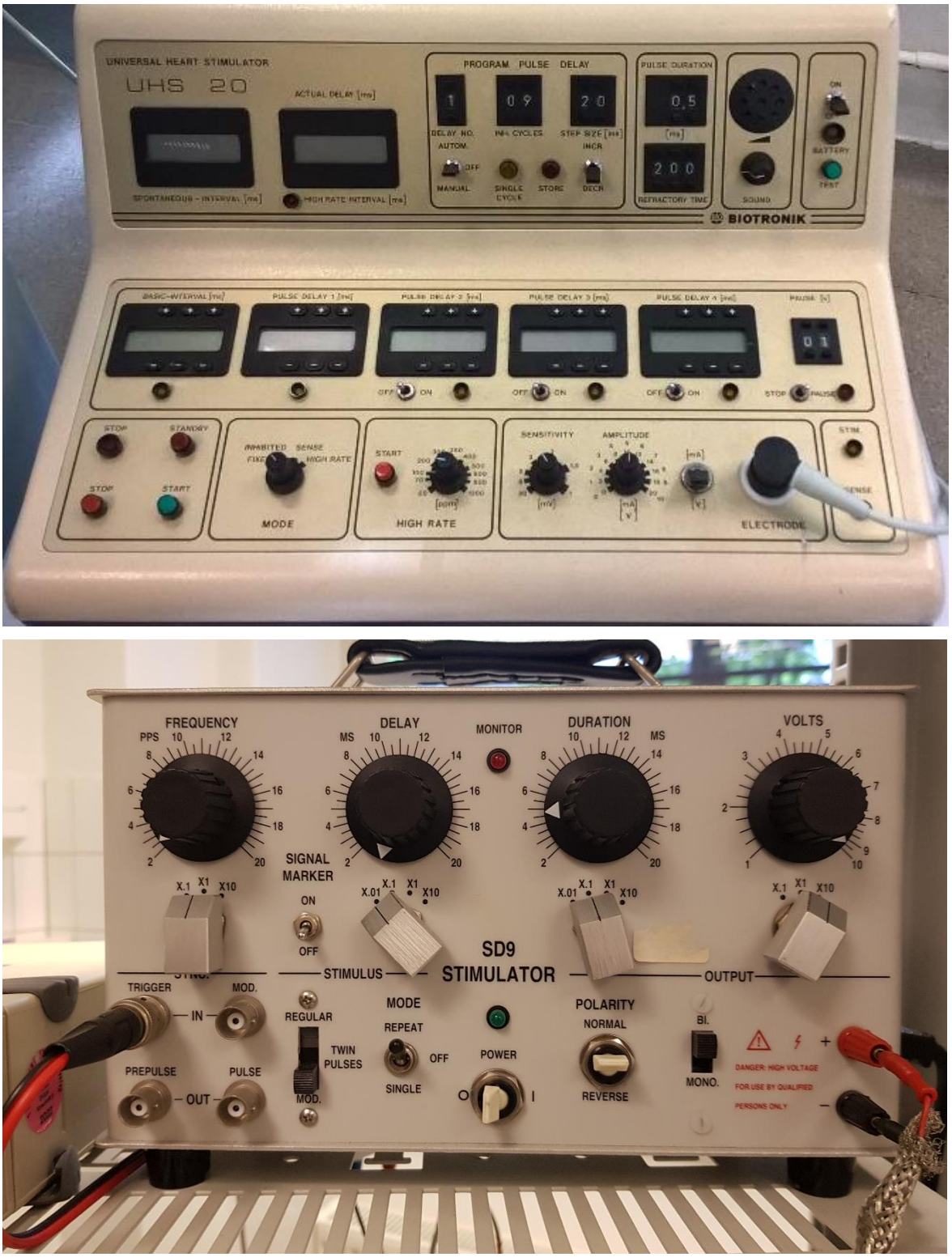

Figure 18. Frequency stimulator setup.

Biotronik stimulator to apply frequency protocols and cycle length adjustment (top) and Grass Product Group stimulator used for adjustment of stimulus duration, voltage and polarity (bottom).

2.1.2.9 Tissue placement

Positioning of each sample in the measuring setup is a crucial point as it influences how easily impalement of the contracting tissue is possible. For preparation the human LV samples were usually only fixated with one needle as their shape did not allow for as much movement in the bath. The rectangular shape of EHTs (length/width ratio of 10:1) however showed substantially more movement making special techniques necessary. Upon harvesting the EHT from the medium in the incubator tissues were either stripped off their silicone posts or embedded in the chamber with their cut off posts. Depending on the structural strength of each tissue the two fixation needles were either impaled through the tissues end where the silicone post had been before, or stuck through the still remaining silicone post on each end. EHTs were pinned down without any stretching to avoid activating mechanosensitive ion channels. In case the EHT developed sideward movement like a guitar-string one or two extra needles were placed below the EHT halfway between both posts. This helped to reduce sideward movement and to create a punctum fixum and allowed AP recordings with less movement artefacts.

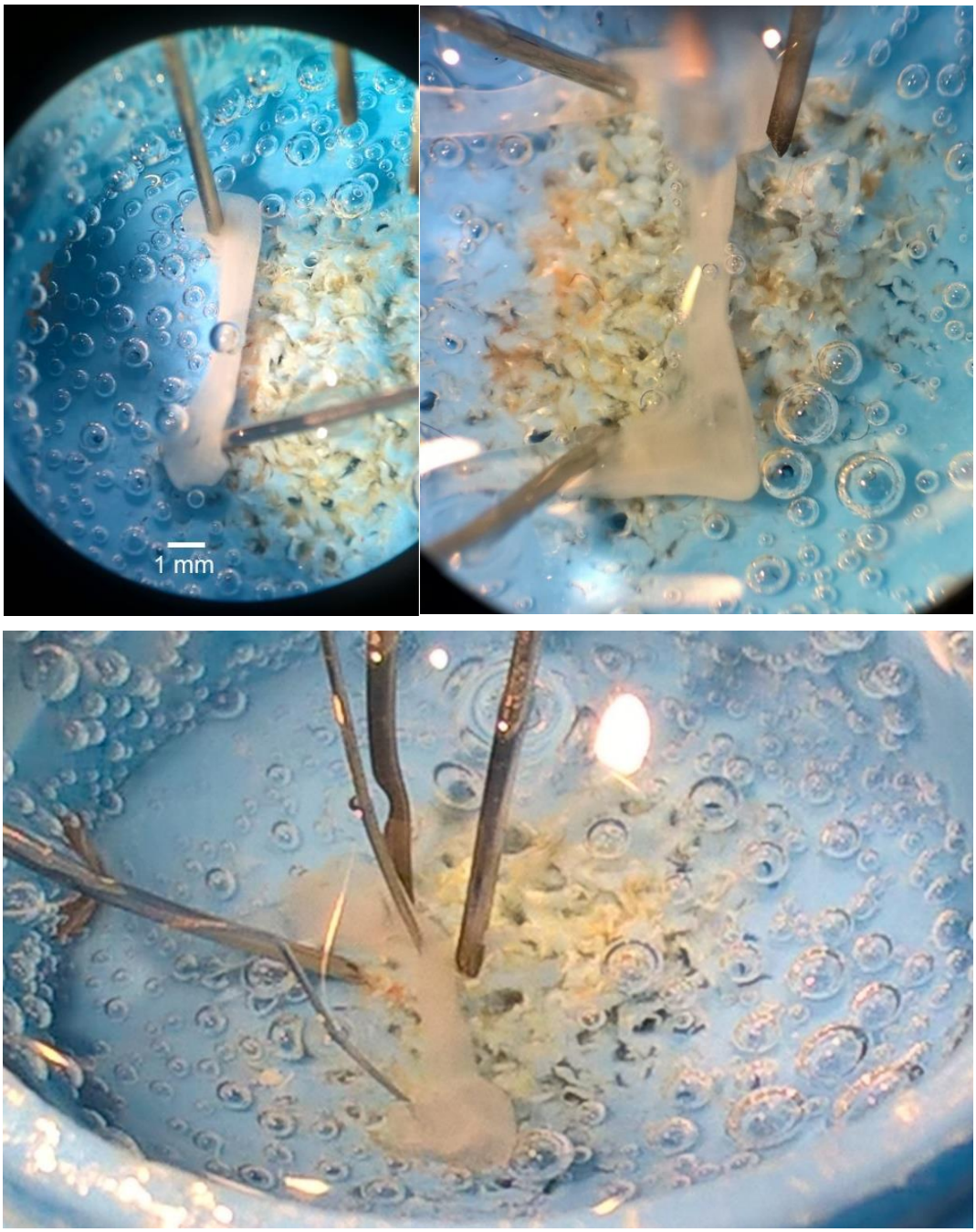

Figure 19. Tissue placement in the chamber.

Fixated engineered heart tissue with needles stuck through each end (top left, scale bar 1 mm) or through remaining silicone posts (top right). Total view of the positioning in the chamber including stabilisation needle below the tissue and stimulation fork electrode (bottom, photographed at an angle).

2.2.2 Execution of the procedure

The AP measuring procedure was carried out by placing the tissue in the silicone recording chamber which was perfused with a pre-heated Tyrode's solution that was oxygenated and pH adjusted by bubbling with carbogen gas (5% CO_2, 95% O_2). The tissue was then pinned to the bottom of the chamber on both ends as described above. The stimulation fork electrode was placed on one side of the tissue close enough to make sure that the electric field between the two poles permeates the EHT to achieve stimulation with minimal necessary voltage. The position and the polarity of stimulation was sometimes adjusted in case of interference of the stimulation artefact with upstroke velocity measurement and thereby AP detection by the analysis software.

For recording the membrane potential; the microelectrode was positioned above the tissue with the mechanical micromanipulator in a way that adjustment of only the Y-axis on the hydraulic micromanipulator would push the glass pipette down to impale the tissue below it. Compensation capacity was adjusted and the resting potential set to 0 mV with the glass electrode placed in the Tyrode's solution outside of the tissue. In the next step electrode resistance was checked. The glass pipettes used in this work had a resistance between 20 and 50 MΩ when filled with 3 mol/L KCl.

In case of not capturing a clean AP at an impalement location the pipette was lifted again, repositioned a few micrometres to any side and reimpaled into the tissue. In between different impalements electrode resistance was checked again, to be sure that the tip was not broken or occluded by debris or tissue. Additionally, it was often useful to perform an extra electrical "buzz" stimulus from the measuring electrode for the signal to properly catch and stay clean and undisturbed. Signal capture was possible at all different places throughout the tissue, however not every single EHT showed stable signals at every impalement location.

2.2.2.1 Baseline measurements

For the standard baseline measurements of APs, the tissue was pinned down in the silicon chamber using thin needles or standard intravenous injection cannulas. It was then impaled with the glass measuring electrode in an area where contraction of the muscle cells occurred, and thus an AP had to be present in the cells. For the LV tissue this was only possible under electric stimulation, whereas in EHT there was a spontaneous generation of APs and contractions. LV tissue's transport solution was washed out in Tyrode's solution for at least 30 minutes (no recirculation), as the transport solution functions as a cardioplegic solution containing a high potassium concentration and thus minimising cellular contraction and oxygen consumption.

EHTs were measured at a spontaneous beating frequency and under frequency-controlled stimulation to be able to compare it to LV. When the spontaneous beating frequency was faster than 1 Hz ivabradine was applied at a concentration of 300 nmol/L to block the funny current, decrease diastolic depolarisation and slow down the AP rate. Upon achieving spontaneous beating rates of under 1 Hz (i.e. >1000 ms cycle length) electrical stimulation of the tissue was used to control the AP frequency and compare it to LV. The required voltage for stimulation was determined by adjusting voltage to the threshold of stimulation where an AP could barely be triggered. Then voltage was increased by an additional 50% to have a margin of safety for stimulations to always have an effect and allow for overall comparability of all tissues.

At a continuous frequency of 1 Hz a stimulation protocol was used to determine the effective refractory period (ERP) This so called S1S2 protocol used a series of standard stimulation intervals of 1000 ms cycle length (CL) S1 followed by one shorter interval S2. This S2 interval was shortened in 10 ms steps from sequence to sequence until it failed to produce another AP. The second to last interval duration was then approximated to be the ERP, indicating the time it takes for the cell's Na^+-channels to reactivate and be able to generate another AP.

2.2.2.2 Rate dependency of APD

Action potential duration and form depend on the beating rate of the tissue. The tissue samples were subjected to a sequence of different frequencies within a physiological range from 0.3 Hz (3000 ms CL, 20 beats per minute) to 3 Hz (333 ms CL, 180 bpm) to check for rate dependency of APD. For this purpose, the Biotronik UHS20 EP lab stimulator was used to set stimulation cycle length to exactly the required duration. Every frequency was applied for at least 500 beats to equilibrate AP properties to the specific beating rate. In some cases, certain frequency ranges were not possible to achieve. When a slower rate was not manageable due to spontaneous activity at too high rate, a slow gradual increase in pacing cycle length (some "overstimulation") was one possible method to gradually habituate the tissues homeostasis to the new, slower rate. In case of a tissue being unable to follow higher frequency stimulation because of the refractory period another method was used. Running the tissue at rates just below the ERP to further shorten APD managed to slowly decrease ERP and allow a capture at the higher pacing frequency.

2.2.2.3 Drug intervention

Applying different drugs and compounds to the experiment was performed in a recycling system of Tyrode's solution. The volume of the bath solution within the system was maintained by feeding the effluent flow from the recording chamber back into the source vessel. The tubing system and bath chamber contained approximately 5 mL of volume and the total volume in the closed system was calculated accordingly. Compound stock solutions from prepared aliquots were then pipetted into the source cylinder, from which it took about 1 minute to reach the recording chamber. The constant bubbling of the carbogen gas provided for quick mixture of the compound in the solution, so no additional mixing was necessary. Some drugs were applied cumulatively by calculating the amount for the respective next concentration step in addition. For performing a washout of the compound, the system was again perfused with standard Tyrode's solution after the intervention for at least 15 minutes with a pumping volume of 3 ml/min and directing the effluent flow into a waste vessel with no recirculation.

2.2.2.4 Freezing and storage of the tissues

After all measurements for one experiment were done the tissue was dried off by briefly letting a soft tissue soak up the remaining liquid on the sample. The EHT or LV tissue was then submerged in liquid nitrogen in a 2 ml Eppendorf tube. Afterwards the frozen samples were stored at -80°C for further potential investigation of protein and/or gene expression.

2.2.2.5 Data analysis and software

Data analysis was performed with Lab-Chart software (ADInstruments, Spechbach, Germany) for AP algorithm analysis. In this software the raw measured signal could be analysed according to pre-defined definitions of AP amplitude peak and minimal peak duration. Detection settings were applied as APA above 60 mV and minimal peak duration at half upstroke height of 11 ms. This analysis produced the following data categories:

Take-off potential (TOP), action potential amplitude, maximum upstroke velocity, maximum negative repolarisation slope, action potential duration at a percentage of repolarisation from 10-90%, action potential triangulation calculated as APD_{90}-APD_{40}, plateau voltage, the count of each peak measured, action potential period in seconds and the time and date of each recorded point. Analysed data was then copied from the table view window for further calculations in Microsoft Excel files.

Values for maximum diastolic potential and diastolic depolarisation in V/s were calculated manually using the data pad function to detect maximum upstroke velocity point in the first derivative of the main data signal and lowest diastolic voltage.

GraphPad Prism 5 (GraphPad Software, San Diego, CA, USA) was used for graphical and numerical data evaluation and figure creation, as well as Microsoft Excel for data collection and management, and Powerpoint (Microsoft Corporation, Redmont WA, USA) for image creation.

Graphical representation in the form of curves consisted of fits to data points from individual experiments. All data were compared using two-tailed paired or unpaired t-tests and a $p<0.05$ was considered to be statistically significant. Group data are presented as mean value±SEM. One-way ANOVA followed by Tukey corrections was used for multiple comparisons.

3 Results

The following section presents the results of our action potential measurements using the sharp microelectrode technique. In total, 51 successful experiments on human left ventricular tissue were conducted, of which 13 were from patients with heart failure, undergoing heart transplantation (HTX) or left ventricular assist device implantation (LVAD), and 38 samples from left ventricular septal myocardium (LVS). Of the 63 EHT experiments in three different hiPSC-cell lines 13 came from iCell² cells, 24 from the TUMi001-A/C25 cell line (C25) and 26 from UKE003i-C/ERC018 cell line (ERC018) samples. For general comparison to LV, EHT data is presented as one pooled group of all three genotypes. An individual breakdown of inter-cell line differences is discussed subsequently.

3.1 Technical issues

Validity of the measured data is very much dependent on a few factors not innate to the tissue or electrophysiological conditions and characteristics itself, but rather the quality of the execution and performance of experiments. Therefore, it was attempted to eliminate as many interfering factors as possible. This included the following factors: temperature, electromagnetic interference with the measuring electrode, electrolyte concentration in bath solutions, conductance/resistance of the measuring electrode and time-based changes in the cells/tissue.

3.1.1 Success rates of experiments

One very plain way to describe the success and quality of an experiment is to look at action potential amplitude (APA), duration of stable AP measurement and amount of contraction artefact. An experiment of good quality was defined as an APA above 90 mV and stable uninterrupted AP recording for more than 10 minutes with a lack of significant contraction artefact. Unstable recordings with interruption of continuous recording under 10 minutes could still be used to interpret APs, however observing an effect of a certain intervention was more intricate in these cases as a new signal at the same or different impalement site had to be used as comparison. Some tissues only showed APs of a small APA or with no continuous measurement at an undisturbed resting membrane potential. These bad signals were useful only in very select aspects of interpretation. In rare cases it was impossible to record any APs at all, despite the fact that a contraction of the tissue was visually observable. EHTs without visual contraction were in general not used in microelectrode measurements. In human LV tissue there were a handful of tissues that never showed any signs of contraction or electrophysiological activity.

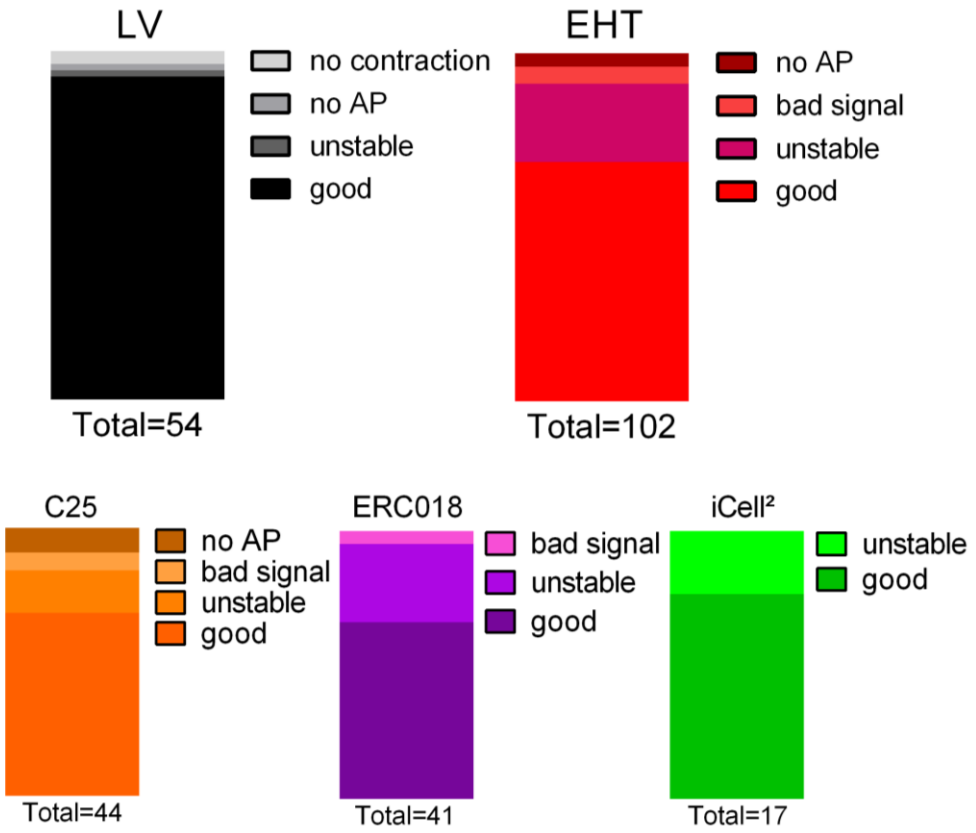

Figure 20. Success rates of action potential measurements in different tissues.

Total quality and quantity of left ventricle and engineered heart tissue are presented in the top row. Single EHT cell lines C25, ERC018 and iCell² are broken down at the bottom.

Since it can be argued that over time a tissue that is subjected to *in vitro* laboratory conditions may develop a change in electrophysiological parameters compared to *in vivo* conditions, the main AP parameter APD_{90} was examined over time. In neither of the groups a significant change was observed over a time control period of at least one hour. It can be confidently stated that even after a longer period of experimental duration in the measuring setup data was still valid and interpretable.

Electric resistance of the measuring electrode made from a glass filament pipette was always evaluated before impalement. Only electrodes with a resistance between 20 and 50 MΩ were used. If the resistance suddenly increased it was sometimes possible to settle this with a few extra electrical impulses applied via the stimulator to clear out possible cell fragments obstructing the pipette opening. Upon a sudden drop in resistance, it was assumed that the pipette's tip had broken off and increased the opening area. In such cases, the glass electrode was replaced.

3.1.2 Stability of AP over time

Stability of a parameter over time makes it easy to measure drug effects. If the parameter does not remain stable over time exact knowledge about the speed of change is necessary to dissect drug effects from spontaneous drift. Very few measurements were perfectly stable over long time periods, but impalement of the signal in these experiments was taken at the same spot in the tissue. Over the course of an experimental day some tissues were stable for more than 6 hours.

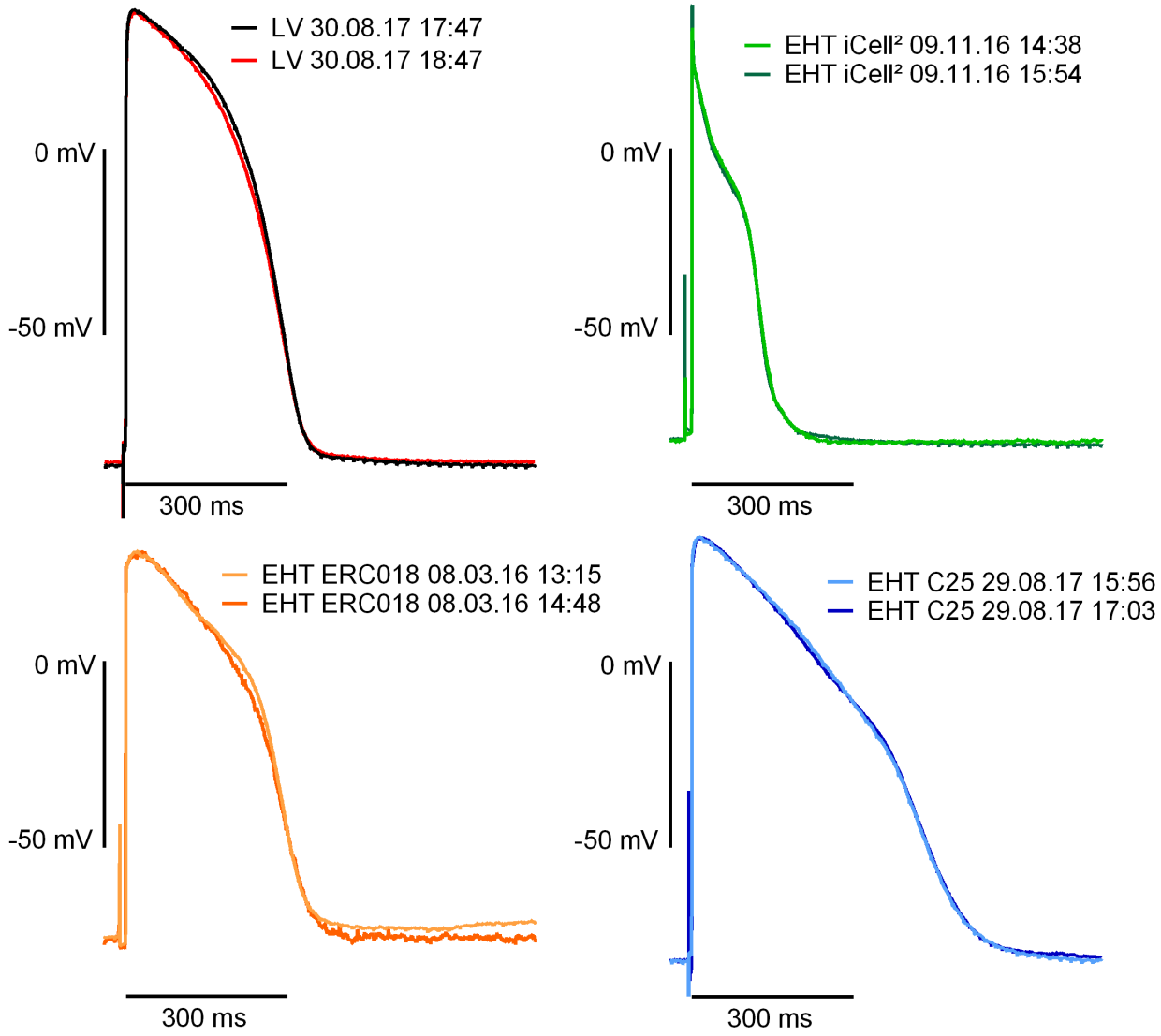

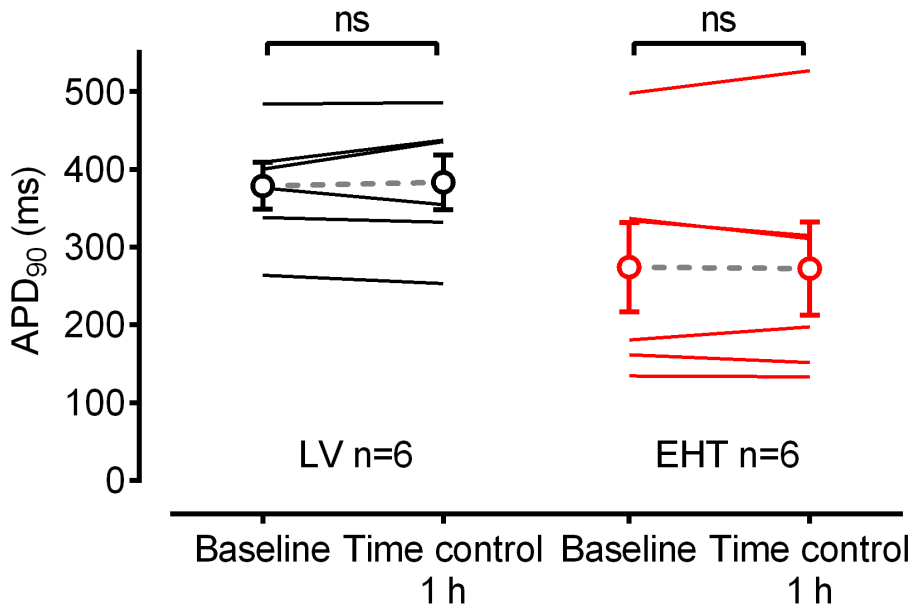

Figure 21. Action potentials parameters in time-matched controls.

Action potential traces of left ventricle (LV, top left) and engineered heart tissue (EHT) in three examples (green iCell², orange and blue ERC018) over a long period of time (>1h). No significant change in action potential duration or shape was observed in either group (bottom).

3.2 Baseline action potential

Initially, the basal action potential characteristics of each preparation were measured. If possible, this was done at a paced frequency of 1 Hz for better comparability at resting physiological heart rate. For spontaneously beating EHT attempts were made to measure spontaneous beating frequency and parameters dependent on it.

3.2.1 Action potential characterisation

3.2.1.1 Human left ventricle

Action potential parameters of human left ventricular tissue preparations from heart failure patients and valvular diseased patients were found to be similar to standard literature values of AP characteristics. The AP showed a wide plateau, without the drastic initial repolarisation typical for atrial AP causedby ultrarapidly activating delayed outward potassium current I_{Kur}. Most preparations did not even show any notch typically caused by the transient outward current I_{to} (Ravens and Christ 2010).

Action potential parameters measured at baseline conditions of 1 Hz stimulated frequency (1000 ms cycle length / 60 beats per minute) presented with a resting membrane potential (RMP) of -78.6±0.7 mV, action potential amplitude (APA) of 108.9±1.2 mV, maximum upstroke

velocity (V_{max}) of 231.2±15 V/s, action potential duration at 50% repolarisation (APD_{50}) 262.8±6.9 ms and at 90% 354.4±7.1 ms (n=51).

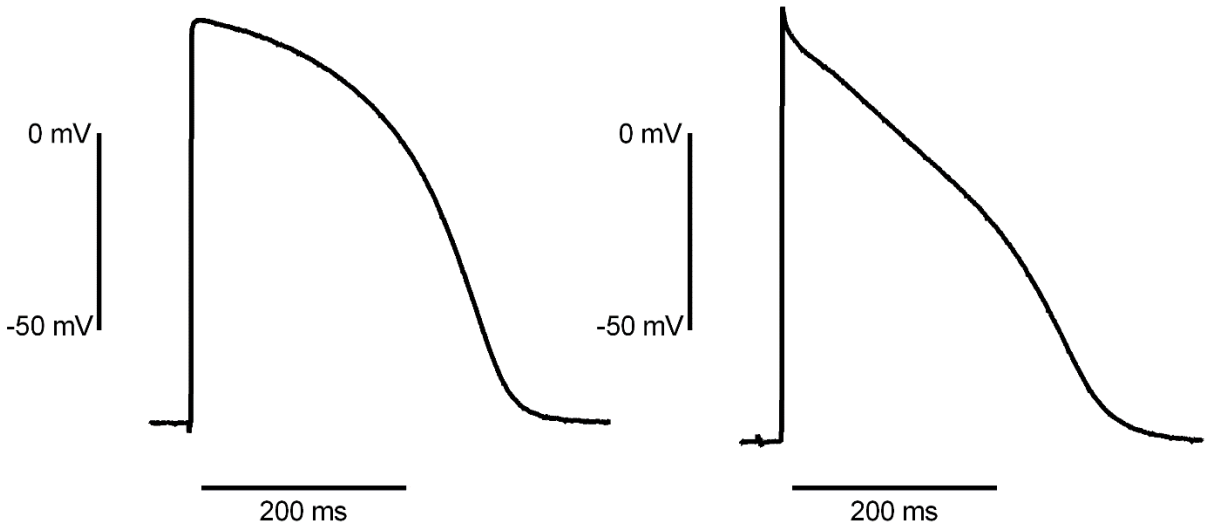

Figure 22. Human left ventricular action potential.

Representative example action potentials of left ventricular tissue, paced at 1 Hz frequency without drug intervention. On the left the most commonly observed shape with a very wide phase 2 plateau, on the right an example with a bigger notch from a different sample.

3.2.1.2 HiPSC-CM in EHT format

In the EHT format, values for most AP characteristics at baseline conditions were found to be the same as in LV. APs recorded at 1 Hz pacing without drug intervention resulted in these values: AP take-off potential (TOP) of -75.7±1.0 mV, APA of 106.3±1.8 mV, V_{max} of 272.1±16.8 V/s. Notable is the fact that the action potential duration was significantly shorter in EHT than in left ventricular tissue (153.2±11.9 ms at 50% repolarisation and 223.8±11.6 ms at 90% repolarisation, n=27, $p<0.001$, see data in table 4). In addition, a diastolic depolarisation (DD) was present in the spontaneously beating EHT akin to that in pacemaking cells (e.g. in the sinoatrial node). DD was quantified as a 5.2±0.8 mV/s (n=27) increase in membrane potential during the diastolic interval between maximum diastolic potential (MDP) and upstroke of next AP. Further exploration will be done in chapter 3.2.2.

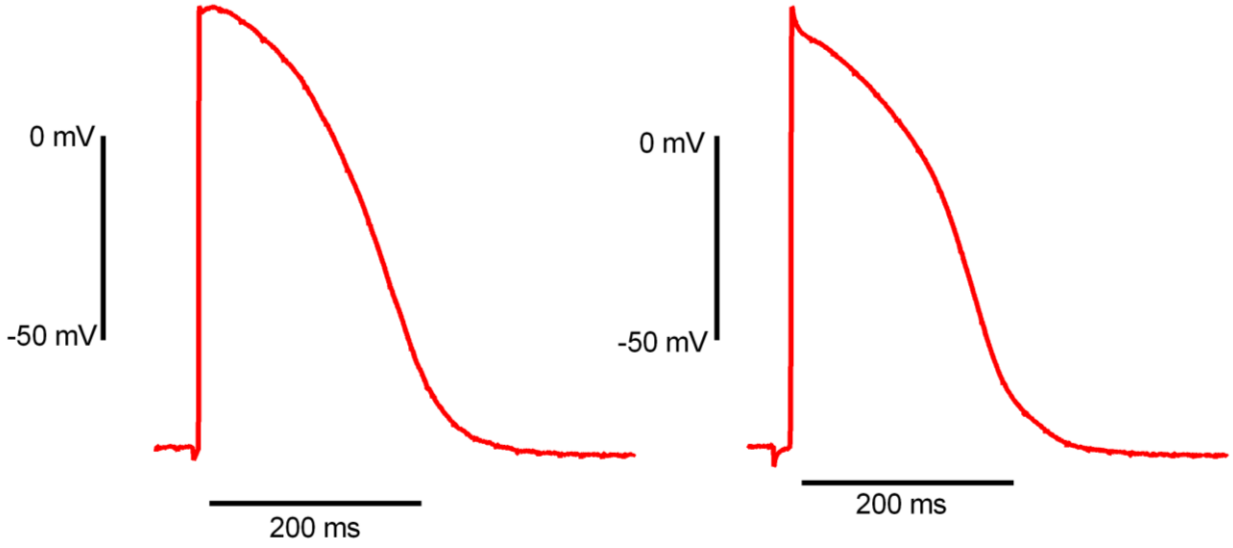

Figure 23. Human induced pluripotent stem-cell engineered heart tissue action potential.

Representative example action potentials, paced at 1 Hz without drug intervention. Similar shape to left ventricular action potential with a slight I_{to}-notch and a noticeably shorter duration on the left and another shape of AP with a bigger notch on the right, which was more common in EHT than in LV.

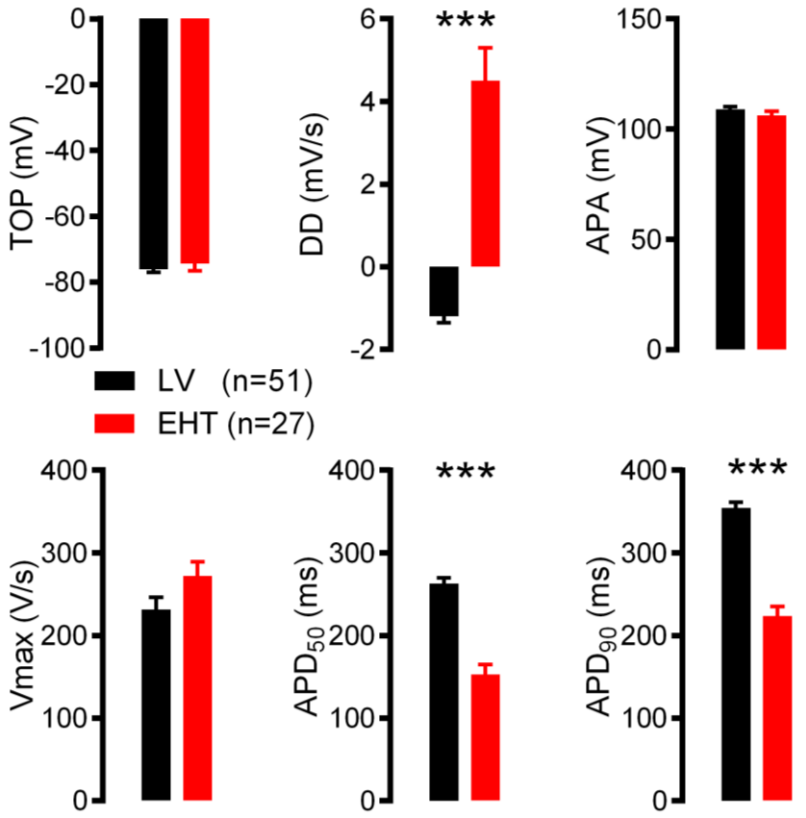

Figure 24. Action potential parameters.

Comparison of left ventricular and engineered heart tissue paced at 1 Hz frequency. Significant difference shows in diastolic depolarisation and action potential duration at 50 and 90% repolarisation $p<0.001$).

Table 4. Baseline AP parameters of LV and EHT. Baseline parameters from Figure 24, left ventricular vs engineered heart tissue comparison, paced at 1 Hz, unpaired T-test. Included is a comparison of maximum diastolic potential (MPD)

Parameter	LV	SEM	n	EHT	SEM	n	p
MDP (mV)	-78.6	0.7	51	-78.3	1.2	27	0.81
DD (mV/s)	-1.2	0.2	51	5.2	0.8	27	<0.01
TOP/RMP (mV)	-77.2	0.7	51	-75.7	1.0	27	0.22
APA (mV)	108.9	1.2	51	106.3	1.8	27	0.22
V_{max} (V/s)	231.2	15.	51	272.1	16.9	27	0.074
APD_{50}	262.8	6.9	51	153.2	12.8	27	<0.01
APD_{90}	354.4	7.1	51	223.8	12.9	27	<0.01

3.2.2 Spontaneous activity

3.2.2.1 Left ventricular tissue is quiescent

The left ventricular tissue never showed any spontaneous activity by itself: It was always quiescent and only showed contraction upon stimulation after washout of the cardioplegic transport solution. Stimulation of tissues was done at an impulse duration of 0.5 ms and a voltage of 150% needed to induce visually controlled contraction of the tissue.

3.2.2.2 Engineered Heart Tissue beats spontaneously

Every EHT did contract spontaneously with a mean beating rate of 1.24±0.1 (n=24) Hz at baseline conditions. During spontaneous activity, membrane voltage showed a diastolic depolarisation of 10.2±1.4 mV/s. This corresponds approximately to the difference in take-off potential (TOP) between -69.4±1.0 mV and maximum diastolic potential (MDP) -60.2±8.8 mV measured in spontaneously beating EHT without drug intervention and pacing.

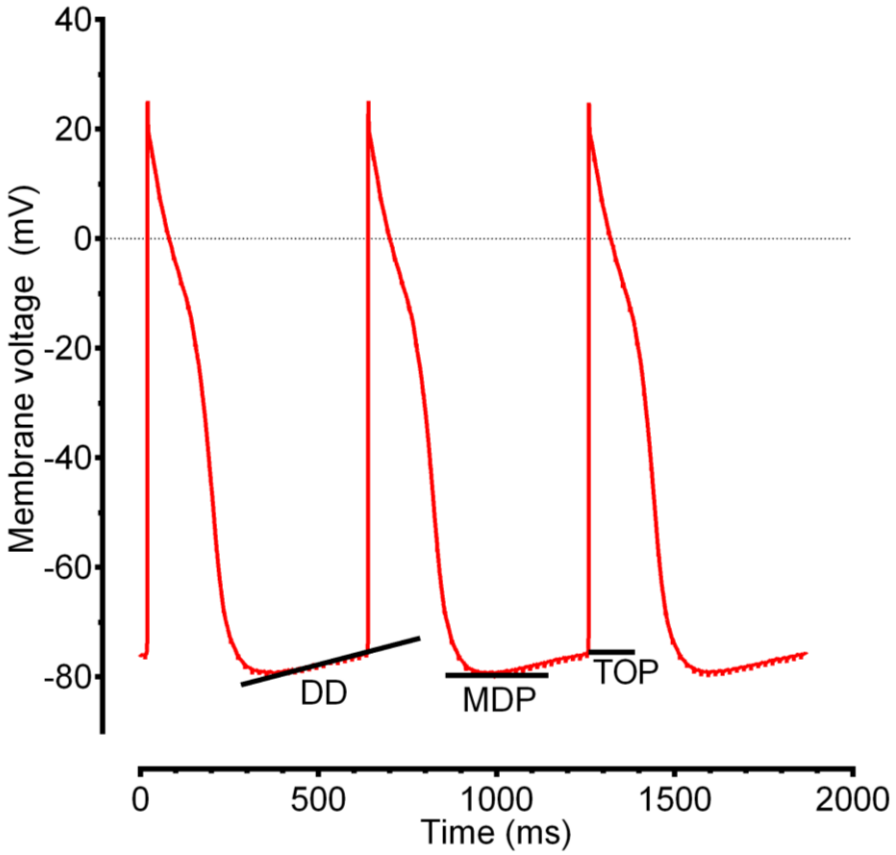

Figure 25. Spontaneous activity and diastolic depolarisation.

Example of spontaneous activity illustrating analysed parameters where diastolic depolarisation (DD) in mV/s describes the amount of voltage increase during the diastolic interval, maximum diastolic potential (MDP) represents the lowest voltage during diastole and take-off potential (TOP) is the point at which the next action potential's upstroke starts.

3.2.2.3 Effect of ivabradine on diastolic depolarisation

It is necessary to bring LV and EHT to the same beating rate to compare their AP parameters. The "funny-current" blocker ivabradine was used to decrease the diastolic depolarisation, since some EHTs beat faster than 1 Hz. In a paired analysis before/after comparison, DD decreased from 7.0±1.0 mV/s to 0.9±0.6 (n=11; paired t-test $p<0.001$) upon I_f block by 300 nmol/L ivabradine. This lowered the take-off potential from -77.1±1.3 to -81.0±1.3 mV (n=11; paired t-test p=0.017) and increased the APA from 108.8±2.4 to 115.5±2.3 mV (n=11; paired t-test p=0.017). The spontaneous beating frequency was lowered from 1.15 Hz (≈930 ms CL) to 0.31 Hz (≈3380 ms CL, n=11; paired t-test $p<0.01$). The latter effect has been reported before (Mannhardt et al. 2016). There is some concern that commonly used concentrations of ivabradine could block other channels than HCN (Lungo et al. 2012). However, 300 nmol/L ivabradine did not affect AP parameters in LV tissue (see Table 6).

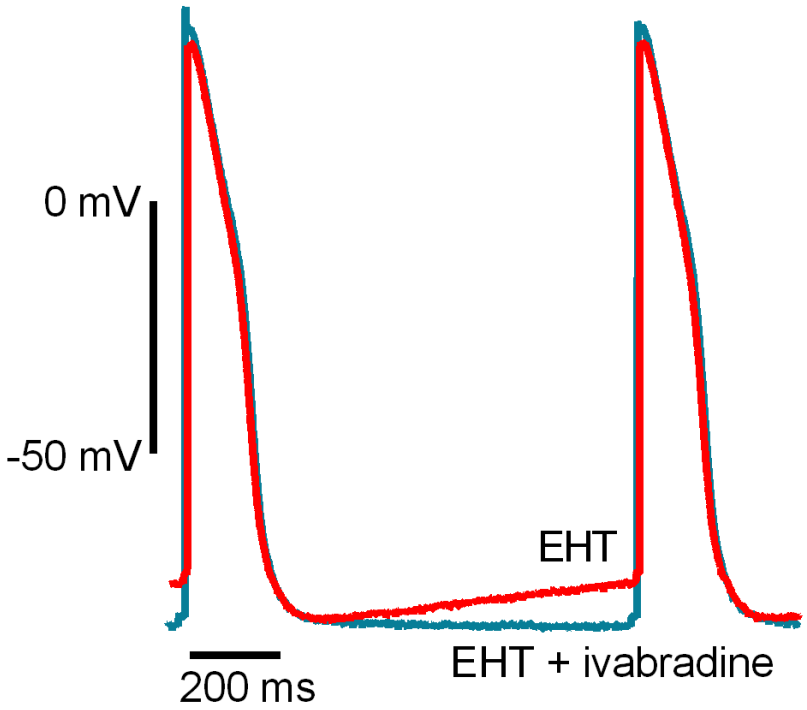

Figure 26. Effect of ivabradine on engineered heart tissue action potential.

Overlaid action potentials before (red) and after (blue) 30 minutes of perfusion with 300 nmol/L ivabradine, paced at 1 Hz.

Table 5. Effect of ivabradine on engineered heart tissue action potential parameters. Paired comparison of 11 preparations before and after 30 minutes of perfusion with 300 nmol/L ivabradine, paired T-test $p<0.05$ was assumed as statistically significant.

Parameter	EHT baseline	SEM	n	EHT + ivabradine	SEM	N	p
MDP (mV)	-82.6	1.3	11	-82.3	1.27	11	0.86
DD (mV/s)	7.0	1.0	11	0.9	0.6	11	<0.01
TOP/RMP (mV)	-77.1	1.3	11	-81.0	1.27	11	0.017
APA (mV)	108.8	2.4	11	115.5	2.3	11	0.017
V_{max} (V/s)	301.7	27.2	11	359.9	47.3	11	0.219
APD_{50} (ms)	146.0	19.5	11	160.8	22.3	11	0.075
APD_{90} (ms)	223.5	23.2	11	241.7	27.8	11	0.196
Frequency (Hz)	1.15	0.1	11	0.31	0.02	11	<0.01

Table 6. Effect of ivabradine on left ventricle action potential parameters. Paired comparison of 5 preparations before and after 30 minutes of perfusion with 300 nmol/L ivabradine, paired T-test p<0.05 was assumed as statistically significant.

Parameter	LV baseline	SEM	N	LV + ivabradine	SEM	N	p
MDP (mV)	-79.0	0.8	5	-77.4	2.5	5	0.47
DD (mV/s)	-1.0	0.6	5	-0.9	0.3	5	0.82
RMP (mV)	-77.9	0.9	5	-77.3	2.2	5	0.72
APA (mV)	110.1	1.5	5	109.0	3.9	5	0.72
V_{max} (V/s)	177.2	25.5	5	200.8	33.5	5	0.45
APD_{50} (ms)	278.9	32.6	5	278.3	31.0	5	0.88
APD_{90} (ms)	367.7	33.7	5	370.1	32.2	5	0.62

A comparison of baseline LV AP parameters and EHT treated with 300 nmol/L ivabradine both paced at 1 Hz shows no particularly different constellation to the comparison of LV and the EHT group without ivabradine. Only the effect on diastolic depolarisation in EHT is to be noted.

Table 7. Comparison of baseline LV and EHT with ivabradine. LV measurements are at baseline conditions, EHT is under the effect of 300 nmol/L ivabradine, both at a pacing frequency of 1 Hz. T-Test p<0.05 was assumed as statistically significant.

Parameter	Baseline LV	SEM	n	EHT + ivabradine	SEM	N	p
MDP (mV)	-78.6	0.7	51	-79.3	1.1	30	0.27
DD (mV/s)	-1.2	0.2	51	-0.2	0.3	30	0.02
RMP (mV)	-77.2	0.7	51	-78.1	1.1	30	0.50
APA (mV)	108.9	1.2	51	110.5	2.0	30	0.50
V_{max} (V/s)	231.2	15.0	51	278.4	24.9	30	0.11
APD_{50} (ms)	262.8	6.9	51	159.1	20.3	30	<0.01
APD_{90} (ms)	354.4	7.1	51	277.6	21.5	30	<0.01

3.2.3 Rate adaptation

With the problem of spontaneous activity of EHT solved by application of ivabradine it was possible to adjust beating rate of both groups via electrical stimulation. A rate dependency stimulation protocol was performed during which the frequencies 0.33, 0.5, 1, 1.5, 2, 2.5 and 3 Hz were applied.

3.2.3.1 APD_{90} rate dependency in LV and EHT

LV tissue showed a maximum APD_{90} of 418.7±21.7 ms at 0.3 Hz (3000 ms CL, n=20), which shortened to 225.2±12.5 at 3 Hz (333 ms CL, n=24). From the base frequency of 1 Hz there was a 16% APD_{90} increase at 0.3 Hz and at 3 Hz a 37.6% shortening from 1 Hz APD_{90} of 361 ms. EHT presented with a shorter maximum APD_{90} of 314±60.9 ms at 0.3 Hz (3000 ms CL, n=10) which shortened to 160.7±9.3 ms at 3 Hz (333 ms CL, n=29). In comparison to base APD_{90} of 247.7 ms at 1 Hz there was a 30.9% APD_{90} increase at 0.3 Hz and at 3 Hz a 37.4% shortening. APD_{90} in both groups was much larger at higher cycle lengths (i.e. lower frequency). EHT behaved similarly to LV but had a shorter APD_{90} at all frequencies.

Table 8. Rate dependency of APD_{90} in LV and EHT. Average APD_{90} of corresponding frequency compared with an unpaired T-test, $p<0.05$ was assumed as statistically significant.

Frequency (Hz)	Average LV APD_{90}	SEM	N	Average EHT APD_{90}	SEM	N	p
0.33	418.7	21.7	20	314.0	60.9	10	0.245
0.5	398.1	21.6	19	308.0	55.1	15	0.233
1	360.9	11.1	34	247.7	21.1	32	<0.001
1.5	307.8	11.3	25	221.9	16.4	31	<0.001
2	273.3	8.1	32	210.2	13.0	35	<0.001
2.5	238.6	8.3	21	197.6	11.1	30	0.007
3	225.2	12.5	24	160.7	9.3	29	<0.001

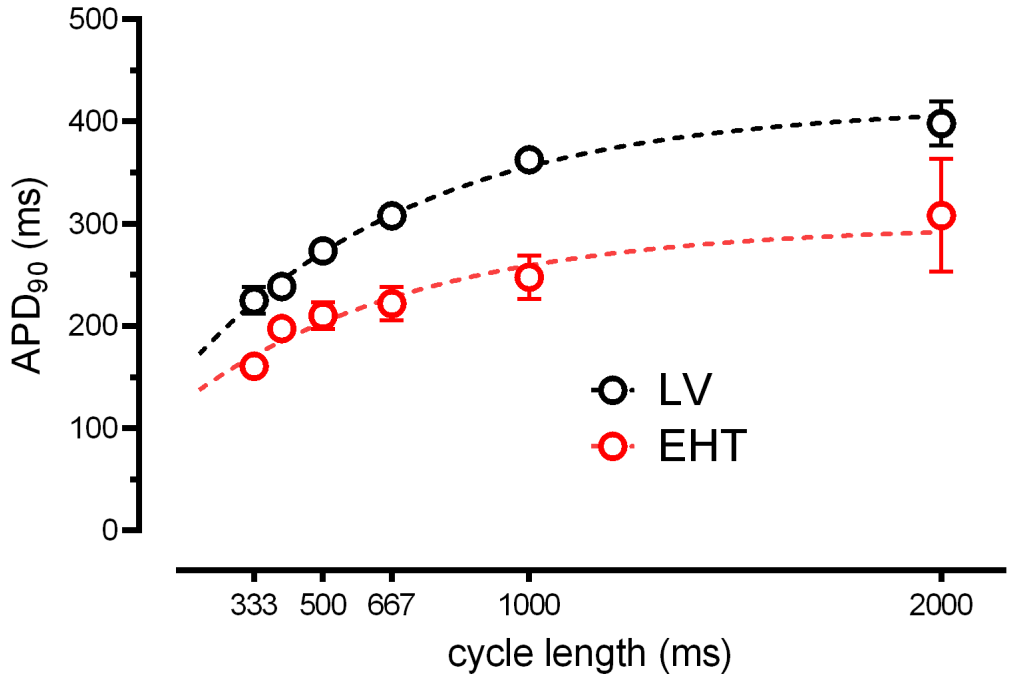

Figure 27. Rate dependency curve of APD_{90} in left ventricular and engineered heart tissue.

Action potential duration dependent on cycle length of stimulation frequency of LV (black) and EHT (red). For comprehensibility frequencies from 3 Hz to 0.5 Hz are depicted as circles with SEM bars. The dotted line presents the regression curve of a simple exponential function. Comparison of exponential regression curves prefers differing curves for each data set (F-test, F ratio=23.62, p<0.0001) but not differing rate constants (n.s.). APD_{90} is lengthening at higher cycle lengths (lower frequency) and shortening at faster pacing with shorter cycle length.

3.2.3.2 Rate correction of APD

APD_{90} was plotted over frequency instead of cycle length to calculate a linear function as guideline for general APD range in order to find an approximation for all possible frequencies between fixed values.

Previously used correction formulas show slight over- or undercorrection for QT-interval values in certain frequency ranges, or have been developed for a specific range. The most frequently used correction formula by Bazett $QTc = \frac{QT\ (ms)}{\sqrt{RR\ (s)}}$ is based on a square root function. QTc calculated by the Bazett formula overcorrects at high frequencies while it undercorrects at low frequencies which may lead to false shorter QTc. Criticism of this formula which is derived from a very small cohort of patients lead to development of other corrections like Friderica $QTFc = QT\frac{ms}{RR^{(\frac{1}{3})}}$ which works better at low frequency and linear correction functions from the Framingham Heart Study $QTLc = QT + 0.154 \times (1 - RR(s))$ (Sagie et al. 1992; Karjalainen et al. 1994).

When applying these correction formulas to this study's data none were able to correct without a higher margin of correction at more extreme rates. Correction formulas developed for QT interval in human ECG recordings may not accurately describe APD of *in vitro* measured tissues. Therefore, another formula was designed inspired by colleagues from Glasgow who measured optical APD_{90} in 2D hiPSC (Lu et al. 2017). Since APD plotted against frequency (in Hz) instead of CL (in ms) is closely modelled by a simple linear regression, this was used to implement a correction formula.

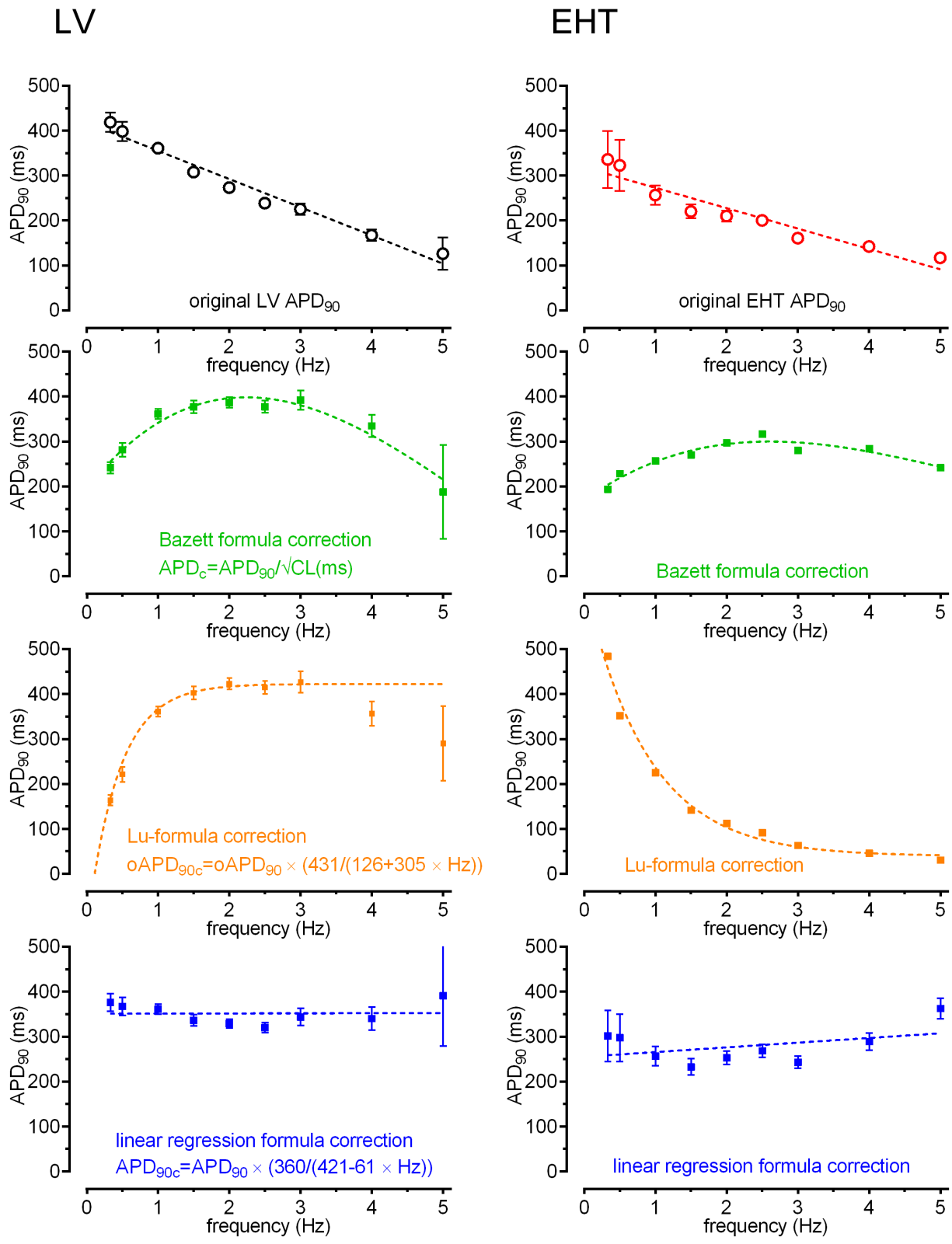

Figure 28. APD-correction for beating rate using different formulas.

APD_{90} plotted against beating frequency in LV (left column) and EHT (right column) showing mean original uncorrected data points (top) and corrected values with different formulas with SEM: Bazett-formula (green), 2D-culture-EHT formula by Lu et. al (orange) and newly designed linear regression formula (blue) with the formula presented on the left side.

A high goodness for a linear regression curve fit (R^2=0.972 for LV and R^2=0.901 for EHT) was found by plotting normalised APD against frequency. More importantly there was no longer a correlation between normalised APD_{90} and rate. In contrast, the Bazett-formula and the formula by Lu et. al tended to overshoot the correction factor for recordings collected in the present study. The newly developed linear regression formula normalised the measured data nicely to be less rate-dependent within the physiological bandwidth around 1 Hz. In this way it was possible to adjust both LV and EHT measured APD_{90} data at various frequencies to a comparable normalised level regardless of pacing frequency. This allowed for comparison in case of non-rate-controlled tissue frequencies without large over- or undercorrection of the APD_{90}.

3.2.3.3 Equilibration of APD in response to stepwise increase in pacing rate

When beating frequency of a cardiac tissue is suddenly changed, it needs a certain time to adjust APD to the new cycle length. To find out how long each of the investigated groups took to adjust, the time for APD-equilibration to 95% of total APD change was analysed. The total APD over time at the point of frequency change was plotted against time. APD data were normalised to APD before the increase in CL (set as 100%). Then a simple exponential function was fitted to the data points to estimate the time needed for 95% adaptation of APD after the frequency jump. For comprehensibility this is presented in the following figure only for the frequency change from 1 to 1.5 Hz. Further calculations were made for different frequency changes from 2 to 2.5 Hz, and 3 to 4 Hz, and the number of APs needed for adjustment was compared between LV and EHT. Based on the emerging data it can be concluded that with a high probability upon changing the pacing frequency of a tissue a number of at least 300 beats would be sufficient to reach a new stable APD_{90}. This was used throughout the work presented here to ensure that in performing rate dependency stimulation protocols a new steady state has been reached.

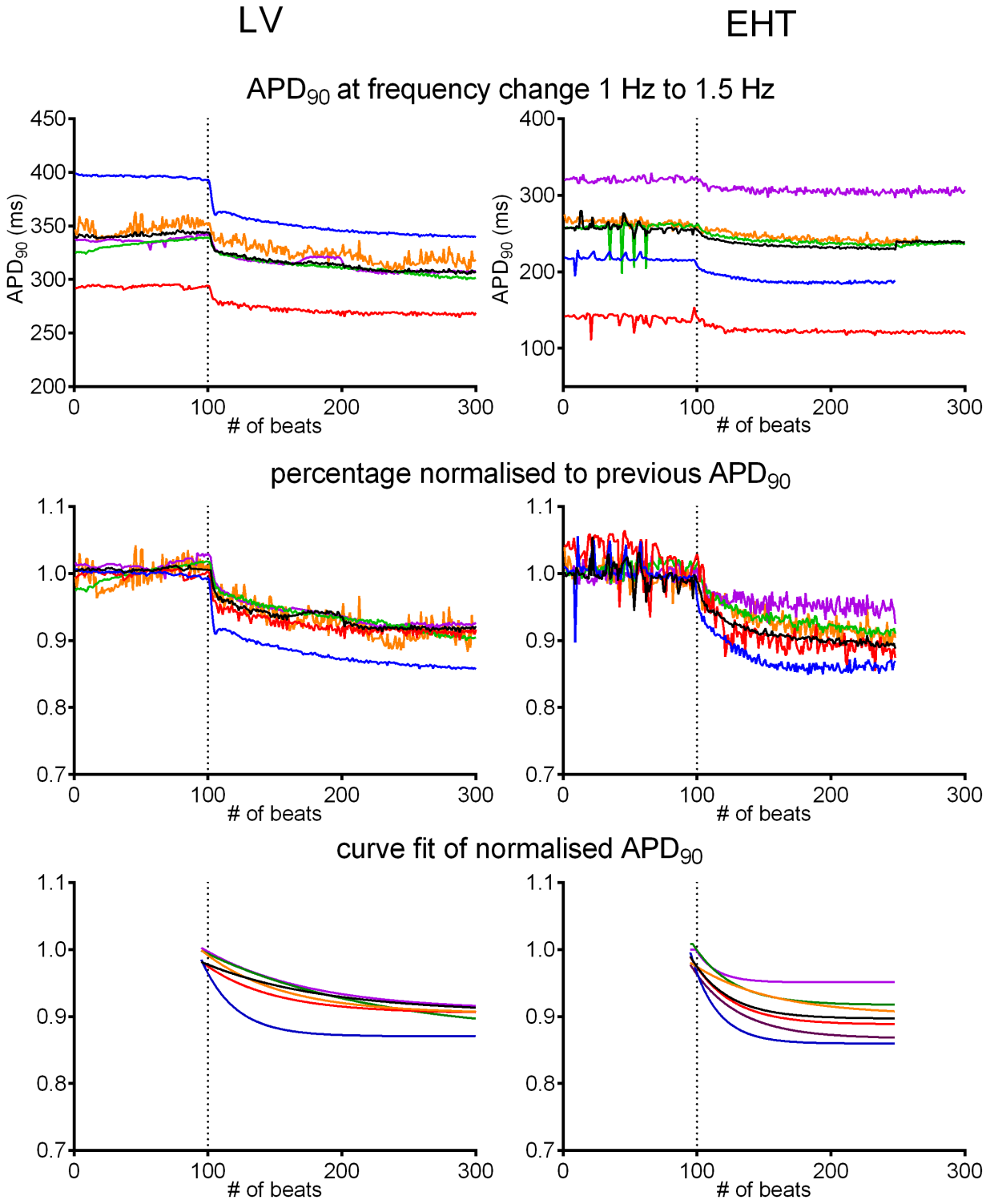

Figure 29. Action potential duration equilibration in response to an abrupt increase in pacing rate

Data for APD_{90} measured in left ventricular (left column) and engineered heart tissue (right column) before and after abrupt increase in pacing rate: Data are presented as absolute APD_{90} in the top row for representative example plots (coloured) and the average APD_{90} (black) at frequency change from 1 Hz to 1.5 Hz at 100 beats. The middle row shows this data as percentage value normalised to the average previous APD_{90} set as 100%, and the bottom row shows a curve fit of this data which was used to determine the exact point of 95% APD-equilibration at the new stimulation frequency.

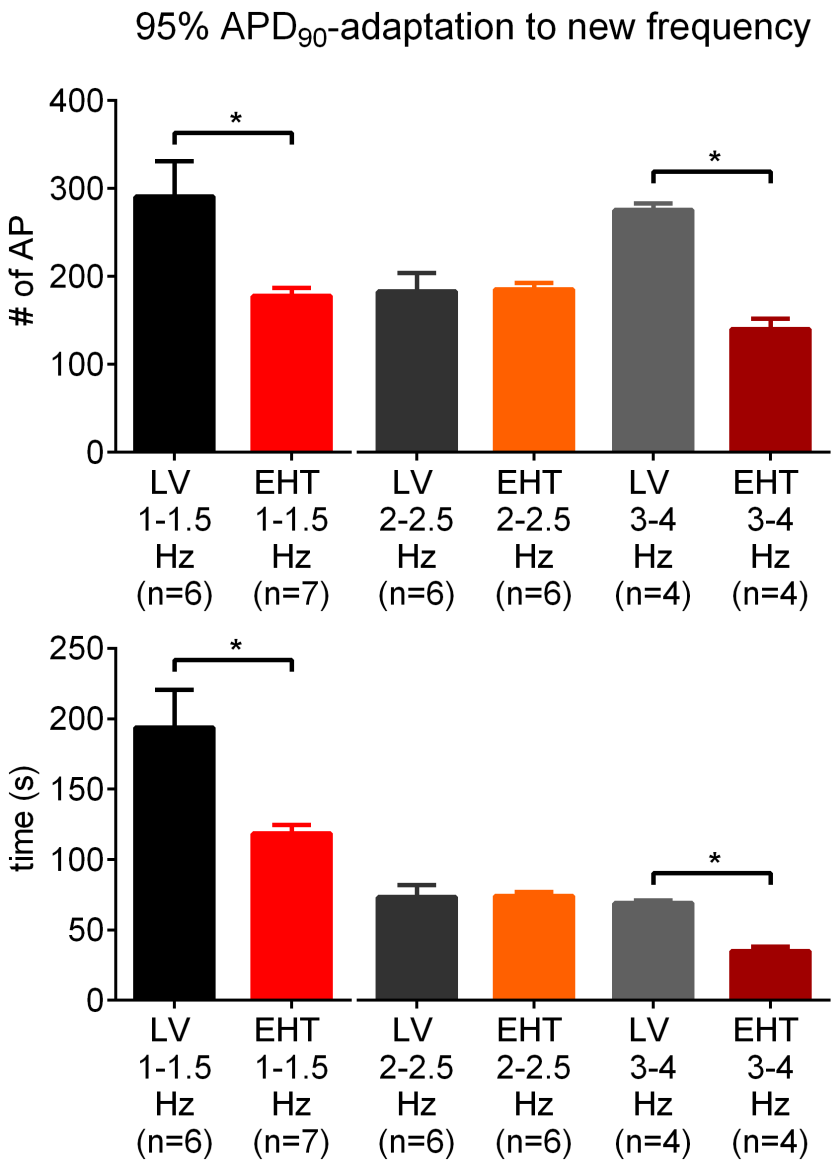

Figure 30. Comparison of action potential duration equilibration for number of beats and time.

For three different steps from 1 to 1.5 Hz, from 2 to 2.5 Hz and from 3 to 4 Hz pacing frequency the number of action potentials (top) and time in seconds (bottom) needed for a 95% APD_{90} equilibration to the new final action potential duration was compared. Overall, equilibration is faster in EHT and a significant difference can be observed in the slower and faster frequency steps of LV in comparison to EHT. Only significant value differences with $p<0.05$ are marked with comparison lines, n-numbers are presented below bars.

3.3 Effect of I_{Kr} block with E-4031 on APD

One of the most feared adverse drug reactions is a prolongation of the cardiac AP. This is usually caused by block of repolarising potassium currents and the most prominent role in the human cardiomyocyte's repolarisation is fulfilled by the rapid delayed rectifier potassium current (I_{Kr}). Reduction of its conductance leads to a slower repolarisation and thus a prolonged AP and a clinical presentation of a long QT interval. This LQTS can be predictive of life-

threatening TdP arrhythmia in which an excitation of the myocardium causes unsynchronised tachycardic contractions that fail to produce a sufficient ejection to provide brain and organs with oxygenated blood.

Consequently, it is of utmost importance in drug development and safety pharmacology to check for possible proarrhythmic effects of new drugs and rule out any repolarisation disturbing elements. The so called *hERG* assay which examines the I_{Kr} response to a certain substance is often performed on rabbit Purkinje fibre (Lu et al. 2005). E-4031 was used to block the I_{Kr} and check for its effect in human LV and EHT to evaluate suitability of this for a *hERG* assay.

3.3.1 Effects of a single high concentration of E-4031

The maximum effect on APD by I_{Kr} blockade was measured with 1 µmol/L E-4031. This included experiments in which the drug was applied in a single concentration, as well as cumulatively applied dosage up to 1 µmol/L. APs were analysed after a perfusion time of 15 minutes.

In LV tissue the APD_{90} increased from a baseline level of 344.1±8.8 ms (n=45) to 436.8±19.5 ms (n=14) in the tissues without amiodarone treatment in patient history or presence of hypertrophic cardiomyopathy.

In EHT the APD_{90} increased much more than in LV from a baseline level of 253.2±15.0 (n=46) to 517.3±25.5 ms (n=32). This dramatic increase presented itself in all cell lines. A detailed breakdown of the individual cell lines can be found in later chapters.

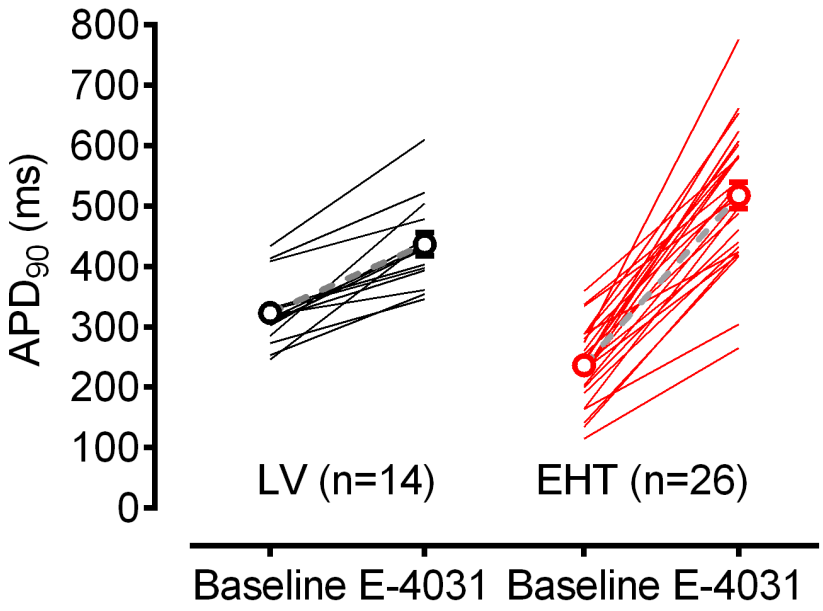

Figure 31. Effect of I_{Kr} block by one single high concentration of E-4031 (1 µmol/L).

Paired data of experiments in which a dose of 1 µmol/L E-4031 was applied with action potential duration (APD_{90}) increase in left ventricle (black) by an average of 113.7 ms in 14 experiments and in engineered heart tissue (red) by 259.6 ms in 26 experiments with a highly significant $p<0.001$ in both cases. Average values are presented by circles and connected by grey dotted line.

3.3.2 Effects of cumulatively increasing concentrations of E-4031

Concentration-response curves were constructed to ascertain the sensitivity of APD prolongation of EHT and LV in response to E-4031. The starting point was a concentration of 1 nmol/L and E-4031 was cumulatively added to this in half-logarithmic steps. The actual prolongation of the AP started slightly above 0 mV membrane voltage, indicating that at higher voltages I_{Kr} does not contribute to regulation of AP shape in LV. The same was true for EHT, however prolongation was much larger than in LV, while starting from a shorter APD_{90}.

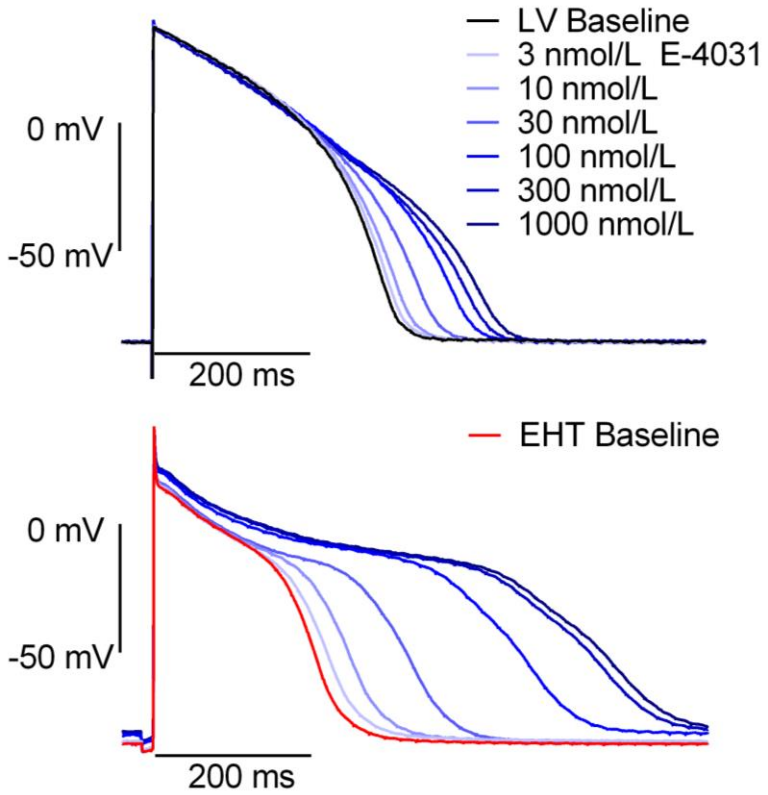

Figure 32. Concentration-dependency of E-4031 on AP shape.

Action potential (AP) recording traces of left ventricle (LV, top) with baseline AP (black), and engineered heart tissue (EHT, bottom) with baseline AP (red) and cumulatively added concentrations of 3, 10, 30, 100, 300 and 1000 nmol/L E-4031 in blue.

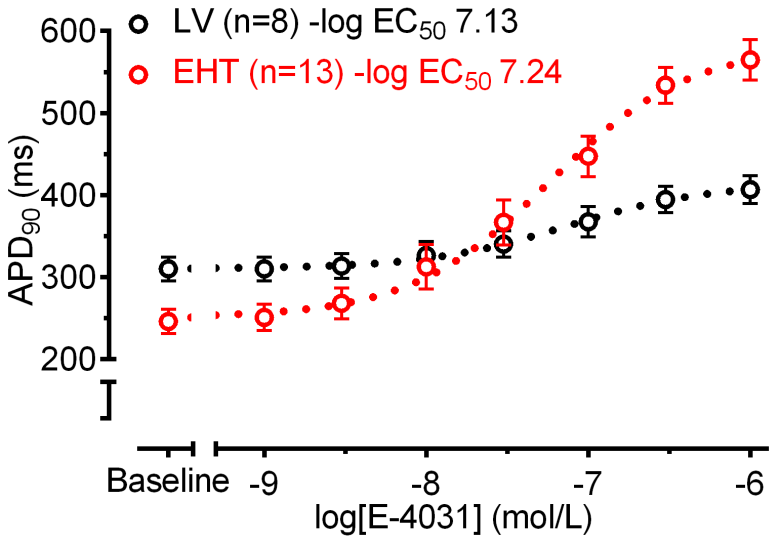

Figure 33. Concentration-response curve for E-4031 effect on action potential duration.

Mean data are depicted for APD_{90} measured in left ventricle (black, LV) and engineered heart tissue (red, EHT) exposed to increasing concentrations of E-4031 (half-logarithmic steps) Dotted lines represent fitted concentration-response curves.

In the sigmoid curve of APD_{90} over logarithmic concentration of E-4031 the shorter baseline and longer elongation of EHT during I_{Kr} block can be noted as well. The half maximal effective concentration was calculated as -log EC_{50} 7.13 in LV vs. 7.24 mol/L in EHT (n. s.) while E_{max} differed significantly F-Test, F-ratio=9, p<0.001).

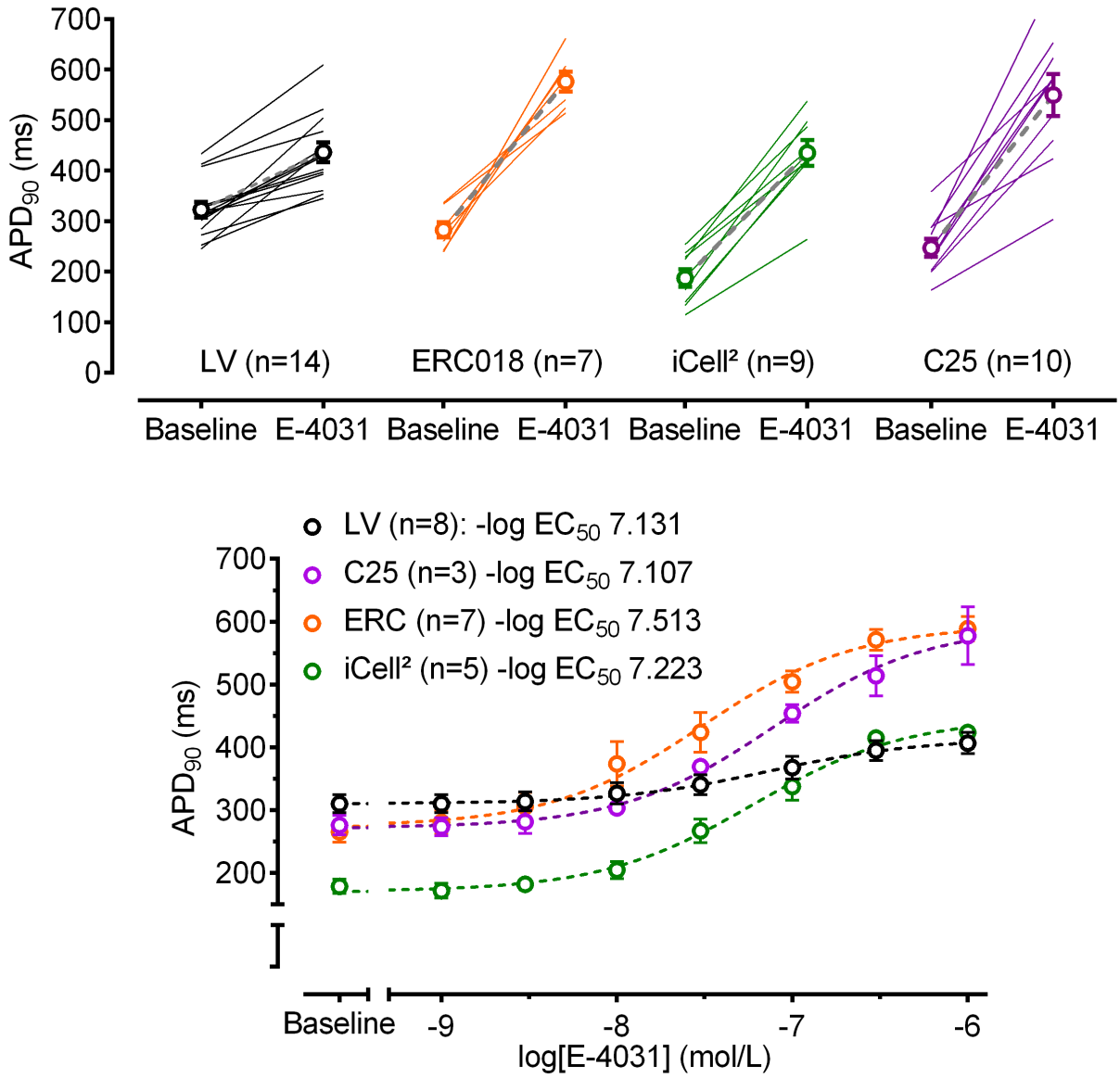

Figure 34. Action potential prolongation by I_{Kr} block in subgroups.

Prolongation of action potential duration at 90% repolarisation of different subgroups of left ventricular (black) and engineered heart tissue (coloured) upon I_{Kr} block with E-4031 in a single concentration of 1 µmol/L (top) showing single experiments and mean value presented by the circle and SEM connected by grey dotted line. Bottom shows the concentration-response curve for the different cell lines with mean values as circles with SEM bars (cumulatively increasing concentrations) Dotted lines represent sigmoidal curves. EC_{50} values (in M) given as inset.

3.3.3 Reverse use dependency of I_{Kr} block-induced prolongation of APD

Classic antiarrhythmic compounds (Class I drugs) show “use dependency” of action. This describes the phenomenon that a drug effect is larger when the target is more active, e.g. an enzyme with a higher reaction rate or an ion channel that is activated more often due to voltage changes. Opposite effects are shown for I_{Kr} blockers: “reverse use dependency”. There is a higher effect of the compound on APD when the target is less frequently activated. With regards to antiarrhythmic drugs APD prolongation correlates inversely with the beating frequency of the tissue/heart, so there is a higher effect of the potassium channel blocker (and thus a bigger prolongation) at lower frequencies.

In the human heart, AP prolongation by I_{Kr} block is typically larger at slower beating rate. (Hondeghem and Snyders 1990; Ohler and Ravens 1994; Vermeulen et al. 1994; Jost et al. 2005). Therefore, we studied effects of I_{Kr} block by E-4031 on APD_{90} at different pacing rates in a subset of experiments.

Reverse use dependency of I_{Kr} block on APD was present in both LV and EHT. In human LV tissue the baseline rate dependency had a higher amplitude than EHT from slowest to fastest beating frequency. The prolongation of APD upon I_{Kr} block however was much higher in EHT from 195.3±9.01 ms at 3 Hz (n=5) to 854.5±79.52 ms at 0.33 Hz (n=4, Δ=659.2 ms) compared to LV with 243.9±15.6 ms at 3 Hz (n=2) to 582.8±51.58 ms at 0.33 Hz (n=5, Δ=338.9 ms, $p<0.01$) This indicates a stronger reverse use dependency of I_{Kr} block in EHT.

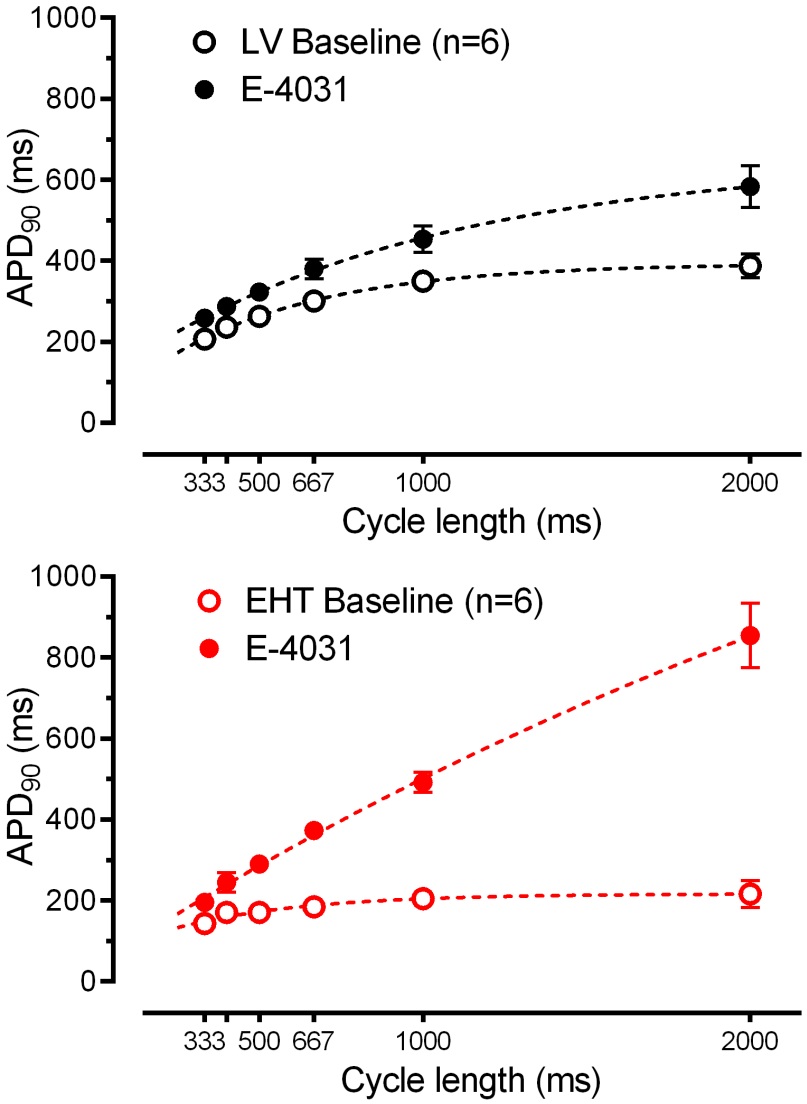

Figure 35. Reverse use dependency of E-4031 in left ventricular and engineered heart tissue.

Mean values for APD_{90} and SEM under baseline conditions and in the presence of E-4031 measured at different cycle lengths. APD_{90} prolongation by E-4031 shows larger prolongation in EHT (F-Test, F-ratio=129.1, p<0.0001) than in LV (F-Test, F-ratio=19.2, p<0.0001) at long cycle lengths, increasing from a shorter baseline APD in EHT to a longer one under compound influence.

3.4 Effects of I_{Ks} Block on APD

Another relevant potassium channel in repolarisation of the cardiac AP is the slow delayed rectifier potassium current I_{Ks}. The I_{Ks} blocker HMR-1556 was used to explore the contribution of this current to the repolarisation reserve.

3.4.1 Effects of a single, high concentration HMR-1556 on APD

HMR-1556 was used in a concentration of 1 µmol/L, which was assumed to block almost 100% of I_{Ks} conductance (Gögelein et al. 2000). From the LQT1 loss-of-function mutation of the *KCNQ1* I_{Ks} is expected to function as one of the key-mechanisms for a QT-regulation and electrical stability.

In human LV HMR-1556 did not significantly change APD_{90} (from 336.7±24 ms to 335.1±24.8 ms, n=9, paired T-test p=0.87). The same was observed in EHT with an APD_{90} of 248±43 ms at baseline vs 249±44 ms with the drug; (n=7, p=0.77, paired T-test)

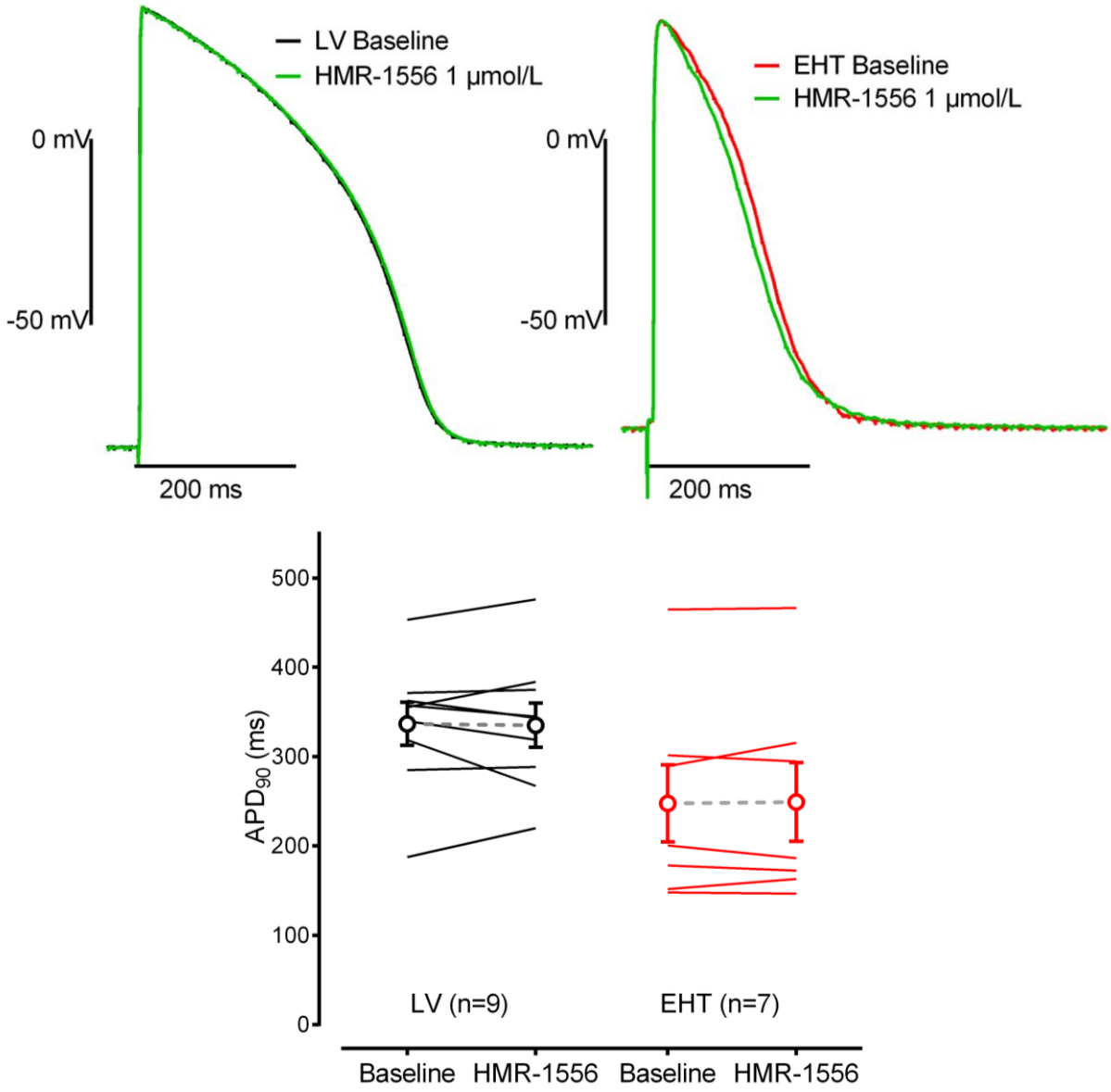

Figure 36. I_{Ks} block by HMR-1556 does not prolong APD in LV and EHT.

Example action potential traces of baseline left ventricle (top left, black) and engineered heart tissue (top right, red) and effect of 1 µmol/L HMR-1556 (green) on both. Individual data of APD_{90} of left ventricle (bottom black) and engineered heart tissue (bottom, red) at baseline

conditions and in the presence of 1 µmol/L HMR-1556. Circles indicate mean values with error bars indicating SEM connected by the dotted grey line.

3.4.2 Effects of I_{Ks} block by HMR-1556 on top of E-4031 I_{Kr} block

HMR-1556 was added to preparations pre-treated with 1 µmol/L E-4031 I_{Kr} block to find out if I_{Ks} contribution on APD can be unmasked in a situation of already impaired repolarisation reserve. The effect was similar to a single dose of HMR-1556 alone, showing only a trend of prolongation. There was neither a significant change in LV (from 465±34 ms to 476±41 ms; n=6, p=0.50, paired T-test) nor in EHT (from 526±49 to 537±51 ms; n=4, p=0.20)

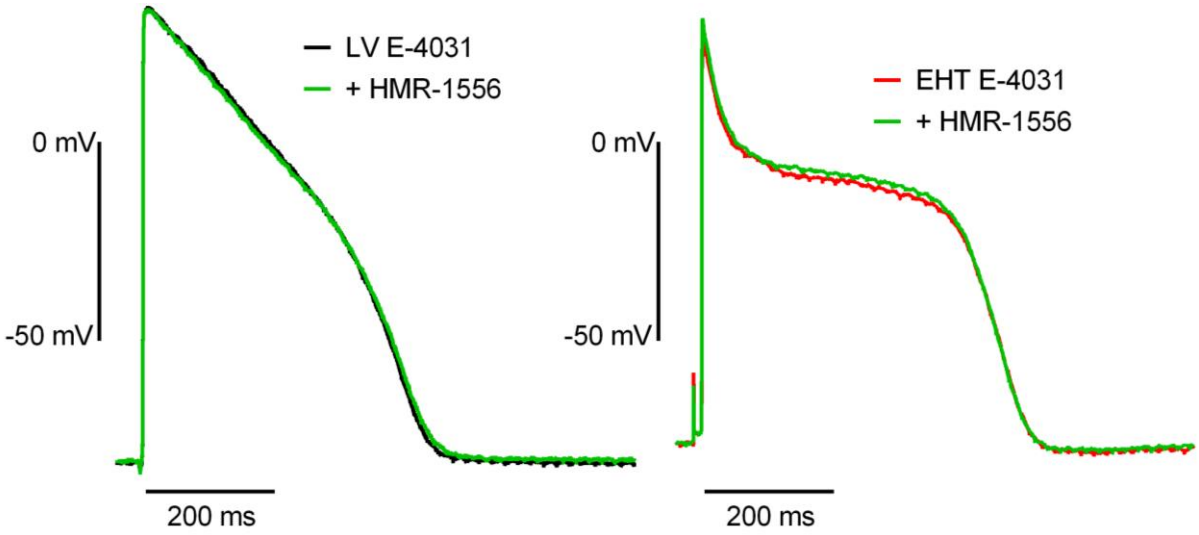

Figure 37. I_{Ks} block by HMR-1556 on top of I_{Kr} block by E-4031.

Example action potential traces recorded in left ventricle (left, black) and EHT (right, red) in the presence of 1 µmol/L I_{Kr} blocker E-4031 showing a big AP prolongation and when I_{Ks} was blocked on top with 1 µmol/L HMR-1556 with little additional effect.

3.4.3 Effect of HMR-1556 under adrenergic stimulation and reduced repolarisation reserve

Patients with LQT1 typically show arrhythmias during physical or emotional stress. In these situations, there is a marked adrenergic stimulation which has been found to increase I_{Ks} contribution. When LV and EHT were pretreated with 100 nmol/L isoprenaline the same concentration of HMR-1556 produced a significant APD_{90} prolongation. When isoprenaline was added on top of E-4031 APD_{90} did not change neither in LV (435±36 ms E-4031 vs. 436±36 ms E-4031+Iso; n=4, p=0.73; paired T-test) nor in EHT (499±32 ms E-4031 vs. 496±38 ms E-4031+Iso; n=4, p=0.7; paired T-test). This might be due to a coactivation of both I_{Ks} and I_{CaL} upon adrenergic stimulation which has been described before (Jost et al. 2005) and a faster activation kinetic of I_{CaL} compared to I_{Ks} (Xie et al. 2013). Upon subsequent addition of

I_{Ks} block with 1 µmol/L HMR-1556 a notable effect in comparison to I_{Ks}-block without adrenergic stimulation can be seen. In LV APD_{90} increased significantly from aforementioned values (from 436±36 ms in the presence of E-4031+Iso to 445±36 ms in the presence of E-4031+Iso+HMR; n=4, p<0.05; paired T-test). An analogous result could be found in EHT (from 496±38 ms in the presence of E-4031+Iso vs. 515±43 ms in the presence of E-4031+Iso+HMR; n=4, p<0.05; paired T-test).

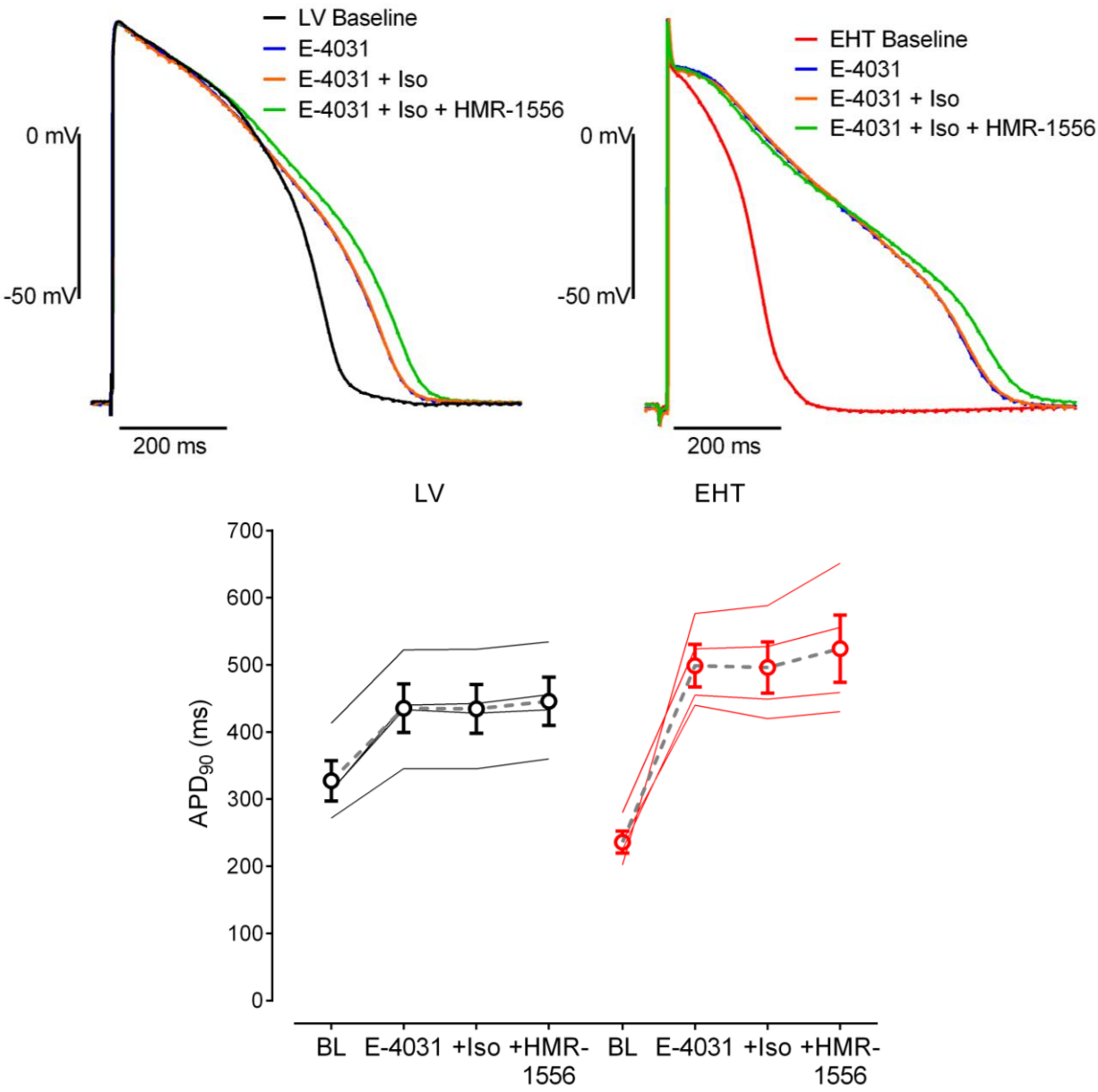

Figure 38. Effects of I_{Ks} block under β-adrenergic stimulation.

Example action potential traces recorded from a human left ventricular preparation (top left) under baseline conditions (BL, black), I_{Kr} blocked by E-4031 (blue), addition of β-adrenoceptor stimulation with isoprenaline (orange) and I_{Ks} block with HMR-1556 (green) and the same procedure for engineered heart tissue (top right). Bottom shows the cumulative effect for action potential duration at 90% repolarisation (APD_{90}) at baseline (BL), 1 µmol/L E-4031 (E-4031), 100 nmol/L isoprenaline (Iso) and 1 µmol/L HMR-1556 (HMR-1556) with mean values in circles with SEM and connected by grey dotted line.

3.5 Effects of I_{K1} block with $BaCl_2$

3.5.1 Effects of a single concentration of $BaCl_2$

The I_{K1} current conducted by the $K_{ir}2.x$ ion channel family is responsible for maintaining the resting membrane potential but also contributes to the final repolarisation phase of the cardiac AP. $BaCl_2$ was used as an I_{K1} blocker in order to evaluate this current's effect on the repolarisation reserve. In a first set of experiments a single concentration of 10 µmol/L $BaCl_2$ was used to determine its repolarisation diminishing effect. From patch clamp experiments in hiPSC-CM one has to expect a block of more than 80% of I_{K1} (Horváth et al. 2018). There was an APD_{90} prolongation from 276.8±22 ms to 300.2±30 ms in LV (n=5; p= 0.06; paired T-test) and from 219.2±15 ms to 239.3±14 ms in EHT (n=6; p<0.01; paired T-test). The absolute difference in prolongation was very similar, suggesting a nearly identical impact of I_{K1} on repolarisation in LV and EHT. 10 µmol/L $BaCl_2$ had no significant impact on the resting membrane potential.

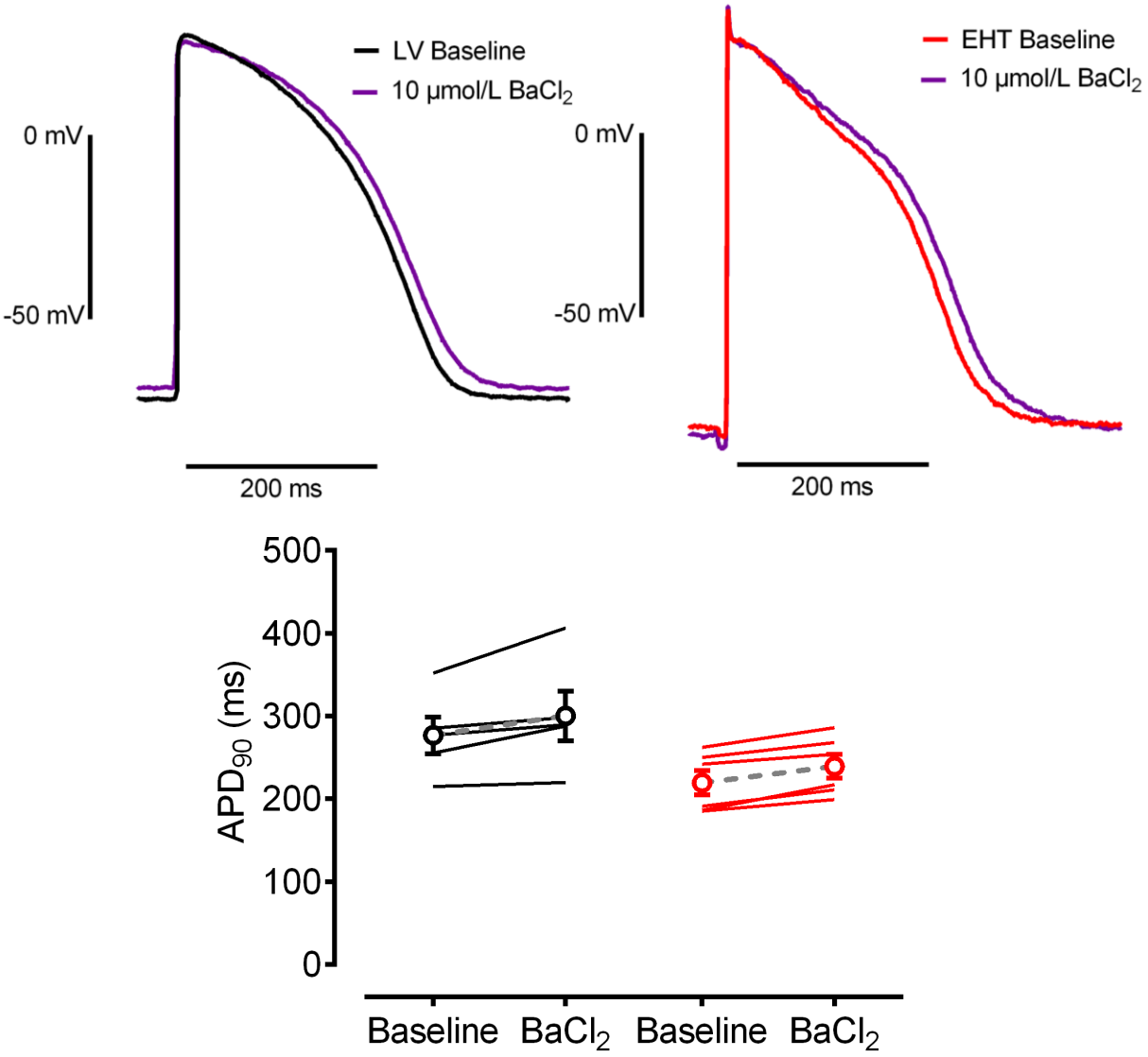

Figure 39. Effect of I_{K1} block by 10 µmol/L barium chloride.

Example AP traces of baseline left ventricular tissue (top left, black) with effect of barium (violet), and engineered heart tissue with baseline trace (top right, red) and barium effect (violet). Bottom shows APD_{90} of left ventricular (black, left) and engineered heart tissue (right, red) at baseline conditions and with 10 µmol/L $BaCl_2$ with mean values in circles connected by grey dotted line and SEM error bars.

Another use of barium in higher concentrations was to attempt to destabilise the resting membrane potential and provoke afterdepolarisations in LV in an impaired repolarisation situation. Result of this will be shown in the following chapters.

3.5.2 Barium chloride concentration-response

Since 10 µmol/L $BaCl_2$ did not depolarise the RMP higher concentrations of $BaCl_2$ were applied. A concentration-effect curve for the effect of $BaCl_2$ on RMP and APD_{90} was constructed in half-logarithmic concentration steps of 10, 30, 100 and 300 µmol/L. Even with very high concentrations of $BaCl_2$ the increase in APD_{90} was modest showing a non-significant trend to longer APD_{90} in LV (393.8±42 ms, n=5, p=0.24) and in EHT (333.1±41 ms, n=5, p=0.117). The effect on RMP was also not significant with a total change in RMP at 300 µmol/L $BaCl_2$ from -74.5±2.8 mV to -72.1±1.8 mV in LV (n=5, p=0.504) and from -79.2±1.1 mV to -69.1±6.5 mV in EHT (n=5, p=0.26)

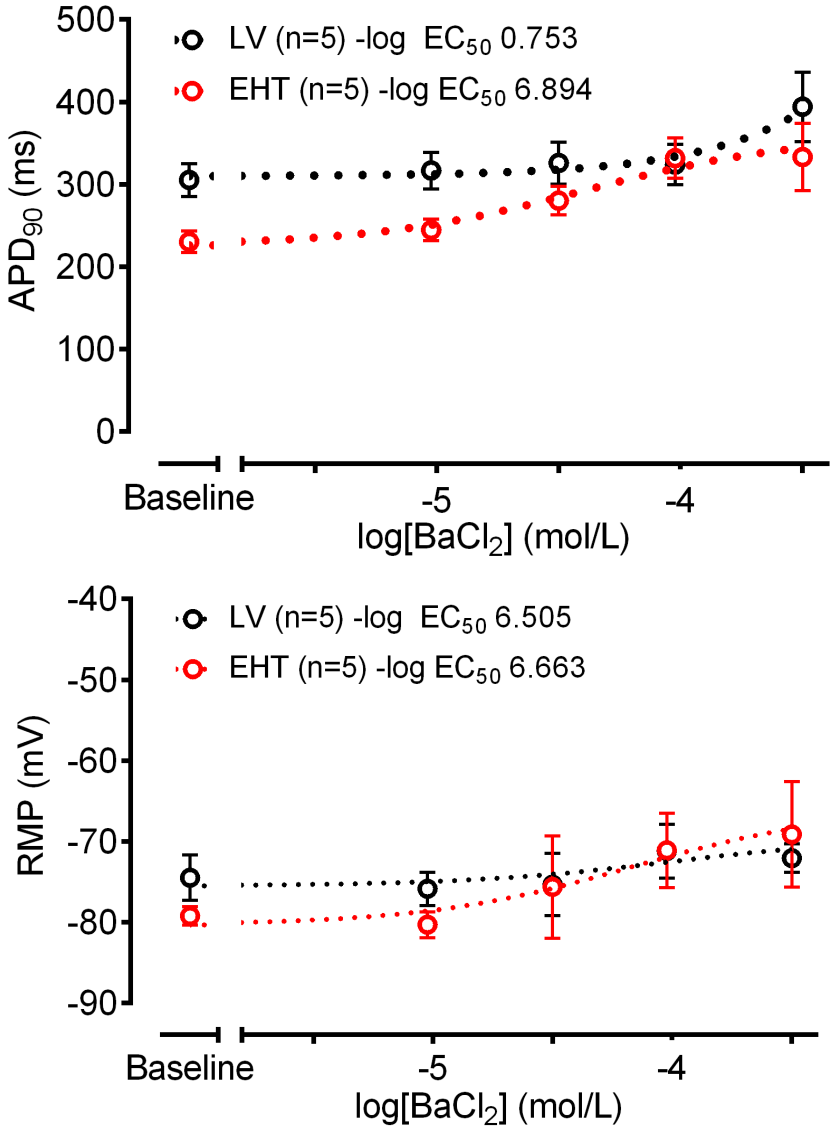

Figure 40. Concentration-response curve for $BaCl_2$ on APD.

Mean values for RMP (bottom) and APD_{90} (top) with SEM under baseline conditions and in the presence of cumulatively increasing concentrations of $BaCl_2$ in left ventricle (black, LV) and engineered heart tissue (red, EHT) on a logarithmic scale showing concentration-response curve for I_{K1} block by $BaCl_2$.

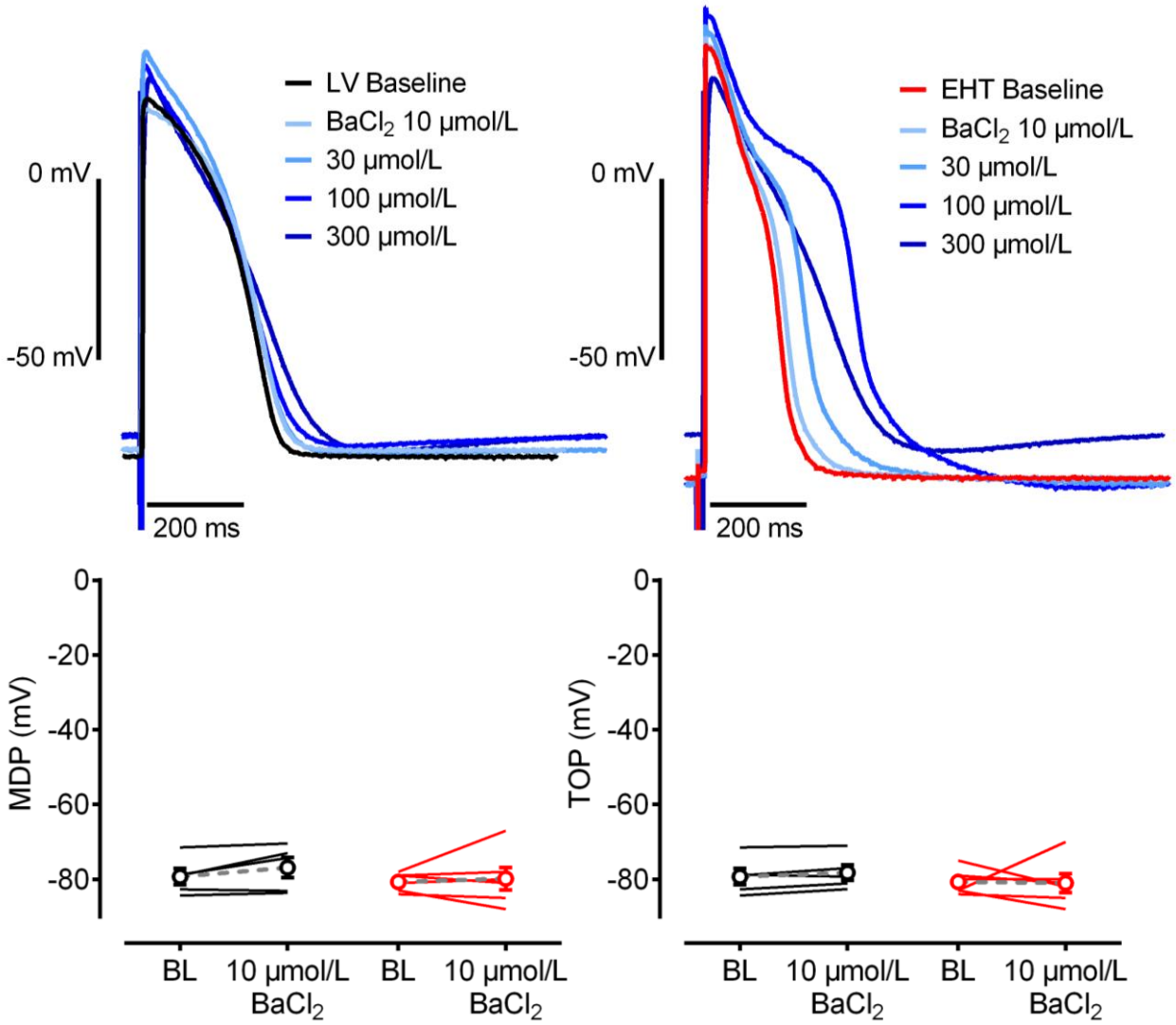

Figure 41. Concentration-dependent effects of barium chloride on AP shape.

Action potential (AP) recording traces of left ventricle (top left, black), and engineered heart tissue (top right, red) and cumulatively added concentrations of 10, 30, 100, 300 µmol/L barium chloride ($BaCl_2$) in blue tones. Bottom shows maximum diastolic potential and take-off potential of left ventricular (black, n=5) and engineered heart tissue (red, n=6) at baseline conditions and with 10 µmol/L $BaCl_2$ with mean values connected by grey dotted line and SEM error bars.

3.6 Early afterdepolarisations in response to potassium channel block in EHT and LV

3.6.1 Shape of EAD in LV & EHT

In any live beating cardiac tissue early afterdepolarisations (EAD) or triggered activity (TA) indicates electrical instability. EADs occur in the so-called vulnerable phase of the AP and can lead to reactivation of sodium and calcium channels. This can cause a disseminated electrical excitation of the tissue and can *in vivo* lead to malignant arrhythmia. Triggered activity results when fast reactivated sodium currents interrupt the repolarisation phase. In measuring APs in cardiac tissue, it is important to ascertain the likelihood of LV and EHT to show EADs and to make conclusions from this to further characterise EHT as a model for arrhythmogenicity. The standard method to invoke arrhythmia in tissues is administration of I_{Kr} blocking E-4031. In addition, we applied some further arrhythmogenic interventions, such as I_{Ks} block, I_{K1} block, lowered potassium concentration, adrenergic stimulation and slow pacing rate.

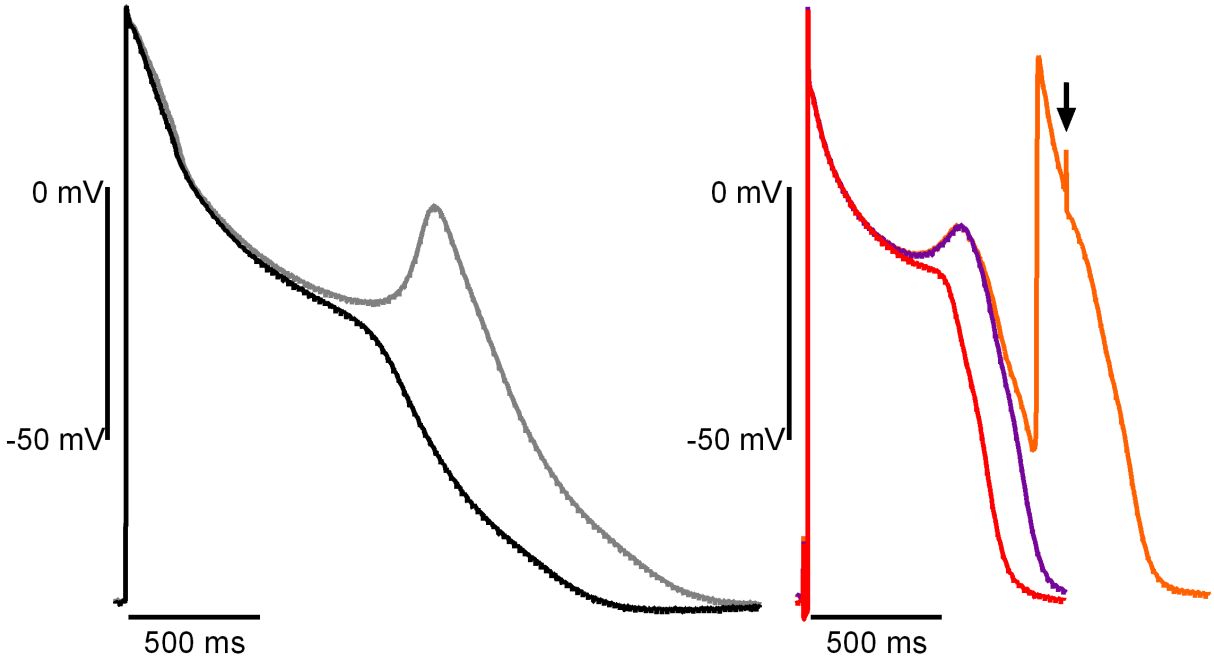

Figure 42. Action potential plots showing early afterdepolarisations.

Action potential traces of an early afterdepolarisation (EAD) in left ventricle (left: black, EAD in grey) at arrythmogenic conditions ($[K^+]$ 2.7 mmol/L, 1 µmol/L E-4031, 1 µmol/L HMR-1556, 300 µmol/L $BaCl_2$, cycle length 3000 ms, 100 nmol/L isoprenaline), and the correspondent in engineered heart tissue upon single I_{Kr} block with 1 µmol/L E-4031 at 1 Hz pacing frequency (right: red prolonged action potential, violet EAD, orange triggered activity, arrow points at pacing artefact).

3.6.2 Amount of APD_{90} prolongation associated with EAD development

I_{Kr} block alone never produced EADs in LV, but slightly prolonged APD_{90} as described above. In EHT however, I_{Kr} block provoked EADs in about 50% of the tissues measured. In some it

even produced triggered activity with a very fast upstroke of a new premature AP. EAD in LV occurred only at much longer APD_{90} than in EHT and could only be precipitated by escalating combinations of arrhythmogenic factors. Triggered activity was not observed in LV at all.

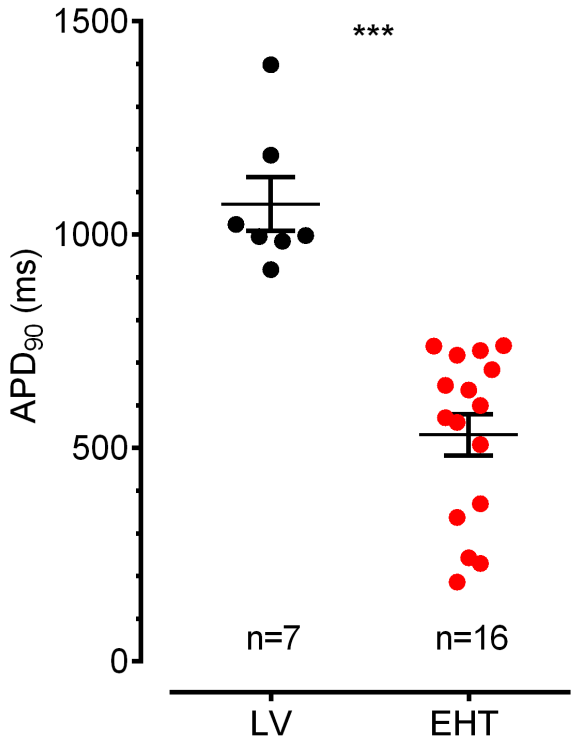

Figure 43. Action potential duration of left ventricle and engineered heart tissue at occurrence of early afterdepolarisations.

Individual APD_{90} of action potentials preceding EADs represented by circles in LV (black, left) and EHT (red, right) with a significantly shorter action potential in EHT of 531 ms±49 vs 1072 ms±63 in LV (unpaired T-test $p<0.001$). Mean values and SEM bars in black.

3.6.3 Precursor of EAD development: AP alternans vs. continuous APD prolongation

In development of EAD during a measurement and after installation of the specific arrhythmogenic trigger two different “modes” of EAD development were found in LV and EHT.

One form of EAD development was an alternans of APD_{90} under arrhythmogenic conditions, in which slightly shorter and longer APs alternated in a 1:1 sequence. In the process the longer AP kept on prolonging slightly until an afterdepolarisation formed during the plateau and increased total APD drastically. This mechanism possibly has to do with shifts of intracellular calcium load during different lengths of diastolic phase and the capacity of the cell to regenerate calcium resources. Another factor could be regeneration time of total ion channel availability during diastole.

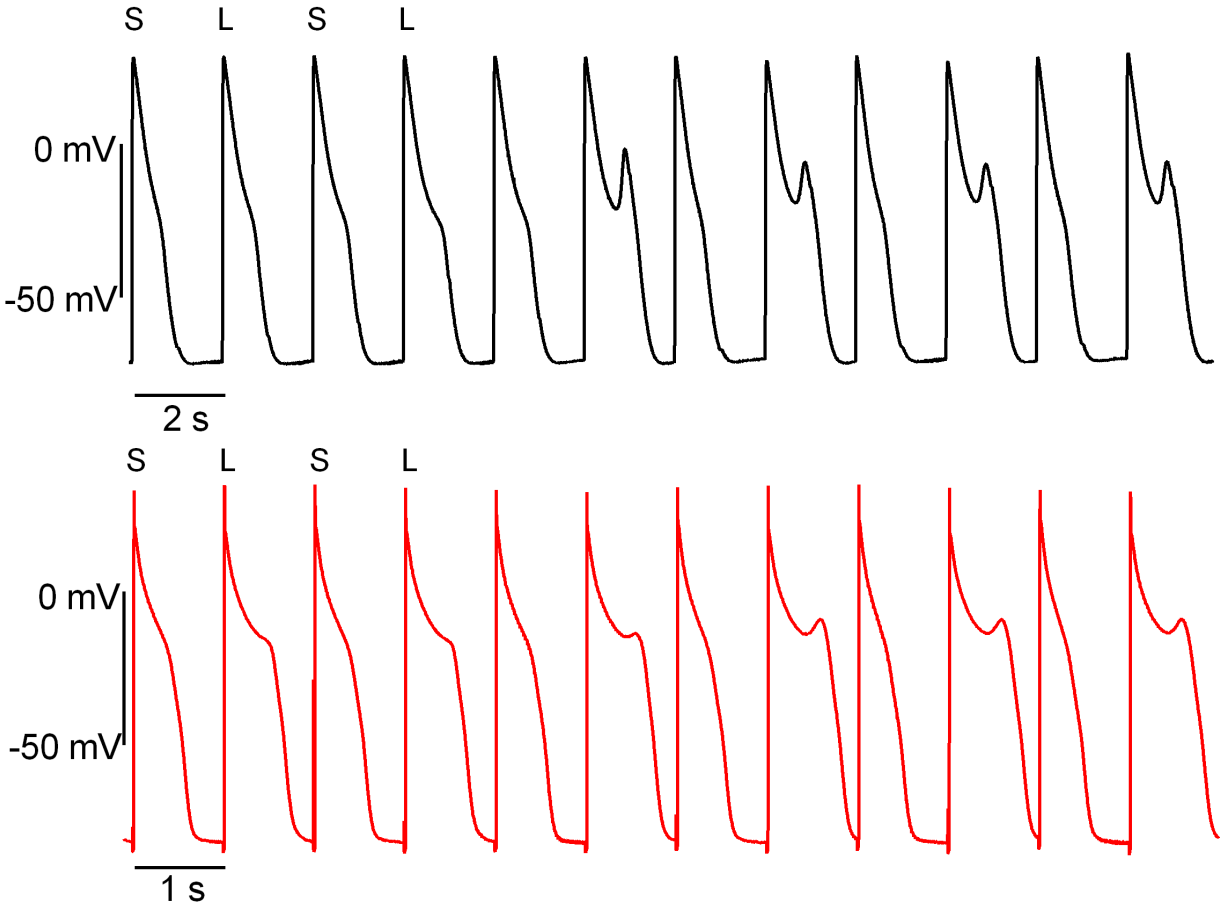

Figure 44. Development of afterdepolarisations in action potential alternans.

Sequence of action potential traces for left ventricle (black, top) at 0.5 Hz pacing frequency and engineered heart tissue (red, bottom) at 1 Hz pacing frequency in a short-long-alternans pattern (S-L-S-L).

Another form of EAD development was the slow constant sequential APD prolongation extending the plateau phase, ultimately resulting in an EAD. In this emergence the EAD occurred before the full maximum effect of the pharmacological intervention (in the case of I_{Kr} block APD prolongation) completed, often shortly after application of a new drug or concentration increase of E-4031. In alternans mode the total prolongation effect of the drug had fully finished after a determined waiting period of at least 10 minutes. The prolongation of the AP plateau results in a reactivation of calcium currents.

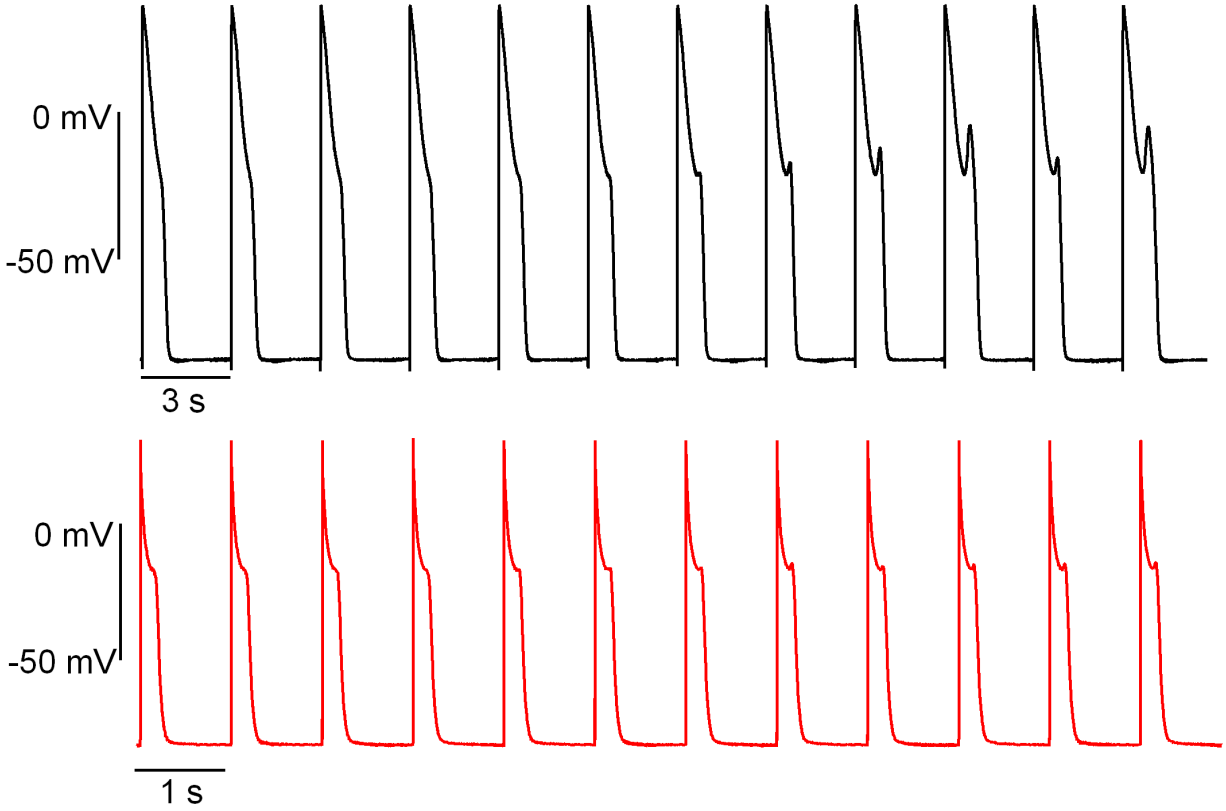

Figure 45. Sequential development of afterdepolarisations in action potential.

Sequence of action potential traces for left ventricle (black, top) at 0.33 Hz pacing frequency and engineered heart tissue (red, bottom) at 1 Hz pacing frequency with continually increasing plateau shoulder leading up to afterdepolarisations.

3.6.4 LV is more resistant to induction of EAD than EHT

Since an I_{Kr} block alone did not evoke EADs in LV tissue an attempt to use several additional arrhythmogenic factors in order to provoke signs of arrhythmia in human tissue was performed. These multiple proarrhythmic factors are shown in figure 46, with a display of its corresponding APD_{90} duration in LV tissue. The relatively low number of EAD occurrences demonstrates how much proarrhythmic stress human myocardial tissue can endure before showing signs of serious arrhythmia.

In addition to ion channel block of the I_{Kr} current another repolarising potassium current (I_{Ks}) was impaired by 1 µmol/L HMR-1556. To deplete the tissue of even more of its repolarisation reserve, the I_{K1} current was blocked by $BaCl_2$ in concentrations of 10, 30, 100 and 300 µmol/L, causing an additional slight destabilisation of the resting membrane potential.

In patients, beta adrenergic receptor activation due to stress/exercise or even because of abrupt withdrawal of pharmacological beta adrenoceptor blockade can lead to arrhythmias, including supraventricular and potentially malign ventricular tachyarrhythmias.

Catecholamines applied under *in vitro* conditions are able to induce arrhythmias (Christ et al. 2014; Flenner et al. 2016). By using isoprenaline at a concentration of 100 nmol/L a situation akin to sympathetic stimulation and stress in physiologic conditions was simulated.

Standard conditions for experiments in LV and EHT alike were a high normal potassium concentration of 5.4 mmol/L and a pacing frequency of 1 Hz (1000 ms cycle length/60 beats per minute). Effects were compared to results obtained at lower potassium concentration (2.7 mmol/L) and a low pacing frequency of 0.33 Hz (3000 ms cycle length or 20 beats per minute). Hypokalaemia (K^+ levels below 3.6 mmol/L) causes a change in the resting membrane potential to more negative values states (Zaza 2009). However, lower extracellular K^+ levels decrease the amount of outward repolarising K^+ currents and thereby prolong APD this way (Khan et al. 2013). Another mechanism at work is the modification of Ca^{2+} homeostasis during hypokalaemia, in which the inhibition of Na^+-K^+-ATPase and thereby reduced NXC activity leads to a Ca^{2+} overload facilitating Ca^{2+} releases and EAD/DAD (Tazmini et al. 2020).

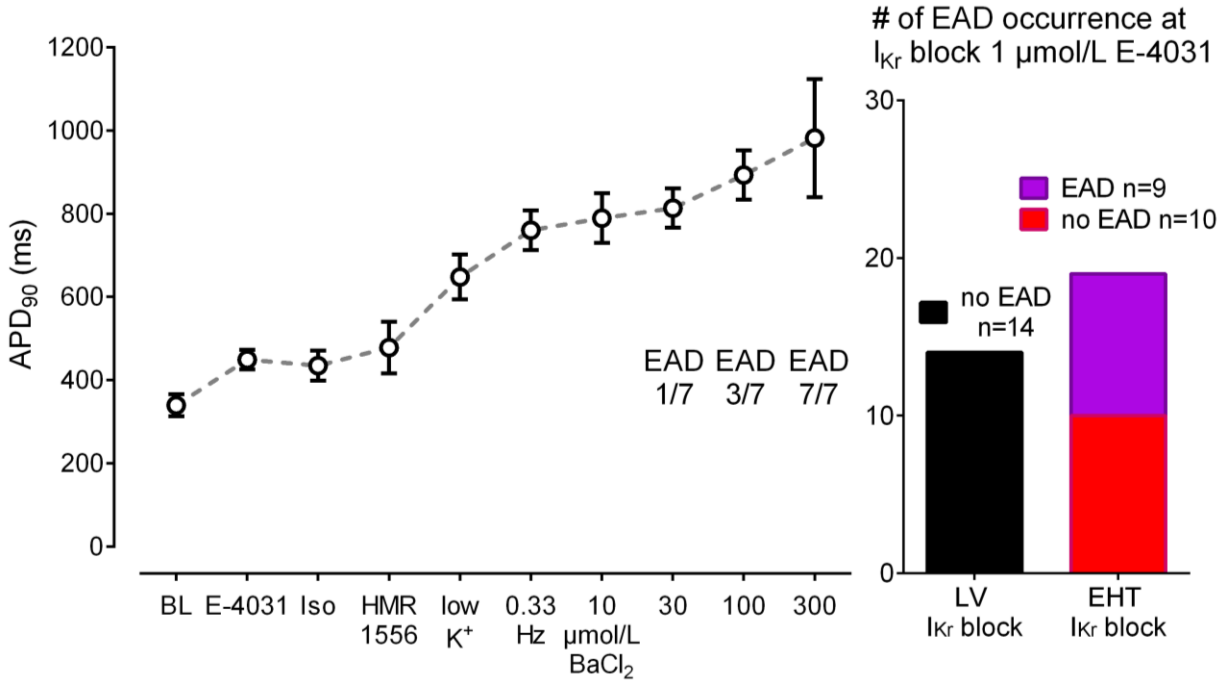

Figure 46. Multiple factors are needed to induce EAD development in left ventricle.

Many different interventions to impair repolarisation reserve are needed to induce afterdepolarisation. Left graph shows the relation between APD_{90} and different proarrhythmic factors that are added consecutively from baseline (BL, left) to barium ($BaCl_2$, right) with concentrations as mentioned before. Occurrence of early afterdepolarisation is indicated by EAD. Right graph shows the number of EAD occurrence by I_{Kr} block alone.

3.6.5 Diastolic interval and EAD development

At longer cycle length during bradycardia, the diastolic interval (DI) and recovery period from the AP is longer. This goes along with an increased period of calcium load in the cell. An

increased intracellular calcium load and Na^+/Ca^{2+} exchanger activity correlate with arrhythmogenesis and a longer plateau phase of the AP can potentially lead to reactivation of Ca^{2+} window currents (January and Riddle 1989; Sipido et al. 2000; Qi et al. 2009).

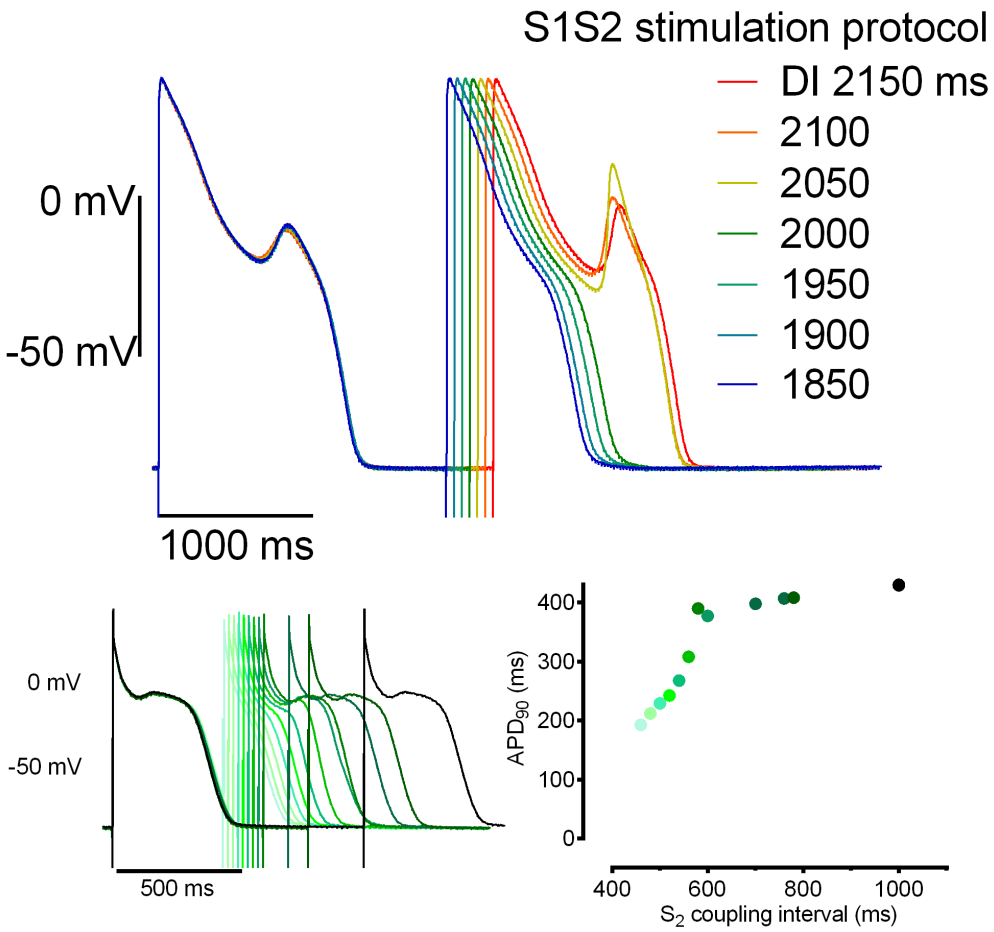

Figure 47. Stimulation protocol in AP showing EAD disappearance at shorter coupling intervals

Action potential sequence of the S1S2 stimulation protocol in left ventricle (top) shows that an incrementally shortened S2 diastolic coupling interval (DI, rainbow-coloured traces with corresponding cycle length) leads to shortening of AP, followed by an increase in EAD amplitude and later the disappearance of afterdepolarisation. Similar results show in engineered heart tissue (bottom left, green). The longer diastolic interval seems to facilitate afterdepolarisations that disappear at shorter S2 coupling intervals also seen in the action potential restitution curve (bottom right).

The activation of calcium window currents and NCX plays a major role during this elongated plateau phase with a strong association to afterdepolarisations (Němec et al. 2016). An AP measurement with consistently occuring EAD during repolarisation was submitted to a S1S2 stimulation protocol in which the standard cycle length impulse was followed by an incrementally shortened interval, and thereby a shorter DI. After a shortening of the S2 interval down to 2000 ms CL the previously constant EAD disappears, suggesting a correlation of

longer DI with EAD development. A similar relationship between DI and following APD was seen in EHT, with EAD occurring at lower pacing rates of 1 Hz already.

3.6.6 Specifity of EAD and arrhythmia detection in EHT I_{Kr} block

Using EHT to detect signs of proarrhythmic potential provides a sensitive test since half of the I_{Kr} blocked EHTs showed EADs. To further determine how specific this test is and whether this applies only to I_{Kr} block by E-4031 other I_{Kr} blocking compounds used in actual patient treatment were tested.

For this specific purpose, an I_{Kr} blocker classified as a non-arrhythmic compound, was tested. Moxifloxacin is a fluoroquinolone antibiotic which produced EADs in single cell cardiomyocytes, however failed to do so in cardiac tissue and did not trigger arrhythmia in animal models (Nalos et al. 2011). In this study moxifloxacin prolonged EHT APD_{90} from a baseline 202±36 ms to 252±52 ms at 10 µmol/L ($p<0.01$) and to an additional 322±58 ms at 100 µmol/L ($p=0.017$; $n=5$) without ever developing signs of EAD.

Verapamil is another example of a non-arrhythmogenic I_{Kr} blocker. The compound is primarily classified as a calcium channel blocker and is widely used in the treatment of high blood pressure, angina pectoris as well as supraventricular tachycardia. It has been identified as an I_{Kr} blocker without torsadogenic effect. Verapamil did not prolong APD_{90} but shortened it (as expected from a Ca^{2+}-channel blocker) from baseline 240±6 ms to 212±10 ms at 1 µmol/L ($p=0.038$, $n=5$). After treatment with verapamil the addition of 1 µmol/L E-4031 caused a prolongation to 282±8 ms without development of EAD ($p<0.01$, $n=5$). This APD prolongation by E-4031 after verapamil (70±13.9 ms) was significantly shorter than I_{Kr} block with E-4031 alone (281.2±18.1 ms, $p<0.01$) which could be explained by the Ca^{2+}-channel blocking effect of verapamil. Thus, it is concluded that EAD development and detection of EHT functions in a more complex mechanism regarding arrhythmic potential and not solely on any I_{Kr} block alone.

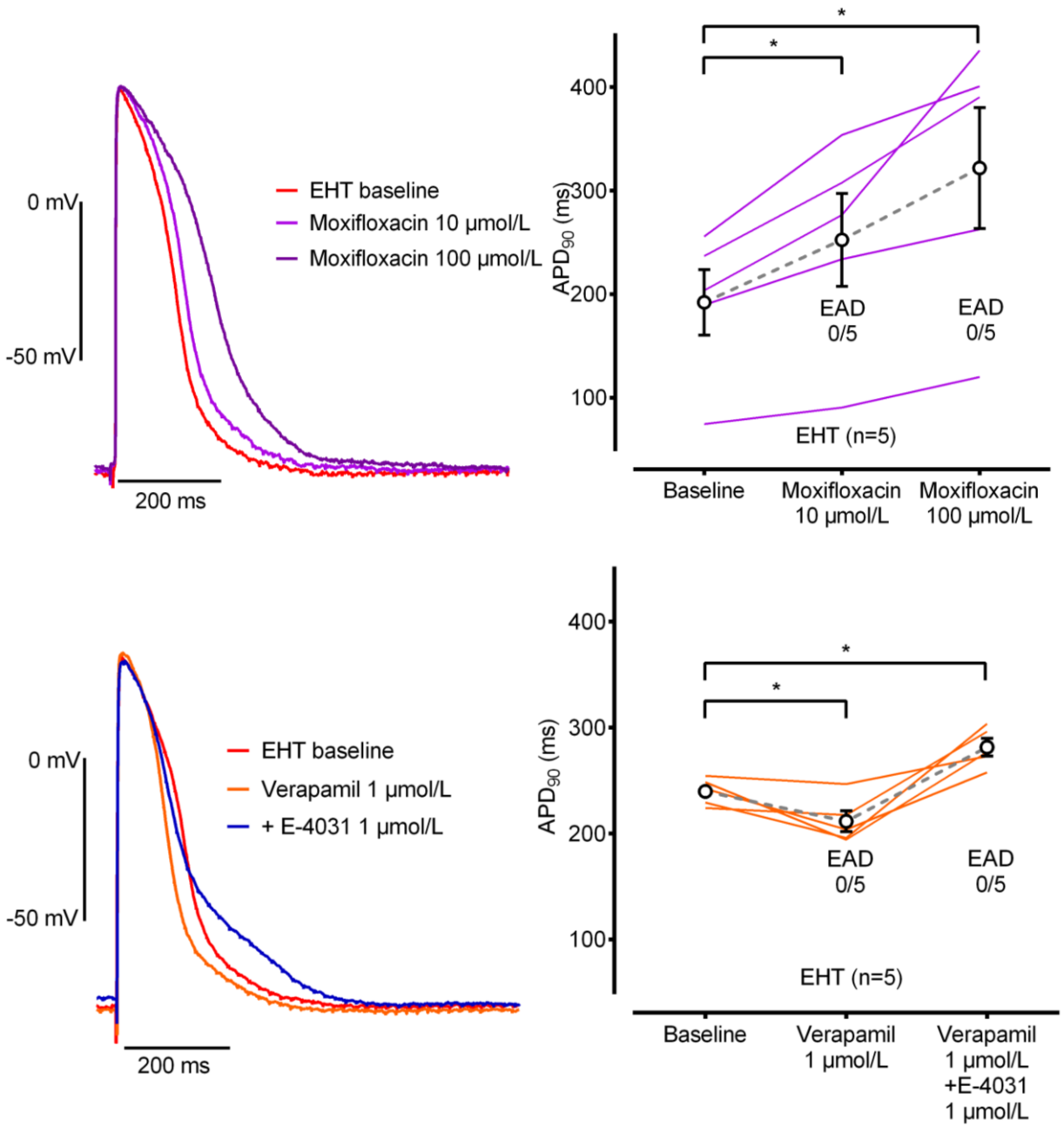

Figure 48. Effects of non-arrhythmogenic I_{Kr} blockers on APD_{90} in EHT

AP illustrating I_{Kr} block not producing early afterdepolarisations with moxifloxacin (top left) or verapamil and E-4031 (bottom left). Action potential duration at 90% of repolarisation of single experiments is shown on the right with significant differences in duration at all interventions.

3.6.7 Predictors for arrhythmic factors

3.6.7.1 Short Term Variability

Several electrophysiological properties of cardiac cells and tissues have been tested to evaluate the prediction likelihood of developing arrhythmia. Among others the short-term variability (STV) of APD was looked at. It is calculated as follows (Thomsen et al. 2004).

$$\mathrm{STV} = \frac{\Sigma\left(\mathrm{APD90(n+1)} - \mathrm{APD90(n)}\right)}{\left[30\sqrt{2}\right]}$$

This formula describes the mean orthogonal distance from the diagonal line of APD_{90} points on a Poincaré plot. In these kind of plots (as seen in Fig. 49, middle) each APD value is plotted against its previous APD, resulting in a cloud of widely spread or closely clustered points. STV was calculated for 30 consecutive beats during a stable AP signal measurement.

STV did not change by E-4031 in any LV. In contrast, some EHTs exhibited stable STV and did not develop EADs, while other EHTs showed a drastic increase in STV, followed by EAD, indicating a mechanistic link between alternans of APD_{90} and development of EAD.

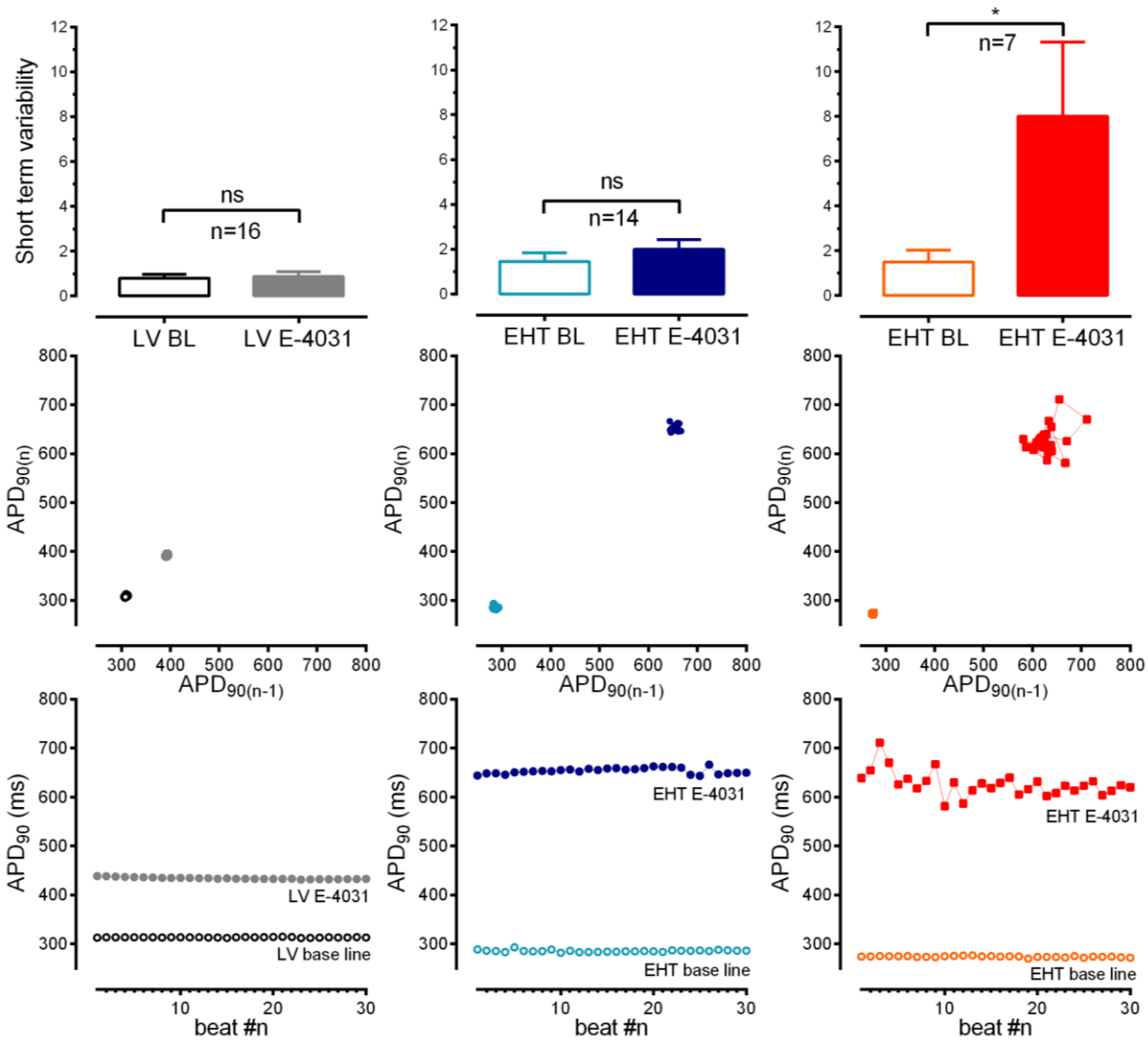

Figure 49. Short term variability of action potential duration in left ventricle and engineered heart tissue in response to E-4031

No significant change in short term variability (STV) occurs in left ventricle (left) and in engineered heart tissue (EHT) that did not develop early afterdepolarisations (EAD) upon I_{Kr} block (middle column). High increase in STV in the group of EHT that did develop EADs later on (right) as can be noted in the calculated value (top row), as well as in the Poincaré plots (middle row) and absolute action potential duration sequence (bottom row).

3.6.7.2 Action potential triangulation

Action potential triangulation (APT) is another arrhythmia predictor taken into consideration. APT was calculated as $APT=APD_{90}-APD_{40}$ and compared EHTs with and without EAD development at baseline conditions and after I_{Kr} block with E-4031 in regard to APT and APD_{90}.

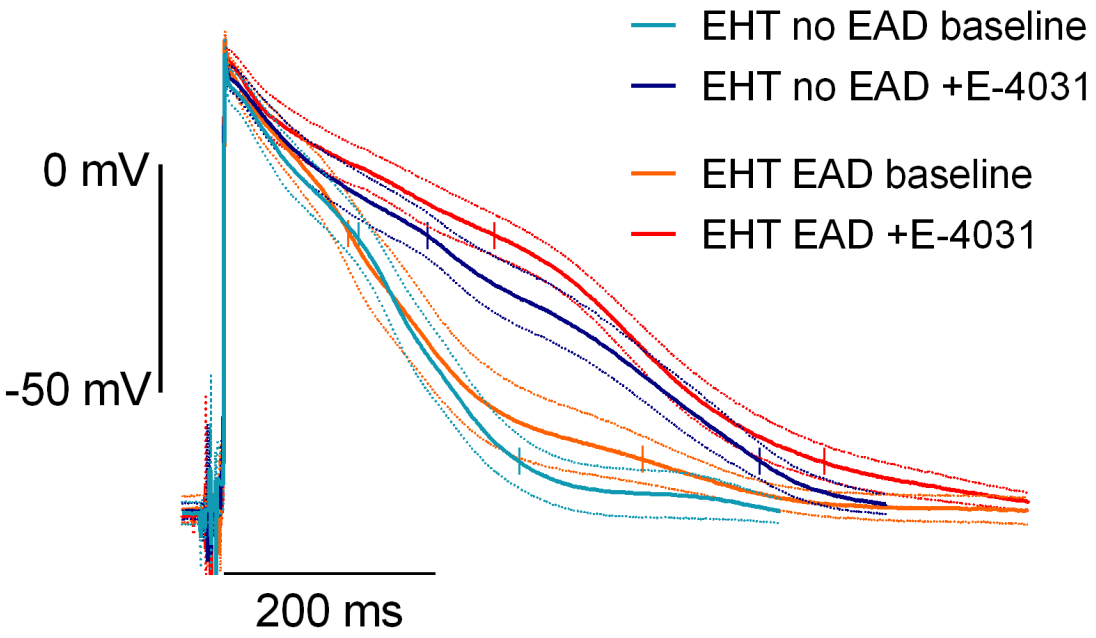

Figure 50. Action potential triangulation plots in engineered heart tissue.

Averaged action potential (AP) traces of engineered heart tissue (EHT) for EHT that developed early afterdepolarisations (EAD) upon I_{Kr} block with E-4031 (orange/red, n=14), EAD or ones that did not (light/dark blue, n=14). The group with EAD shows a longer AP both at baseline and after I_{Kr} block. Traces are marked by upright ticks at APD_{40} and APD_{90} to visualise triangulation.

EHTs with EAD development showed a longer APD in particular in the range below -50 mV. This correlates well with the voltage level at which I_{Kr} currents are most active. It can be assumed that this finding may indicate a lower I_{Kr} contribution in these EHTs. In addition, the longer plateau phase in the presence of E-4031 in EAD-developing tissues (Fig. 50. red curve) might be caused either by larger depolarizing currents via calcium channels and/or NCX or due smaller repolarising potassium currents like I_{Ks} in these individual preparations.

When looking at predictive markers for subsequent arrhythmia APD is one of the most frequently used parameters. It was tested whether APD or AP triangulation of EHTs correlates better with EAD development. APD_{90} of measurements at baseline and I_{Kr} block did not show a significant difference between groups with and without EADs. In contrast APT showed a significant difference between the two groups both at baseline and I_{Kr} block. This might point to APT being a more sensitive predictor in arrhythmia evaluation of *in vitro* engineered heart tissue.

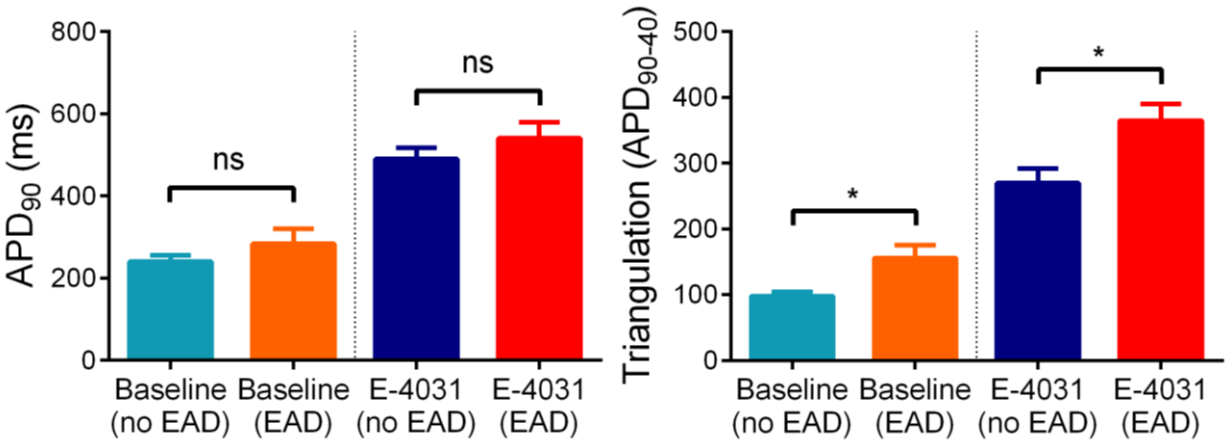

Figure 51. Comparison of action potential duration and triangulation as predictor for arrhythmia in EHT

Engineered heart tissues with (EAD, n=15) and without early afterdepolarisation (no EAD, n=21) development upon I_{Kr} block showing a bigger triangulation in the EAD group. In comparison there was no significance in APD_{90} difference between groups.

4. Discussion

The aim of this study was to characterise AP properties of engineered heart tissue produced from hiPSC-CM and compare them to human left ventricular myocardial tissue. For this purpose, sharp microelectrodes were used to measure intracellular recordings of APs was used by which it was possible to keep the tissue in a live beating system as close to physiological conditions as possible. The analysis of APs recorded under different conditions, including variation in beating frequency, influence of pharmacological ion channel block and manipulation of physiological conditions clearly demonstrates that EHT shares many electrophysiological properties of human adult ventricular tissue. The aim was to find out whether hiPSC-CM EHTs are a valid method to study electrophysiology and arrhythmia with regards to safety pharmacology and how they compare to native human tissue. With this comparison in mind a few major key points of discussion have emerged.

4.1 Diastolic depolarisation of hiPS-CM EHT

In 24 out of 27 EHT experiments there was a relevant amount of spontaneous diastolic depolarisation following an AP. This behaviour is very much unlike any adult working myocardial cell physiology. In working myocardium cells show a stable RMP and need to be critically depolarized from the neighbouring cells. A somewhat spontaneous excitation may exist in working myocardium. However, this rhythm is at a much slower pace and usually acts as an escape rhythm or idioventricular rhythm of cells from either the atrio-ventricular node, His-bundle, Tawara-branches or Purkinje fibres with an increasing interval between excitations when the normal atrio-ventricular conduction does not work (Perez Riera et al. 2010). The spontaneous excitation in EHTs developed at a mean beating frequency of about 1.24 Hz (≈800 ms cycle length or 75 bpm) which is undeniably faster than the normal cardiac escape rhythm of ca. 30-40 bpm (~ 0.6 Hz) in Purkinje fibres (McAllister et al. 1975). In fact, it is closer to the mean resting heart rate dictated by the sinoatrial node in the high right atrium, which is driven by the hyperpolarisation-activated cyclic nucleotide-gated channels (HCN) conducting the pacemaker or “funny current” (I_f). From developmental studies the impact of I_f to pacemaking in ventricular cardiomyocytes is thought to increase during embryonic and fetal development, which might be analogous to hiPSC-CM cultured in EHT (Louch et al. 2015).

The mechanism of pacemaking in EHT is still a matter of debate. There is no doubt that *funny currents* and HCN-channels are involved. These channels mediate a depolarising inward cation current, which activates at more negative membrane potentials and in the presence of cAMP (Baruscotti et al. 2005). They are sensitive to ivabradine, which is used in patients to slow sinus rate (Di Francesco and Camm 2004). Here it was found that beating rates of EHTs

were very sensitive to ivabradine, which is in accordance with own prior data (Mannhardt et al. 2016), but at variance to previous reports in single cell hiPSC-cardiomyocyte cultivation (Kim et al. 2016). Diastolic depolarisation could be reduced almost completely and spontaneous beating rate dropped by 73%. This suggests that a strong diastolic depolarisation does indeed correlate with automaticity in the EHT and a faster spontaneous beating rate.

Since a small effect of ivabradine on repolarisation reserve has been shown in previous studies the substance was also applied to the human left ventricular tissue preparations. It has been reported that at high concentrations of 10 µmol/L evoke a small AP prolongation (Koncz et al. 2011). Here we found no significant effect of 300 nmol/L ivabradine on LV AP parameters, and no impact on AP shape in either healthy myocardial tissue (from patients with compensated AS, AI) or diseased LV preparations (HCM, LVAD, HTX) in our experiments. Therefore, it was assumed that at the concentration of 300 nmol/L no further interference with the analysis of parameters was to be expected.

The efficacy of ivabradine as a DD inhibitor points to the "*funny current*" being the major driving force behind spontaneous diastolic depolarisation EHT and this characteristic of electrophysiological behaviour.

However, spontaneous activity was not completely lost in the EHT format in the presence of ivabradine. This may relate to incomplete block of I_f by 300 nmol/L ivabradine (EC50 ~ 50 nmol/L (Thollon et al. 2007; Mannhardt et al. 2016) or point to other mechanisms, such as the calcium triggered automaticity in cells contributing to spontaneous activity.

4.2 HiPS-CM oversensitive to I_{Kr} block compared to human LV

Blocking relevant ion channels in arrhythmia evaluation revealed substantial differences between LV and EHT. I_{Kr} blockade in EHT from hiPSC-CM prolonged APD_{90} with a higher effect size than it did in LV tissue. AP prolongation started at membrane voltage below -0 mV and was more than twice as high in EHT than in LV (260 ms vs 114 ms). At 1 Hz pacing rate the percentile APD prolongation of E-4031 in LV of about 27% was markedly smaller than the one in EHT of about 104%. The half maximal inhibitory concentration (IC_{50}) of E-4031 was the same in EHT subgroups, with ERC018 being the outlier with a lower IC_{50}.

The more pronounced APD prolongation might be partly explained by ion channel densities in the corresponding cell membranes of hiPSC-CM EHT and LV. Higher expression levels of the *KCNH2 hERG* gene product responsible for the I_{Kr}-channel have been found in hiPSC-CM EHTs so it would be expected that a blockade does have a bigger impact on them (Lemoine et al. 2018).

The phenomenon of a substance showing higher efficacy at higher beating rate is called “use dependency” as known for sodium channel blockers. The opposite effect “reverse use dependency” is typically seen in potassium channel blockers, where a faster pacing rate leads to a lower response and effect size. This also means there is a bigger effect at lower frequencies of heart rate or in this case tissue stimulation. At 1 Hz the APD of LV was about 30% prolonged by I_{Kr} block, in EHT about 86%. At faster rate (2 or 3 Hz) prolongation was distinctly lower, while still larger in EHT than LV. At very slow beating rates of 2000 ms CL or 0.5 Hz the EHT showed a massively larger prolongation of 395% more in comparison to LV’s 51%.

This reverse use dependency was not only detectable in EHT but also surprisingly larger than in LV. Some animal models like guinea pig or rabbit have failed to demonstrate a reverse use dependency of APD prolongation by I_{Kr} block (Ohler and Ravens 1994; Lu et al. 2005). This is relevant since bradycardia is adanger in patients treated with reverse use dependent substances, especially when a predisposition for arrhythmia like genetic LQT syndrome or dysregulated electrolytes is present. A preautomatic pause or long diastolic interval after an extrasystole can be a trigger of bradycardia associated arrhythmias due to AP prolongation, EADs or TdP (Viskin et al. 1996; Kirchhof et al. 2009). The above-mentioned animal model should be unable to detect such a response pattern.

For this reason, it is important to find a model in which many different arrhythmogenic mechanisms can be studied sufficiently and simultaneously to further increase understanding of certain pathomechanisms.

4.3 APD prolongation by I_{Ks} block hard to detect? Similarities to human ventricles

Activity of the sympathetic nervous system and its effects on the myocardium is a critical point in arrhythmogenesis. Beta blocker treatment is one of the most important short- and long-term primary and secondary prevention methods in ventricular arrhythmia. One potassium channel involved in human ventricular repolarisation that is adjusted by adrenergic stimulation is the I_{Ks} slow delayed rectifier current, especially in situations when repolarisation reserve is impaired already (Li et al. 1996; Jost et al. 2005; Christ et al. 2015).

Under *ex vivo* conditions I_{Ks} block by HMR-1556 did not show any significant effect on APD or other AP parameters of either LV or EHT format. The same was observed under impaired repolarisation conditions with I_{Kr} block by 1 µmol/L E-4031. Only upon previous adrenergic stimulation using 100 nmol/L isoprenaline an increase in APD upon I_{Ks} block was found in I_{Kr} blocked LV and EHT tissues. The effect size was relatively small, but more importantly did not differ much between EHT and LV. This reproduces the finding that contribution of I_{Ks} to AP

shape depends critically on an adrenergic stimulus as previously described for human LV (Jost et al. 2005). There was a trend for isoprenaline to shorten APD in EHT (27.5 ms, p=0.08). HMR-1556 on top of isoprenaline prolonged APD_{90}.

Sympathetic nerve activation leads to arrhythmia in many forms of ventricular tachycardia and its influence in LQTS and development of TdP is severe enough that therapeutic approaches include extensive beta blockade and even sympathetic denervation of the left stellate ganglion and thoracic T2-T4 ganglia (Antonopoulos et al. 2017). The EHT system or excised human LV tissues alone however do not seem to represent highly sensitive methods to evaluate this factor very much since a complex autonomous nervous system and its regulation cannot be replicated in the EHT format yet.

4.4 EAD development mechanisms

Human left ventricular myocardium showed afterdepolarisations only at conditions with multiple arrhythmogenic triggers including multiple different potassium channel blocks (I_{Kr}, I_{Ks}, I_{K1}), changes in potassium concentration, pacing frequency and adrenergic stimulation. In some cases, EADs were not even seen under exhaustion of these stressors. In contrast, hiPSC-CM EHT presented a much higher likeliness to develop EADs; in about half the experiments even at I_{Kr} block only. It is notable that EHT APD has a shorter baseline and carries out a bigger proportionate prolongation that leads to higher total APD which generally correlates with arrhythmogenicity.

The mechanisms behind this difference in arrhythmogenicity are not completely understood, however there are a few characteristics that might have an impact on this behaviour. In specific, there are two kinds of factors to be considered: cellular characteristics of induced pluripotent stem cell cardiomyocytes themselves, and structural conditions of the EHT format. Calcium and potassium currents are crucially determining in the cellular mechanisms in particular.

Previous studies have shown that calcium ion influx across the cell membrane is significantly larger in hiPSC-CM than in human LV, as I_{CaL} density is higher, especially in the EHT cell culture format. Furthermore, another calcium channel which is completely absent in human adult LV myocardium is present and active in hiPSC-CM EHT. This T-type calcium current I_{CaT} however, shows a much smaller contribution to the total Ca^{2+} influx than the L-type calcium channel (Uzun et al. 2016).

Computer simulation models indicate that an increased I_{CaL} density in hiPSC-CM EHT contributes significantly to lowering the EAD threshold upon I_{Kr} blockade, while modulation of

I_{K1} to LV human-like density and the addition of I_{CaT} had just a minor proarrhythmic effect (Lemoine et al. 2018). An important balance in the AP is facilitated by the modified I_{Kr} which appears much stronger in EHT and therefore has a bigger part in repolarisation reserve and arrhythmia development. It even seems plausible that the increased I_{Kr} cation outward current equilibrates for the increased cation inward currents I_{CaL} and I_{CaT} and performs in an antiarrhythmic way.

During higher degrees of I_{Kr} block this counterbalance is turned down and the repolarising current is weaker and therefore the time to reach more negative membrane potentials is longer. In this increased AP phase 3 voltage dependent calcium inward currents are active longer and can become large enough to induce EAD.

I_{CaL} activation voltage range starts at around 10 mV and is halved at approximately -10 mV in hiPSC-CM EHT (Uzun et al. 2016). This means that especially AP prolongation as seen in I_{Kr} block has a positive feedback mechanism by prolonging calcium current opening windows, potentially reactivating channels and stretching plateau duration further. Quantification of the ongoing process can be represented as action potential triangulation as opposed to total APD_{90} (Figures 50 & 51). A comparison of APD and APT shows a better correlation of arrhythmic potential in tissues by looking at triangulation derived by plateau duration.

Related to this, the dependency of APD and beating rate comes into play. The tissue experiences a relatively longer diastolic period during slower frequencies of stimulation. During this diastolic interval the cell regulates intracellular and sarcoplasmatic calcium load via SERCA-ryanodine receptor, NCX and Na^+-K^+-ATPase systems. If a longer period of SR-loading occurs during the diastole, a subsequent beat producing a calcium-induced calcium release could have a potentially higher release of Ca^{2+} into the cytoplasm, thus producing a bigger electric membrane change and potentially more AP-plateau prolongation. Accordingly a longer NCX and Ca^{2+} window-current would favour EAD (Louch et al. 2012).

In a single experiment in LV tissue, it was possible to suppress the EAD spike using SEA0400 which is a substance known to block the sodium-calcium-exchanger. This decrease of the EAD amplitude could be observed already with 1 µmol/L. EAD were completely suppressed by 10 µmol/L. However, since it was so difficult to produce EAD in LV this was not yet pursued much further.

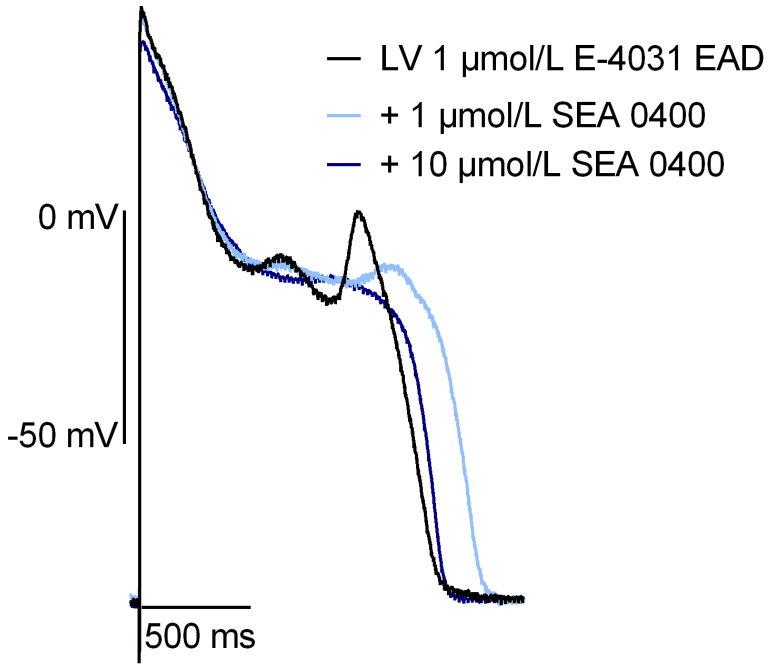

Figure 52. Effect of Na^+/Ca^{2+} exchanger block on early afterdepolarisations.

Action potential traces of left ventricular tissue with stable early afterdepolarisations upon I_{Kr} block when the sodium-calcium exchanger blocker SEA0400 was added. Note the disappearance of EAD shape during repolarisation upon SEA0400.

The structural characteristics of the EHT format are another factor that has to be considered in the behaviour of arrhythmogenesis. The EHT format produces a more rod shaped form of cardiomyocytes, as opposed to the more spherical cell shape in monolayer format or isolated cells (Lemoine et al. 2017). Three dimensional tissue engineereing overall develops a more maturated phenotype (Eschenhagen et al. 2012), but there is still the obvious and distinct difference between human LV myocardium and hiPSC-CM in cell size with hiPSC-CM being two to three-fold smaller than human cardiomyocytes (Uzun et al. 2016). Structural distinctions in EHT include underdeveloped mitochondrial density, intercellular connections, and t tubule structure among others (Mannhardt et al. 2016). The lower cell density of these tissues may also result in less functional electromechanical coupling of the myocardial cells, as there is potentially lower surface area and cell capacitance to properly excite neighbouring cell's electrophysiological mechanisms such as voltage gated Na^+ and Ca^{2+}channels (Eder et al. 2015; Lemoine et al. 2017).

Resulting from this, one might also expect discrepancies in the source-sink behaviour of electric conduction along the tissue. In a less dense tissue the excitation from a cell (as the source) might be connected to less neighbouring cells receiving the electrical conduction (as the sink). Thus, a block in conduction could occur, potentially leading to an increase in dispersion of repolarisation and promotion of arrhythmia (Huang et al. 2016). But less sink in

a tissue also means that there is a decreased capacity of the surrounding tissue to buffer for abnormal conduction patterns such as EADs. Especially in models with less dense three dimensional tissue formation, but rather a more spread out and linear conduction these effects seem to be pronounced (Xie et al. 2010).

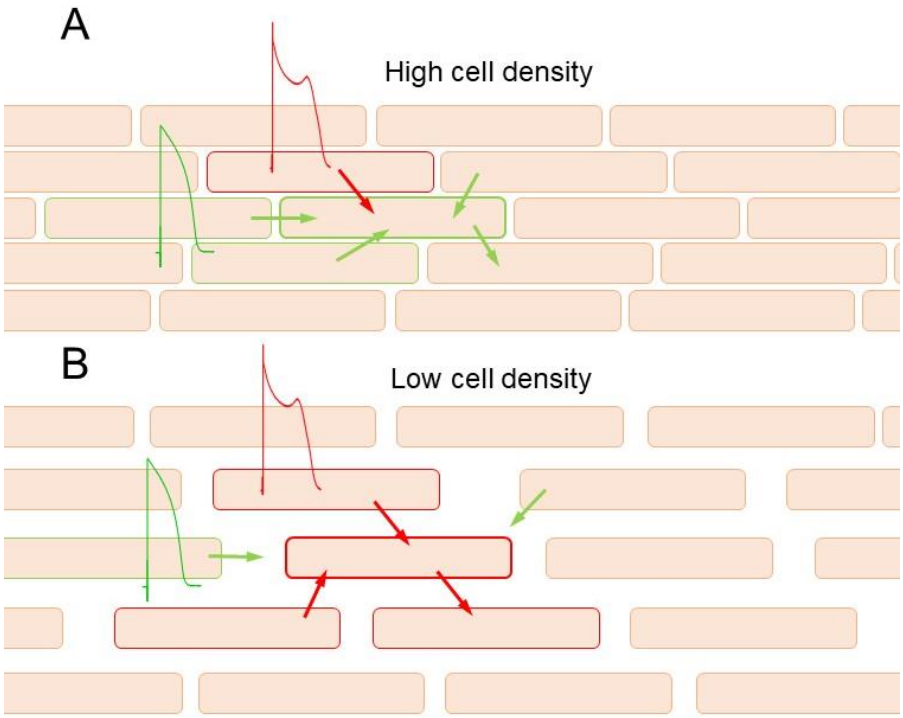

Figure 53. Source sink model of conduction in myocardium.

Electric cell to cell conduction in higher density myocardium (A) and lower cell density tissue (B) with red action potential and arrows signifying proarrhythmic conduction patterns (i.e. afterdepolarisations) and green ones showing normal or less arrhythmic conduction.

4.5 EHT as a model for Purkinje fibres?

In regard to their electrophysiological properties hiPSC-CM EHTs show some notable differences to human LV tissue. Looking closer at the combination of some of these parameters a profile of characteristics emerges, in which similarity to the specific cardiac conduction system more so than to the working myocardium of the ventricle becomes clear. In drug testing and studying arrhythmia Purkinje fibres play an important role, as they present an integral part in arrhythmogenesis of certain entities. The factors that EHT and Purkinje fibres have in common will be discussed below.

Both EHT and rabbit Purkinje fibre showed a marked prolongation in AP duration upon I_{Kr} block using E-4031 or other QT prolonging drugs. This is typically useful in safety pharmacology and LQT assays as a sensitive method to identify potentially proarrhythmic substances. Their high susceptibility to produce afterdepolarisations is another key point in this regard. In this study

about half of the I_{Kr} blocked EHT preparations resulted in EADs upon exclusive use of E-4031 at 1 µmol/L. In experiments with rabbit and canine Purkinje fibres EADs could usually be provoked as well (Nattel and Quantz 1988; Lu et al. 2005; Jonsson et al. 2010), while human and rabbit LV never stood out in this way (Vermeulen et al. 1994; Jost et al. 2005; Lu et al. 2005). Thus, Purkinje fibres can understandably be preferred to ventricular tissue in safety pharmacology to unmask even small risks of arrhythmogenicity.

Furthermore, EHT and Purkinje fibres showed a cellular peculiarity in their calcium channel composition. Next to the common L-Type Ca^{2+} channel conducting the I_{CaL} current found in EHT, LV and Purkinje fibres there is a presence of *CACNA1G*-Gene coded T-type Ca^{2+} channels in EHT (Lemoine et al. 2018) and canine Purkinje fibres and also an expression of T-Type channel protein subunit Cav3.1 (α_{1G}) in human Purkinje fibre cells (Tseng and Boyden 1989; Gaborit et al. 2007). How much these actually contribute to electrophysiological function remains to be investigated.

Lastly, investigations in canine Purkinje fibres have shown results not unlike the ones found in this study regarding ivabradine sensitive diastolic depolarisation in EHT. A spontaneously beating tissue under influence of increasing concentrations of ivabradine resulted in a slower beating rate and decreased DD without any significant change in APD_{90} (Koncz et al. 2011).

Overall, it can be concluded that the hiPSC-CM EHT model can be as sensitive in detecting proarrhythmic factors as previously used Purkinje fibres and shows several striking characteristic similarities. However, for a detailed evaluation a direct comparison study of EHT and Purkinje fibres would most likely be necessary, albeit difficult to realise as acquiring Purkinje fibres in relevant quantity poses an obvious obstacle.

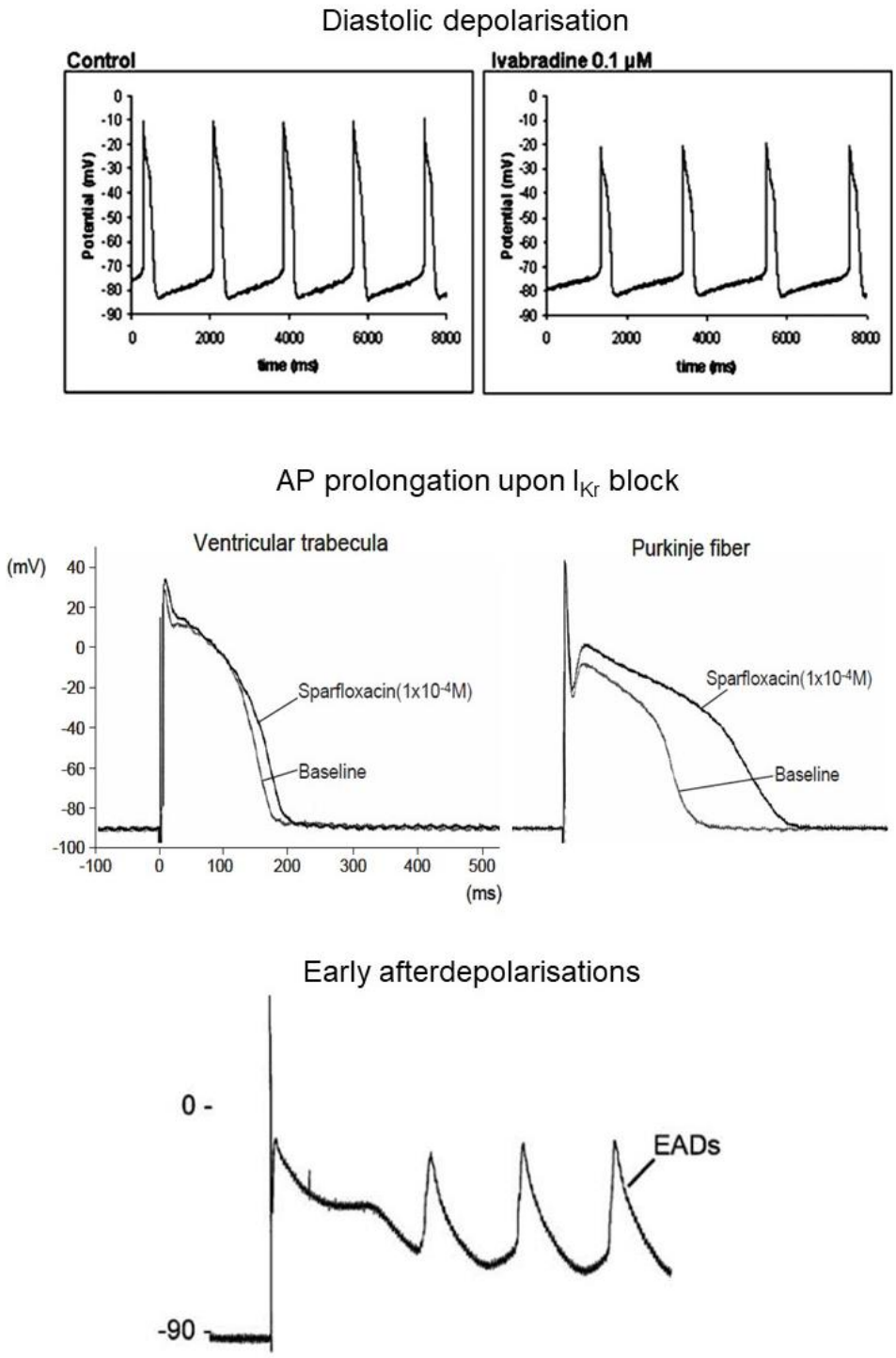

Figure 54. Characteristics of Purkinje fibre tissue.

Purkinje fibres show some response patterns that can be found in stem cell engineered heart tissue (spontaneous diastolic depolarisation, pronounced action potential prolongation upon I_{Kr} block, and development of early afterdepolarisations) are present in some Purkinje fibre tissues. The top shows canine Purkinje fibres and the effect of ivabradine on diastolic depolarisation (Koncz et al. 2011). Middle presents proarrhythmic effect of I_{Kr} block with sparfloxacin in ventricle and Purkinje fibres of rabbits and its consequences at the bottom using sertindole and bradycardia at 0.2 Hz pacing frequency (Lu et al. 2005).

4.6 Error analysis and limitations

In live experimentation there is always room for different kinds of errors and therefore following misinterpretations, inapplicable data due to bias or technical difficulties. The relevant factors and limitations of this project will be discussed in the following.

In the setup of experiments a technique was used which has been established for a long time. Maintenance of the sophisticated microelectrode set-up was a relevant time factor including all noise-reducing interventions and optimisations of puller settings after every change of the filament. However, this mostly affected the time management and planning of experiments and less so the actual quality of measurements, as for every experiment the usability of all parts and systems was tested and if necessary adjusted. Examples of this include the breaking of micromanipulator and stimulator devices, broken heating filaments of the electrode puller and soiled tubing systems of liquid solutions which were all replaced upon notice. Infrequently the grounding electrode in the recording chamber had to be cleaned off residues and trapped air bubbles to allow for a clean undisturbed signal. Upon impalement of the tissue the contact of the glass electrode will be slightly different every time and the breaking of the tip of the electrode cannot be fully prevented and controlled. Therefore, electrode resistance was examined before every new impalement and a range between 20 and 50 MΩ resistance was used to monitor this factor.

In rare cases a whole batch of EHT could be not investigated successfully due to very high baseline frequencies, minimal contraction and inability to find good spots to record APs. The influences on tissue generation and culture are not completely understood and too extensive to discuss in short, thus are not the focus of this work. All EHT cell lines were (by chance) generated from female donors, and data on sex specific AP factors in hiPSC-CM are still unclear.

A presentation of success rates in experiments was given in a previous figure that mentioned criteria to assess the quality of an experiment. One possible form of confirmation bias could be in effect here as AP measurements of worse quality were less likely to be included. AP amplitude was used to monitor for false longer or shorter measured signals as a characteristic of sufficiently realistic values.

Natural variation in AP size, duration and detection of the analysis algorithm add into inaccuracy of analysis. This was counteracted by collecting sample sizes sufficiently large enough to generate robust mean values. In some cases, long stable series of APs could not be maintained and analysis was limited to generating single data points not from averages of tens or hundreds of APs but merely as many as possible with a minimum number of 10 AP per acceptable data point.

Remnants of previously used substances in experiments were washed out of the system with Tyrode's solution and distilled water as well as possible. However, a 100% elimination can never be guaranteed. It was assumed that sufficiently long washout periods of at least 15 minutes managed to clear out substances in concentrations where drug effects could be expected.

Patient's medications and interpersonal physiology of myocardial tissue is another point of concern. Especially patients treated with potassium channel blocking medications such as amiodarone need to be considered more prone to measuring or experimental errors due to differently adjusted cell and tissue electrophysiology and were therefore excluded from the study. Additionally, tissue samples were obtained from patients with valvular or heart failure disease, are thus possibly affected in other disease specific mechanisms.

4.7 Prospects and future outlook

In a potential outlook on future projects further characterisation of hiPSC-CM EHT could be assessed in some aspects that have only briefly been discussed here.

HiPSC-CM have T-type currents in contrast to adult human cardiomyocytes. The physiological relevance is unclear. T-type calcium channel-selective blockers could be used to determine the impact of T-type calcium channels on automaticity, AP shape and arrhythmogenicity.

Another interesting target is the sodium-calcium-exchanger, which is blocked by SEA0400. Its effects on AP plateau, EAD behaviour and even spontaneous activity could be interesting to study. However, it is difficult to engage in this type of research without taking into consideration the whole homeostasis of Na^+ and Ca^{2+} and all factors playing into their balance, including intracellular Ca^{2+} handling of the sarcoplasmic reticulum, SERCA activity etc. In conjunction with these types of mechanisms it could be useful to further investigate L-type calcium channels and their role in calcium handling and arrhythmogenesis.

An approach different from classic ion channel manipulation could be on the level of genes and protein expression. Knockouts of certain genes in EHT coding for proteins like calsequestrin, T-Type Ca^{2+} channel or others could reveal information regardless of pharmacological blockade or drug interaction in the tissue and cells. In this endeavour it would be important to keep in mind the different conditions in which the EHT will culture and grow and possibly adapt or upregulate certain mechanisms to counteract genetic modification.

5 Summary

In this dissertation the main objective was to characterise the cardiac electrophysiological properties of engineered heart tissue (EHT) made from human induced pluripotent stem-cells and to compare it to original human left ventricular myocardium (LV). Especially the *hERG* channel conducting the I_{Kr} ion current was observed in order to find out how EHT fares as a screening system for drug testing with regard to arrhythmogenesis in safety pharmacology.

For this purpose, laboratory grown EHT was compared to human cardiac tissue retrieved from heart surgery. The method of choice for electrophysiological action potential (AP) measurements was intracellular impalement using sharp microelectrodes. This technique allowed for live measurements of beating tissue and manipulation of beating frequency via electric stimulation as well as pharmacological intervention with ion current altering drugs. Conditions of experiments were maintained in a small chamber perfused with physiological Tyrode's solution which was heated to body temperature and supplied with oxygen and pH adjustment by gas inflow.

The main findings of the experiments include a few distinct characteristics of EHT. In contrast to human myocardium, EHT showed autonomous beating and spontaneous diastolic depolarisation. Beating rates often surpassed the physiological range of resting heart rate necessary for proper comparison. Application of the HCN channel-blocking ivabradine diminished both diastolic depolarisation and spontaneous beating rate. Under this condition, external electric stimulation ensured a consistent frequency. This allowed for execution of the same procedure used in LV which showed no reaction to ivabradine. Other baseline AP characteristics did not differ from LV except for AP duration, which was considerably shorter in EHT.

A rate dependency stimulation protocol of different frequencies from 0.33 to 3 Hz revealed that EHT reacted with a similar AP prolongation at slower and shortening at faster frequency. Ion channel blockade of the I_{Kr} current using E-4031 lead to a markedly higher AP prolongation in EHT than in LV in single dose and cumulative application of a concentration of 1 µmol/L. This effect and the reverse-use dependency of this mechanism became especially clear in rate dependency protocols under I_{Kr} blockade, which produced a much higher AP prolongation at lower frequencies in EHT than in LV resulting in very long APD. I_{Ks} block with HMR-1556 did not result in relevant AP prolongation. In fact, it only really showed a slight AP duration increase under beta-adrenergic stimulation with isoprenaline. I_{K1} blockade with $BaCl_2$ increased AP duration in both groups to the same extent and at the same time depolarised the resting membrane potential.

Arrhythmic events on a cellular level, such as early or delayed afterdepolarisations (EAD, DAD) could be induced by applying proarrhythmic stress. In EHT about half of the tissues showed EADs upon I_{Kr} block with E-4031, while LV never did. Investigations using the non-arrhythmogenic I_{Kr} blocking agents moxifloxacine and verapamil showed no EAD inducing effect and prolonged AP by less than E-4031 did. EADs could be provoked in LV only using multiple arrhythmic factors including lowering potassium concentrations, slowing beating frequency, high barium concentrations and adrenergic stimulation. Analysis of a few AP patterns unveiled possible predictor factors for arrhythmogenesis. Short term variability of AP duration increased much more upon I_{Kr} block in EHT that did later develop EADs. At the same time action potential triangulation (APD_{90-40}) was already higher in EAD-developing EHT at baseline conditions before I_{Kr} block, providing basis for discussion of the mechanisms for arrhythmogenesis.

An oversensitive reaction of EHT to I_{Kr} block by E-4031 marks the most dramatic finding. The hERG-channel is one of the most important factors in drug development, as substances with such arrhythmogenic effect cannot safely be used in clinical routine. Especially the reverse use dependency effect, which is ever so present in human electrophysiology, poses an interesting characteristic not observed in most previously used animal models. I_{Ks} blockade on the level of tissue samples and EHT systems seems to play a less significant role in rhythmology which parallel the ex vivo experiments in LV tissue. Bigger significance in other settings including whole hearts and autonomous innervation may be possible. A more prominent role in this setting is played by mechanisms contributing to EAD development in EHT. The interactions between cellular substrate, including ion current composition of I_{Kr}, I_{Ks}, I_{K1}, L- and T-type calcium channels as well as Na^+/Ca^{2+} exchanger, their activation and reactivation thresholds make for excellent basis for further investigation. Structural and culture related context must not be disregarded.

Finally, the many interesting peculiarities of hiPSC-CM EHT point towards a similarity with Purkinje fibres, which are an elementary unit in cardiac conduction and arrhythmogenesis and have been used in electrophysiology for a long time. Expanding on some of these findings may very well lead to important steps in uncovering methods to further progress in drug development screening and using human tissue in arrhythmia research and safety pharmacology.

6 Zusammenfassung der Dissertation

Kardiale ventrikuläre Tachyarrhythmien sind lebensgefährliche Ereignisse, bei denen es zu einer schnellen myokardialen Erregung und Kontraktion des Ventrikels kommt. Eine Verlängerung des Aktionspotentials (AP) und des QT-Intervalls führt zu einem erheblichen Risiko für Torsade-de-Pointes-Tachykardien (Long-QT-Syndrom, LQTS). Ursachen für die AP-Verlängerung können Ionenkanalmutationen oder medikamenteninduzierte Kanaldysfunktion sein. In der Sicherheitspharmakologie werden Substanzen auf eine mögliche proarrhythmische Wirkung auf repolarisierende Kaliumkanäle untersucht. Die Wirkung auf einen einzelnen Ionenkanal kann in Expressionssystemen getestet werden, aber AP-Messungen sind notwendig, um den Nettoeffekt von Substanzen auf die Repolarisation einzuschätzen. Da humanes Herzgewebe nur in begrenztem Umfang zur Verfügung steht werden Messungen in Tiermodellen durchgeführt. Hierbei gibt es erhebliche Unterschiede in der AP-Regulation verschiedener Spezies. Sind humane induzierte pluripotente Stammzell-Kardiomyozyten (hiPSC-CM) in der Lage die Lücke zu Tiermodellen zu schließen? Bislang ist der Beitrag einzelner Kaliumkanäle zur Repolarisation hiPSC-CM in *engineered heart tissue* (EHT) noch nicht vollständig charakterisiert. Im Rahmen dieser Arbeit soll untersucht werden, wie sehr EHT dem menschlichen ventrikulären Gewebe in Bezug auf die Repolarisation ähnelt, und ob das EHT Testsystem etablierten tierischen Gewebemodellen überlegen ist.

Methoden: EHT wurde aus hiPSC-CM hergestellt. Humanes linksventrikuläres (LV) Gewebe wurde von Patienten während Herzoperationen gewonnen. Für Aktionspotentialmessungen wurde die *sharp microelectrode* Technik verwendet. Aktionspotentiale konnten über Stunden stabil gemessen werden, was die Anwendung von Stimulationsprotokollen sowie pharmakologische Interventionen mit ionenkanalblockierenden Medikamenten ermöglichte.

Ergebnisse: Im Gegensatz zu LV zeigte EHT spontane diastolische Depolarisation, Erregung und Kontraktion, die durch Ivabradin-induzierte Blockierung des *funny current* I_f weitgehend aufgehoben werden konnten. Die AP-Form im EHT ähnelte der des menschlichen LV, aber die AP-Dauer im EHT war kürzer. I_{Kr}-Block durch E-4031 induzierte eine größere AP-Verlängerung und zeigte eine stärkere Umkehrverwendungsabhängigkeit als LV. Eine mögliche Ursache hierfür könnte die höhere Kanaldichte und Genexpression des *hERG*-Kanals sein. I_{Ks}-Block verlängerte die APD nur, wenn Beta-Adrenozeptoren stimuliert wurden; der Anstieg der APD war deutlich geringer als bei I_{Kr}-Blockade. Nach I_{Kr}-Blockade entwickelte die Hälfte der EHTs frühe Nachdepolarisationen (EAD), die mit Arrhythmie assoziiert sind. Im Gegensatz dazu waren mehrere proarrhythmische Faktoren notwendig, um EADs im LV zu provozieren.

Schlussfolgerung: Insgesamt weisen LV und EHT gemeinsame Merkmale in der Repolarisation auf, aber die Repolarisationsreserve ist im EHT kleiner, und der I_{Kr} dominiert

die Repolarisation. Der Beitrag von I_{Ks} ist in beiden Geweben eher gering und hängt von der Beta-Adrenozeptor-Stimulation ab. Die Daten legen nahe, dass EHT ein vielversprechendes Modell in der Sicherheitspharmakologie ist, da es im Vergleich zu Tiermodellen ein vollständigeres Modell der menschlichen Elektrophysiologie bietet.

7 References

Journals

Altomare C, Bartolucci C, Sala L, et al (2015) IKr Impact on Repolarization and Its Variability Assessed by Dynamic Clamp. Circ Arrhythmia Electrophysiol 8:1265–1275. doi: 10.1161/CIRCEP.114.002572

Antonopoulos A, Lawrence D, Patrini D, et al (2017) The role of sympathectomy in long QT syndrome. 9:3394–3397. doi: 10.21037/jtd.2017.08.45

Baruscotti M, Bucchi A, DiFrancesco D (2005) Physiology and pharmacology of the cardiac pacemaker ("funny") current. Pharmacol Ther 107:59–79. doi: 10.1016/j.pharmthera.2005.01.005

Bers DM (2002) Cardiac excitation–contraction coupling. Nature 415:198–205. doi: 10.1038/415198a

Bhoelan BS, Stevering CH, van der Boog a TJ, van der Heyden M a G (2014) Barium toxicity and the role of the potassium inward rectifier current. Clin Toxicol (Phila) 52:584–93. doi: 10.3109/15563650.2014.923903

Birinyi P, Acsai K, Bányász T, et al (2005) Effects of SEA0400 and KB-R7943 on Na+/Ca2+ exchange current and L-type Ca2+ current in canine ventricular cardiomyocytes. Naunyn Schmiedebergs Arch Pharmacol 372:63–70. doi: 10.1007/s00210-005-1079-x

Breckwoldt K, Letuffe-Brenière D, Mannhardt I, et al (2017) Differentiation of cardiomyocytes and generation of human engineered heart tissue. Nat Protoc 12:1177–1197. doi: 10.1038/nprot.2017.033

Brette R, Destexhe A (2012) Intracellular recording.

Bussek A, Wettwer E, Christ T, et al (2009) Cellular Physiology and Biochemistr y Biochemistry Tissue Slices from Adult Mammalian Hearts as a Model for Pharmacological Drug Testing. Cell Physiol Biochem 24:527–536.

Camm JA, Fozzard HA, Janse MJ, et al (1991) The ' Sicilian Gambit ' A new approach to the classification of antiarrhythmic drugs based on their actions on arrhythmogenic mechanisms. Eur Heart J 12:1112–1131.

Christ T, Horvath A, Eschenhagen T (2015) LQT1-phenotypes in hiPSC: Are we measuring the right thing? Proc Natl Acad Sci 112:E1968–E1968. doi: 10.1073/pnas.1503347112

Christ T, Kovács PP, Acsai K, et al (2016) Block of Na+/Ca2+ exchanger by SEA0400 in human right atrial preparations from patients in sinus rhythm and in atrial fibrillation. Eur J Pharmacol 788:286–293. doi: 10.1016/j.ejphar.2016.06.050

Christ T, Rozmaritsa N, Engel A, et al (2014) Arrhythmias, elicited by catecholamines and serotonin, vanish in human chronic atrial fibrillation. Proc Natl Acad Sci 111:11193–11198. doi: 10.1073/pnas.1324132111

Dhamoon AS, Jalife J (2005) The inward rectifier current (IK1) controls cardiac excitability and is involved in arrhythmogenesis. Hear Rhythm 2:316–324. doi: 10.1016/j.hrthm.2004.11.012

DiFrancesco D (1993) Pacemaker mechanisms in cardiac tissue. Annu Rev Physiol 55:455–472. doi: 10.1146/annurev.physiol.55.1.455

Difrancesco D, Camm JA (2004) Heart Rate Lowering by Specific and Selective I f Current Inhibition with Ivabradine. Drugs 64:1757–1765.

DiFrancesco D, Ojeda C (1980) Properties of the current if in the sino-atrial node of the rabbit

compared with those of the current iK, in Purkinje fibres. J Physiol 308:353–67. doi: 10.1113/jphysiol.1980.sp013475

DiFrancesco D, Tortora P (1991) Direct activation of cardiac pacemaker channels by intracellular cyclic AMP.

Eder A, Vollert I, Hansen A, Eschenhagen T (2015) Human engineered heart tissue as a model system for drug testing. Adv Drug Deliv Rev. doi: 10.1016/j.addr.2015.05.010

Eschenhagen T, Eder A, Vollert I, Hansen A (2012) Physiological aspects of cardiac tissue engineering. Am J Physiol. doi: 10.1152/ajpheart.00007.2012

Flenner F, Friedrich FW, Ungeheuer N, et al (2016) Ranolazine antagonizes catecholamine-induced dysfunction in isolated cardiomyocytes , but lacks long-term therapeutic effects in vivo in a mouse model of hypertrophic cardiomyopathy. Cardiovasc Res 90–102. doi: 10.1093/cvr/cvv247

Gaborit N, Le Bouter S, Szuts V, et al (2007) Regional and tissue specific transcript signatures of ion channel genes in the non-diseased human heart. J Physiol 582:675–693. doi: 10.1113/jphysiol.2006.126714

Gögelein H, Brüggemann A, Gerlach U, et al (2000) Inhibition of I Ks channels by HMR 1556. Naunyn Schmiedebergs Arch Pharmacol 480–488. doi: 10.1007/s002100000284

Goldenberg I, Thottathil P, Lopes CM, et al (2012) Trigger-specific ion-channel mechanisms, risk factors, and response to therapy in type 1 long QT syndrome. Hear Rhythm 9:49–56. doi: 10.1016/j.hrthm.2011.08.020

Heath BM., Terrar DA. (1996) THE DEACTIVATION KINETICS OF THE DELAYED RECTIFIER COMPONENTS IKr AND IKs IN GUINEA-PIG ISOLATED VENTRICULAR MYOCYTES. Exp Physiol 81:605–621. doi: doi: 10.1113/expphysiol.1996.sp003962

Hodgkin AL, Huxley AF (1939) Action Potentials Recorded from Inside a Nerve Fibre. Nature 144:710–711. doi: 10.1038/144710a0

Hondeghem LM, Snyders DJ (1990) Class III antiarrhythmic agents have a lot of potential but a long way to go. Reduced effectiveness and dangers of reverse use dependence. Circulation 81:686–90. doi: 10.1161/01.CIR.81.2.686

Horváth A, Lemoine MD, Löser A, et al (2018) Low Resting Membrane Potential and Low Inward Rectifier Potassium Currents Are Not Inherent Features of hiPSC-Derived Cardiomyocytes. Stem Cell Reports. doi: 10.1016/j.stemcr.2018.01.012

Huang X, Kim TY, Koren G, et al (2016) Spontaneous initiation of premature ventricular complexes and arrhythmias in type 2 long QT syndrome. Am J Physiol Heart Circ Physiol. doi: 10.1152/ajpheart.00500.2016

Jagadeesh G, Balakumar P, Maung-u K (2015) Pathophysiology and pharmacotherapy of Cardiovascular disease.

January CT, Riddle JM (1989) Early Afterdepolarizations: Mechanism of Induction and Block. Circ Res 977–990.

Jonsson MKB, Duker G, Tropp C, et al (2010) Quantified proarrhythmic potential of selected human embryonic stem cell-derived cardiomyocytes. Stem Cell Res 4:189–200. doi: 10.1016/j.scr.2010.02.001

Jost N, Virág L, Bitay M, et al (2005) Restricting excessive cardiac action potential and QT prolongation: A vital role for IKs in human ventricular muscle. Circulation 112:1392–1399. doi: 10.1161/CIRCULATIONAHA.105.550111

Jost N, Virág L, Comtois P, et al (2013) Ionic mechanisms limiting cardiac repolarization reserve in humans compared to dogs. J Physiol 591:4189–206. doi: 10.1113/jphysiol.2013.261198

Karjalainen J, Viitasalo M, Mänttäri M, Manninen V (1994) Relation between QT intervals and heart rates from 40 to 120 beats/min in rest electrocardiograms of men and a simple method to adjust QT interval values. J Am Coll Cardiol 23:1547–1553. doi: 10.1016/0735-1097(94)90654-8

Khan E, Spiers C, Khan M (2013) The heart and potassium : A banana republic. Acute Card Care 15:17–24. doi: 10.3109/17482941.2012.741250

Khan IA (2002) Long QT syndrome: Diagnosis and management. Am Heart J 143:7–14. doi: 10.1067/mhj.2002.120295

Kim JJ, Yang L, Lin B, et al (2016) Mechanism of automaticity in cardiomyocytes derived from human induced pluripotent stem cells. J Mol Cell Cardiol 81–93. doi: 10.1016/j.yjmcc.2015.01.013.Mechanism

Kirchhof P, Franz MR, Bardai A, Wilde AM (2009) Giant T – U Waves Precede Torsades de Pointes in Long QT Syndrome. J Am Coll Cardiol. doi: 10.1016/j.jacc.2009.03.043

Koncz I, Szél T, Bitay M, et al (2011) Electrophysiological effects of ivabradine in dog and human cardiac preparations : Potential antiarrhythmic actions. Eur J Pharmacol 668:419–426. doi: 10.1016/j.ejphar.2011.07.025

Lemoine MD, Duverger JE, Naud P, et al (2011) Arrhythmogenic left atrial cellular electrophysiology in a murine genetic long QT syndrome model. Cardiovasc Res 92:67–74. doi: 10.1093/cvr/cvr166

Lemoine MD, Krause T, Koivumäki JT, et al (2018) Human Induced Pluripotent Stem Cell–Derived Engineered Heart Tissue as a Sensitive Test System for QT Prolongation and Arrhythmic Triggers. Circ Arrhythmia Electrophysiol. doi: 10.1161/CIRCEP.117.006035

Lemoine MD, Mannhardt I, Breckwoldt K, et al (2017) Human iPSC-derived cardiomyocytes cultured in 3D engineered heart tissue show physiological upstroke velocity and sodium current density. Sci Rep 7:1–11. doi: 10.1038/s41598-017-05600-w

Li G, Feng J, Yue L, et al (1996) Evidence for Two Components of Delayed Rectifier K + Current in Human Ventricular Myocytes. Circ Res 78:689–696.

Li Y, Hof T, Baldwin TA, et al (2019) Regulation of I Ks Potassium Current by Isoproterenol Adenylyl Cyclase. Cells 8:1–16. doi: doi:10.3390/cells8090981

Liu DW, Antzelevitch C (1995) Characteristics of the delayed rectifier current (IKr and IKs) in canine ventricular epicardial, midmyocardial, and endocardial myocytes. A weaker IKs contributes to the longer action potential of the M cell. Circ Res 76:351–65. doi: 10.1161/01.RES.76.3.351

Louch WE, Koivum JT, Tavi P (2015) Calcium signalling in developing cardiomyocytes : implications for model systems and disease. J Physiol 5:1047–1063. doi: 10.1113/jphysiol.2014.274712

Louch WE, Stokke MK, Sjaastad I, et al (2012) No Rest for the Weary : Diastolic Calcium Homeostasis in the Normal and Failing. Physiology 27:308–323. doi: 10.1152/physiol.00021.2012

Lu HR, Hortigon-Vinagre MP, Zamora V, et al (2017) Application of optical action potentials in human induced pluripotent stem cells-derived cardiomyocytes to predict drug-induced cardiac arrhythmias. J Pharmacol Toxicol Methods 87:53–67. doi: 10.1016/j.vascn.2017.05.001

Lu HR, Vlaminckx E, Teisman A, Gallacher DJ (2005) Choice of cardiac tissue plays an important role in the evaluation of drug-induced prolongation of the QT interval in vitro in rabbit. J Pharmacol Toxicol Methods 52:90–105. doi: 10.1016/j.vascn.2005.04.007

Lu Z, Kamiya K, Opthof T, et al (2001) Density and kinetics of I(Kr) and I(Ks) in guinea pig and rabbit ventricular myocytes explain different efficacy of I(Ks) blockade at high heart rate in guinea pig and rabbit: implications for arrhythmogenesis in humans. Circulation 104:951–956. doi: 10.1161/hc3401.093151

Lungo M Del, Melchiorre M, Guandalini L, et al (2012) Novel blockers of current with isoform selectivity in recombinant cells and native tissue. Br J Pharmacol 602–616. doi: 10.1111/j.1476-5381.2011.01782.x

Mannhardt I, Breckwoldt K, Letuffe-Brenière D, et al (2016) Human Engineered Heart Tissue: Analysis of Contractile Force. Stem Cell Reports 7:29–42. doi: 10.1016/j.stemcr.2016.04.011

McAllister R., Noble D, Tsien RW (1975) Reconstruction of the electrical activity of cardiac Purkinje fibres. J Physiol 1–59.

Nalos L, Varkevisser R, Jonsson MKB, et al (2011) Comparison of the I Kr blockers moxifloxacin , dofetilide and E-4031 in five screening models of pro-arrhythmia reveals lack of specificity of isolated cardiomyocytes. Br J Pharmacol 165:467–478. doi: 10.1111/j.1476-5381.2011.01558.x

Nattel S, Quantz MA (1988) Pharmacological response of quinidine induced early afterdepolarisations in canine cardiac Purkinje fibres : insights into underlying ionic mechanisms. Cardiovasc Res 22:808–817.

Němec J, Kim JJ, Salama G (2016) The link between abnormal calcium handling and electrical instability in acquired long QT syndrome – does calcium precipitate arrhythmic storms? Prog Biophys Mol Biol 120:210–221. doi: 10.1016/j.pbiomolbio.2015.11.003.The

Nerbonne JM, Kass RS (2005) Molecular physiology of cardiac repolarization. Physiol Rev 85:1205–1253. doi: 10.1152/physrev.00002.2005.

Niggli E, Kléber A, Weingart R (2006) Founder of cardiac cellular electrophysiology: Honouring Silvio Weidmann, 7 April 1921– 11 July 2005. J physiol 3:431–432. doi: 10.1113/jphysiol.2005.101550

Ohler A, Ravens U (1994) Effects of E-4031, Almokalant and Tedisamil on Postrest Action-Potential Duration of Human Papillary-Muscles. J Pharmacol Exp Ther 270:460–465.

Okada Y, Ogawa S, Sadanaga T, Mitamura H (1996) Assessment of Reverse Use-Dependent Blocking Actions of Class III Antiarrhythmic Drugs by 24-Hour Holter Electrocardiography. Am Coll Cardiol 27:1–4. doi: 10.1016/0735-1097(95)00424-6

Peng S, Lacerda AE, Kirsch GE, et al (2010) The action potential and comparative pharmacology of stem cell-derived human cardiomyocytes. J Pharmacol Toxicol Methods 61:277–286. doi: 10.1016/j.vascn.2010.01.014

Perez Riera AR, Barbosa Barros R, de Sousa FD, Baranchuk A (2010) Accelerated Idioventricular Rhythm : Chronology of the Main Discoveries. Indian Pacing Electrophysiol J 10:40–48.

Prondzynski M, Lemoine MD, Zech ATL, et al (2019) Disease modeling of a mutation in a -actinin 2 guides clinical therapy in hypertrophic cardiomyopathy. EMBO Mol Med 1–18. doi: 10.15252/emmm.201911115

Qi X, Yeh Y, Chartier D, et al (2009) The Calcium/Calmodulin/Kinase System and Arrhythmogenic Afterdepolarizations in Bradycardia-Related Acquired Long-QT Syndrome. Circ Arrhythmia Electrophysiol 2:295–304. doi: 10.1161/CIRCEP.108.815654

Ravens U, Christ T (2010) Atrial-selective drugs for treatment of atrial fibrillation. Herzschrittmachertherapie + Elektrophysiologie 4:217–221. doi: 10.1007/s00399-010-0088-8

Roden DM, Viswanathan PC (2005) Genetics of acquired long QT syndrome. J Clin Invest. doi: 10.1172/JCI25539.fit

Sagie A, Larson MG, Goldberg RJ, et al (1992) An improved method for adjusting the QT interval for heart rate (the Framingham Heart Study). Am J Cardiol 70:797–801. doi: 10.1016/0002-9149(92)90562-D

Salata J, Jurkiewicz NK, Jow B, et al (1996) IK of rabbit ventricle evidence for IKS is composed of two currents: evidence for IKs.

Sanguinetti MC (1992) Modulation of Potassium Channels by Antiarrhythmic and Antihypertensive Drugs. Hypertens J Am Hear Assoc 19:228–236.

Sanguinetti MC, Curran ME, Zou A, et al (1996) Coassembly of KVLQT1 and minK (IsK) proteins to form cardiac IKS potassium channel. Nature 384:80–83.

Santulli G, Xie W, Reiken SR, Marks AR (2015) Mitochondrial calcium overload is a key determinant in heart failure. Proc Natl Acad Sci 112:11389–11394. doi: 10.1073/pnas.1513047112

Schwartz PJ, Ackerman MJ, George ALJ, Wilde AAM (2013) Impact of Genetics on the Clinical Management of Channelopathies. J Am Coll Cardiol 62:169–180. doi: 10.1016/j.jacc.2007.01.076.White

Shen WK, Sheldon RS, Benditt DG, et al (2017) 2017 ACC/AHA/HRS Guideline for the Evaluation and Management of Patients With Syncope. J Am Coll Cardiol 70:39–110. doi: 10.1016/j.jacc.2017.03.003

Sipido KR, Volders PGA., de Groot M, et al (2000) Enhanced Ca 2+ Release and Na/Ca Exchange Activity in Hypertrophied Canine Ventricular Myocytes. Circulation 102:2137–2144.

Spector PS, Curran ME, Keating MT, Sanguinetti MC (1996) Class III Antiarrhythmic Drugs Block HERG, a Human Cardiac Delayed Rectifier K+. Circ Res 78:499–503.

Stengl M, Volders PGA, Thomsen MB, et al (2003) Accumulation of slowly activating delayed rectifier potassium current (I Ks) in canine ventricular myocytes. Physiol Soc 777–786. doi: 10.1113/jphysiol.2003.044040

Tanaka H, Nishimaru K, Aikawa T, et al (2002) E€ ffect of SEA0400, a novel inhibitor of sodium-calcium exchanger, on myocardial ionic currents. Br J Pharmacol 135:1096–1100. doi: 10.1038/sj.bjp.0704574

Tazmini K, Frisk M, Lewalle A, et al (2020) Hypokalemia Promotes Arrhythmia by Distinct Mechanisms in Atrial and Ventricular Myocytes. Circ Res 889–906. doi: 10.1161/CIRCRESAHA.119.315641

Tester DJ, Ackerman MJ (2011) Genetic Testing for Potentially Lethal, Highly Treatable Inherited Cardiomyopathies/Channelopathies in Clinical Practice. Circulation 123:1021–1037. doi: 10.1080/10810730902873927.Testing

Thollon C, Bedut S, Villeneuve N, et al (2007) Use-dependent inhibition of hHCN4 by ivabradine and relationship with reduction in pacemaker activity. Br J Pharmacol 150:37–46. doi: 10.1038/sj.bjp.0706940

Thomas D, Karle C, Kiehn J (2004) Modulation of HERG potassium channel function by drug action. Ann Med 36:41–46. doi: 10.1080/17431380410032580

Thomas GP, Gerlach U, Antzelevitch C (2003) HMR 1556 , A Potent and Selective Blocker of Slowly Activating Delayed Rectifier Potassium Current. J Cardiovasc Pharmacol 41:140–147.

Thomsen MB, Verduyn SC, Stengl M, et al (2004) Increased short-term variability of repolarization predicts d-sotalol-induced torsades de pointes in dogs. Circulation 110:2453–2459. doi: 10.1161/01.CIR.0000145162.64183.C8

Tristani-Firouzi M, Tawil R Andersen-Tawil Syndrome, Sixth Edit. Elsevier Inc.

Tseng GN, Boyden PA (1989) Multiple types of Ca2+ currents in single canine Purkinje cells. Circ Res 65:1735–1750. doi: 10.1161/01.RES.65.6.1735

Uzun AU, Mannhardt I, Breckwoldt K, et al (2016) Ca2+-currents in human induced pluripotent stem cell-derived cardiomyocytes effects of two different culture conditions. Front Pharmacol. doi: 10.3389/fphar.2016.00300

Vandenberg JI, Perry MD, Perrin MJ, et al (2012) hERG K+ CHANNELS: STRUCTURE, FUNCTION, AND CLINICAL SIGNIFICANCE. Physiol Rev 92:1393–1478. doi: 10.1152/physrev.00036.2011

Vermeulen JT, Mcguire MA, Opthof T, et al (1994) Triggered activity and automaticity in ventricular trabeculae of failing human and rabbit hearts. Cardiovasc Res 28:1547–1554. doi: 10.1093/cvrese/28.10.1547

Viskin S, Alla SR, Barron H v, et al (1996) Mode of Onset of Torsade de Pointes in Congenital Long QT Syndrome. J Am Coll Cardiol 28:1262–1268. doi: 10.1016/S0735-1097(96)00311-7

Wallace E, Howard L, Liu M, et al (2019) Long QT Syndrome : Genetics and Future Perspective. Pediatr Cardiol 40:1419–1430. doi: 10.1007/s00246-019-02151-x

Weinsberg F, Bauer C, Schwarz J (1997) The class III antiarrhythmic agent E-4031 selectively blocks the inactivating inward-rectifying potassium current in rat anterior pituitary tumor cells (GH3 / B6 cells). Pflugers Arch Eur J Physiol 434:9094250. doi: DOI: 10.1007/s004240050356

Wettwer E, Hála O, Christ T, et al (2004) Role of IKur in controlling action potential shape and contractility in the human atrium: Influence of chronic atrial fibrillation. Circulation 110:2299–2306. doi: 10.1161/01.CIR.0000145155.60288.71

Xie Y, Grandi E, Puglisi JL, et al (2013) β-Adrenergic Stimulation Activates Early Afterdepolarizations Transiently via Kinetic Mismatch of PKA targets. J Mol Cell Cardiol 1:153–161. doi: 10.1016/j.yjmcc.2013.02.009.

Xie Y, Sato D, Garfinkel A, et al (2010) So little source, so much sink: Requirements for afterdepolarizations to propagate in tissue. Biophys J 99:1408–1415. doi: 10.1016/j.bpj.2010.06.042

Yap YG, Camm AJ (2003) Drug induced QT prolongation and torsades de pointes. Heart 89:1363–72. doi: 10.1007/s00508-008-0940-6

Zaza A (2009) Serum potassium and arrhythmias †. Europace 11:421–422. doi: 10.1093/europace/eup005

Contribution work

Brette R, Destexhe A (2012) Chapter 3 „Intracellular recording“ In Handbook of Neural Activity Measurement. Cambridge 44-91

Gintant G and Valentin JP. (2015) Chapter 49 “Drug-Induced Prolongation of the QT Interval: Present and Future Challenges for Drug Discovery” In Pathophysiology and Pharmacotherapy of Cardiovascular Disease. Gowraganahalli Jagadeesh, Pitchai Balakumar, Khin Maung-U (Hrg.) Springer International Publishing Switzerland, 977-1002

Jost N, Muntean DM, and Christ T. (2015) Chapter 46 “Cardiac Arrhythmias: Introduction, Electrophysiology of the Heart, Action Potential and Membrane Currents.” In Pathophysiology and Pharmacotherapy of Cardiovascular Disease. Gowraganahalli Jagadeesh, Pitchai Balakumar, Khin Maung-U (Hrg.) Springer International Publishing Switzerland, 977-1002

Schleifer JW and Srivathsan K. (2015) Chapter 48 “Proarrhythmic Effects of Antiarrhythmic and Non-antiarrhythmic Drugs” In Pathophysiology and Pharmacotherapy of Cardiovascular Disease. Gowraganahalli Jagadeesh, Pitchai Balakumar, Khin Maung-U (Hrg.) Springer International Publishing Switzerland, 977-1002

Tristani-Firouzi M, Tawil R. (2014) Chapter 94 „Andersen-Tawil Syndrome“ in Cardiac Electrophysiology: From Cell to Bedside (Sixth Edition). Elsevier Inc. 947-952

Internet sources

E-4031 - National Center for Biotechnology Information. (2017) PubChem Compound Database; CID=3185, https://pubchem.ncbi.nlm.nih.gov/compound/3185 (accessed May 11, 2017).

HMR-1556 - National Center for Biotechnology Information. (2017) PubChem Compound Database; CID=9887834, https://pubchem.ncbi.nlm.nih.gov/compound/9887834 (accessed May 11, 2017).

Isoprenaline - National Center for Biotechnology Information. (2020) PubChem Database. Isoprenaline, CID=3779, https://pubchem.ncbi.nlm.nih.gov/compound/Isoprenaline (accessed on Feb. 18, 2020)

Ivabradine - National Center for Biotechnology Information. (2017) PubChem Compound Database; CID=132999, https://pubchem.ncbi.nlm.nih.gov/compound/132999 (accessed June 27, 2017).

Moxifloxacin - National Center for Biotechnology Information (2020). PubChem Compound Summary for CID 152946, Moxifloxacin. Retrieved August 4, 2020 from https://pubchem.ncbi.nlm.nih.gov/compound/Moxifloxacin

SEA0400 - National Center for Biotechnology Information (2020). PubChem Compound Summary for CID 644100. Retrieved August 4, 2020 from https://pubchem.ncbi.nlm.nih.gov/compound/sea0400

Verapamil - National Center for Biotechnology Information (2020). PubChem Compound Summary for CID 2520, Verapamil. Retrieved August 4, 2020 from https://pubchem.ncbi.nlm.nih.gov/compound/Verapamil

8 Supplement

Detailed description of the EHT production and tissue engineering

The generation and culture of human induced pluripotent stem cell-derived cardiomyocytes in engineered heart tissue and monolayer format has been described and referenced in previous works from this institute by Breckwoldt et. al (2017). This segment is an abbreviation of the process.

The undifferentiated hiPSC line C25 (kind gift from Alessandra Moretti, Munich, Germany) was expanded in FTDA medium1 and differentiated in a three-step protocol based on growth factors and a small molecule Wnt inhibitor DS07 (kind gift from Dennis Schade, Dortmund, Germany) as previously published2. ERC018 iPS cells were generated in-house from skin fibroblasts of a healthy subject using the CytoTuneTM-iPS Sendai Reprogramming Kit (Thermo Fisher Scientific) and differentiated to cardiomyocytes as described for C25. ICell² cardiomyocytes is a commercially available hiPSC-CM cell line bought from Cellular Dynamics. Aliquots of iCell² cardiomyocytes were thawed according to the manufacturer's instructions. All iPS cell lines were generated from female donors.

The generation of engineered heart tissue (EHT) was performed as described previously.3 In brief, fibrin-based EHTs were generated in agarose casting moulds with solid silicone racks in a 24-well format with $1x10^6$ hiPSC-CM in a fibrin matrix (total volume 100 µl) consisting of 10 µl/100 µl Matrigel [BD Bioscience, 256235], 5 mg/ml bovine fibrinogen (200 mg/ml in NaCl 0.9% [Sigma, F4753] plus 0.5 µg/mg aprotinin [Sigma, A1153]), 2x DMEM, 10 µmol/L Y-27632 and 3 U/ml thrombin [Biopur, BP11101104]). EHTs were cultured at 37 °C, 7% CO2, 40% O2 humidified cell culture incubated with a medium consisting of DMEM (Biochrom; F0415), 10% heat-inactivated horse serum (Gibco 26050), 1% penicillin/streptomycin (Gibco 15140), insulin (10 µg/ml; Sigma I9278) and aprotinin (33 µg/ml; Sigma A1153). EHTs started coherent and stable beating at day 10-14 after casting and were used between day 25 and 100 for electrophysiological measurements.

Effect of ivabradine on left ventricle action potential shape

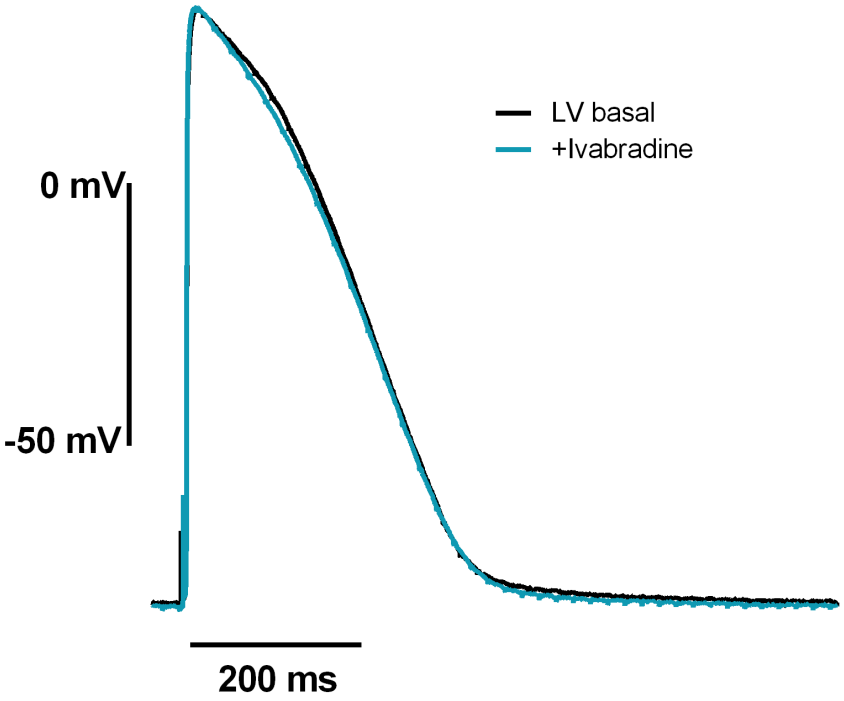

Supplement Figure 1. Effect of ivabradine on left ventricle action potential shape.

$BaCl_2$ concentration-response plots

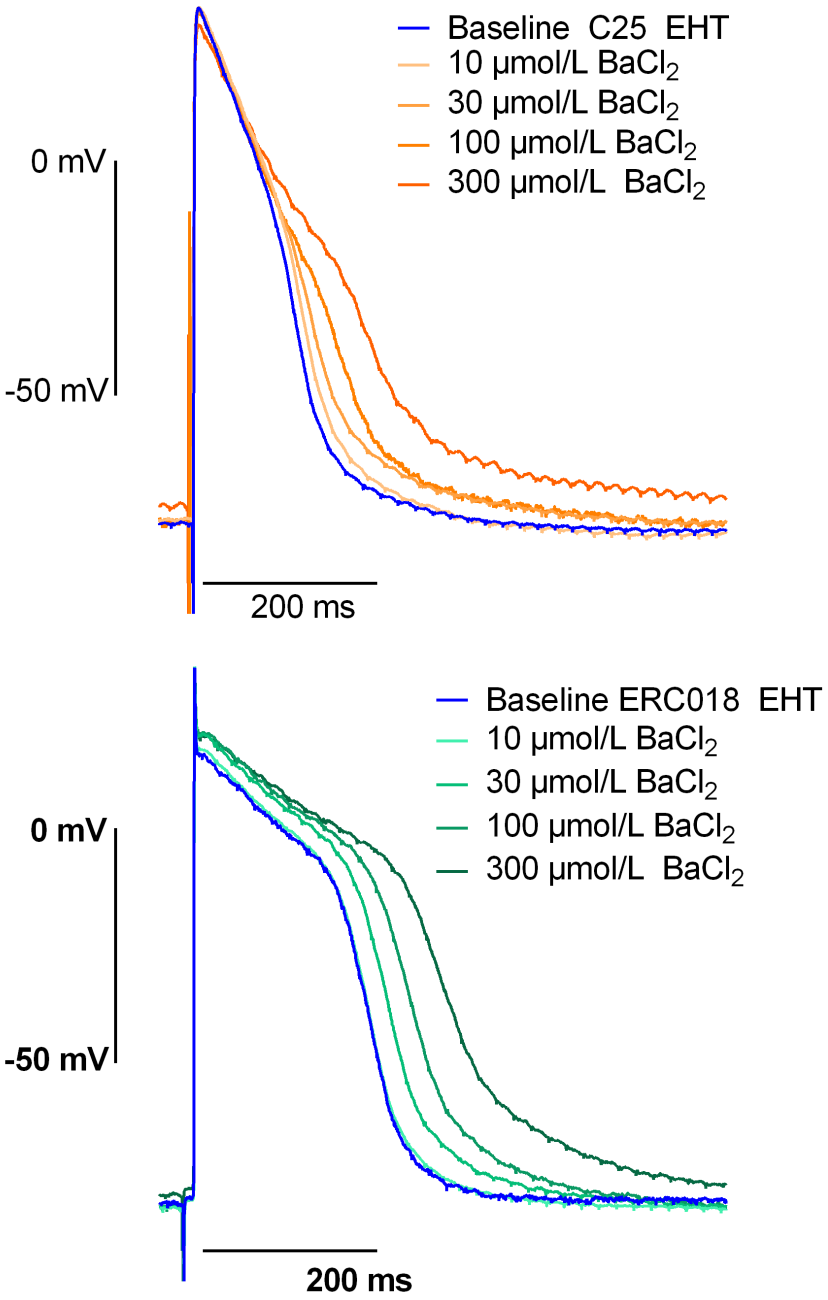

Supplement Figure 2. Examples of $BaCl_2$ concentration-response in different cell lines.

EHT action potential shapes in different genotypes

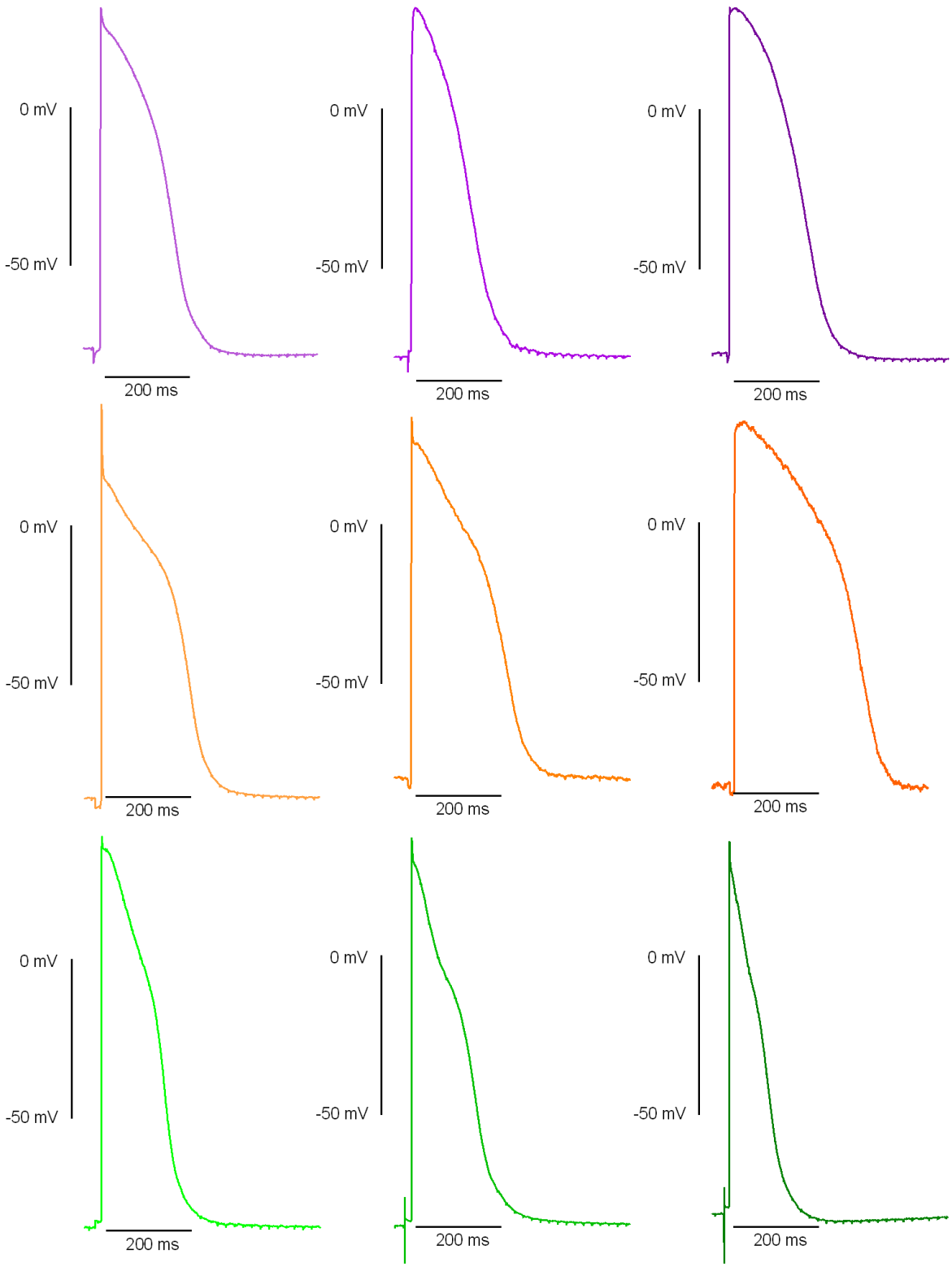

Supplement Figure 3. Action potential shapes in different cell lines of engineered heart tissue. Three different cell lines of EHT tissue paced at 1 Hz under baseline conditions: C25 in violet, ERC018 in orange and iCell^2 in green.

EHT E-4031 concentration-response in different genotypes

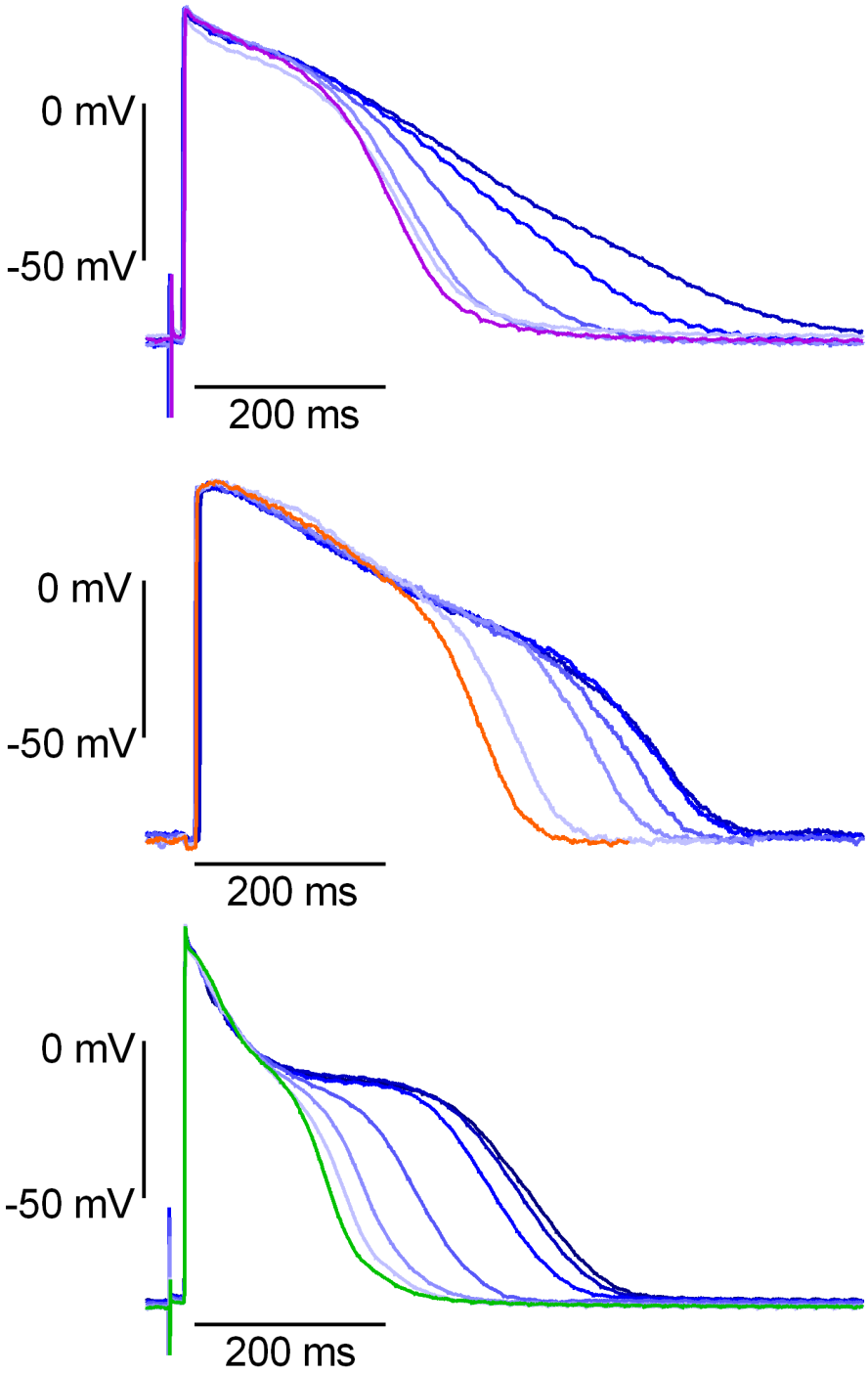

Supplement Figure 4. Concentration-response to E-4031 I_{Kr} block in different cell lines of engineered heart tissue. Three cell lines C25 in violet, ERC018 in orange and iCell^2 in green shown under incremental I_{Kr} block in half-logarithmic steps blue tones (3 nmol/L to 1 µmol/L)

Patient Data belonging to the ventricular tissue used for experiments

Supplement Table 1. Patient data. Patient data, including premedication, pre- and postoperative electrocardiogram and echocardiogram, cardiovascular preconditions have been collected via the university clinic's internal network Soarian.

	Left ventricular tissue
Total patients	34
Gender [m / f]	19/15
Age [years]	60.8±2.6
Operation	
Left ventricular assist device, n	3/34
Heart transplantation, n	4/34
Aortic valve replacement, n	24/34
Cardiovascular disease	
Hypertension, n	31/34
Diabetes mellitus, n	6/34
Coronary artery disease, n	7/34
Dilatated cardiomyopathy, n	6/34
Valve disease, n	28/34
LVEF [%]	51.2±2.9
Cardiovascular medication	
Na^+-channel blocker, n	0/34
β-blockers, n	21/34
Amiodarone, n	0/34
Ca^{2+}-channel- blockers, n	2/34
Digitalis, n	2/34
Diuretics, n	16/34
ACE-Inhibitors / AT_1-blockers, n	28/34

9 Curriculum vitae

Lebenslauf wurde aus datenschutzrechtlichen Gründen entfernt.

10 Danksagung

Abschließend möchte ich allen Personen danken, die an der Entstehung dieser Arbeit beteiligt waren und dies ermöglicht haben.

Zuerst gilt mein Dank Prof. Dr. med. Thomas Eschenhagen für die Möglichkeit meine Dissertation am Institut für Experimentelle Pharmakologie und Toxikologie des Universitätsklinikums Hamburg-Eppendorf zu schreiben und hier unter exzellenter Leitung sehr viel zu lernen.

Weiterhin danke ich meinem Doktorvater PD Dr. med. Torsten Christ, dessen langjährige elektrophysiologische Expertise und humorvolle Art diese zu vermitteln, die Grundlage für die Entstehung dieser Arbeit gebildet haben. Ein besonderer Dank gilt meinem Betreuer Dr. med. Marc Lemoine für die Einarbeitung in die Materie und experimentelle Technik, Unterstützung bei sämtlichen Fragen im Prozess der wissenschaftlichen Arbeit, und nicht zuletzt für die karriereweisende Hilfestellung als Arzt in der klinischen Elektrophysiologie.

An alle MitarbeiterInnen des Instituts geht ein Dank für die angenehme Arbeitsatmosphäre und die entspannte und internationale Zusammenarbeit. Ganz besonders natürlich an alle Personen, die uns ihre mühsam gezüchteten EHT-Gewebeproben für die elektrophysiologischen Experimente zur Verfügung gestellt haben, und an die KollegInnen des universitären Herzzentrums ohne die es nie möglich gewesen wäre an echtes menschliches Herzgewebe zu kommen.

“*Grazie mille*” an PhD Marta Lemme und Dr. rer. biol. hum. Julia Krause für die Solidarität und Inspiration durch ihre ebenfalls vielen geduldig verbrachten Stunden am *sharp microelectrode*-Setup, und all den KollegInnen und DoktorandInnen, die den Aufwand und die Schwierigkeiten nachvollziehen können.

Zuletzt ein großer Dank an meine FreundInnen und Familie, die mich immer moralisch unterstützt haben im langen Prozess und deren Fragen “wie weit denn die Doktorarbeit ist?” nie fordernd, sondern immer motivierend waren.

11 Eidesstattliche Versicherung

Ich versichere ausdrücklich, dass ich die Arbeit selbständig und ohne fremde Hilfe verfasst, andere als die von mir angegebenen Quellen und Hilfsmittel nicht benutzt und die aus den benutzten Werken wörtlich oder inhaltlich entnommenen Stellen einzeln nach Ausgabe (Auflage und Jahr des Erscheinens), Band und Seite des benutzten Werkes kenntlich gemacht habe.

Ferner versichere ich, dass ich die Dissertation bisher nicht einem Fachvertreter an einer anderen Hochschule zur Überprüfung vorgelegt oder mich anderweitig um Zulassung zur Promotion beworben habe.

Ich erkläre mich einverstanden, dass meine Dissertation vom Dekanat der Medizinischen Fakultät mit einer gängigen Software zur Erkennung von Plagiaten überprüft werden kann.

Inhalte dieser Arbeit wurden publiziert in Circulation: Arrhythmia and Electrophysiology

Lemoine MD et al (2018) Human Induced Pluripotent Stem Cell–Derived Engineered Heart Tissue as a Sensitive Test System for QT Prolongation and Arrhythmic Triggers. doi: 10.1161/CIRCEP.117.006035

Unterschrift: 

Hamburg, 21.01.2021 Tobias Krause